

## PDF hosted at the Radboud Repository of the Radboud University Nijmegen

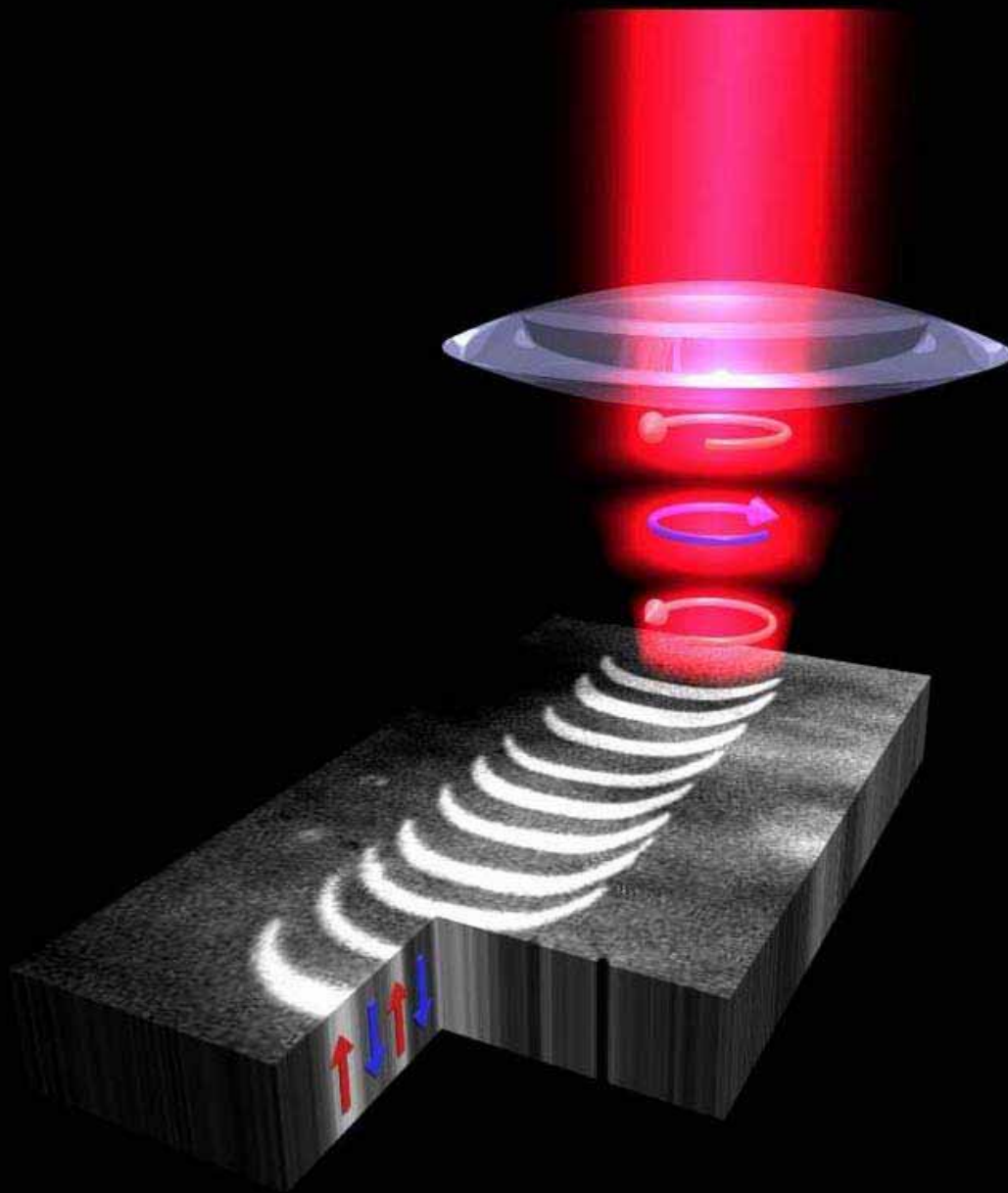
The following full text is a publisher's version.

For additional information about this publication click this link.

<http://hdl.handle.net/2066/65585>

Please be advised that this information was generated on 2018-07-08 and may be subject to change.

**LASER - INDUCED**  
**FEMTOSECOND**  
**MAGNETIC RECORDING**



CLAUDIU DANIEL STANCIU



# **Laser-Induced Femtosecond Magnetic Recording**

**Claudiu Daniel Stanciu**

---

Laser-Induced Femtosecond Magnetic Recording  
Stanciu, Claudiu Daniel  
PhD Thesis, Radboud University Nijmegen, The Netherlands - 2008  
Illustrated with references, summary in English, Dutch and Romanian  
ISBN/EAN: 978-90-9023402-1  
Front cover: All-Optical Magnetic Recording with Circularly Polarized Light  
Cover design by C. D. Stanciu and F. Hansteen.  
Printed by PrintPartners Ipskamp, Enschede, The Netherlands  
Copyright © 2008, by Claudiu Daniel Stanciu  
An electronic version of this thesis can be found at: <http://www.stanciu.nl>

# Laser-Induced Femtosecond Magnetic Recording

Een wetenschappelijke proeve op het gebied van de  
Natuurwetenschappen, Wiskunde & Informatica

Proefschrift

ter verkrijging van de graad van doctor  
aan de Radboud Universiteit Nijmegen  
op gezag van de Rector Magnificus prof. dr. S.C.J.J. Kortmann,  
volgens besluit van het College van Decanen  
in het openbaar te verdedigen op vrijdag 3 oktober 2008  
om 12:00 uur precies

door

Claudiu Daniel Stanciu

geboren op 20 december 1979  
te Pitești, Romania

**Promotor:**

Prof. dr. Th. Rasing

**Copromotores:**

Dr. A. V. Kimel  
Dr. A. Kirilyuk

**Manuscriptcommissie:**

Prof. dr. M. Katsnelson

Prof. dr. R. W. Chantrell

Department of Physics,  
University of York,  
York, U.K.

Prof. dr. M. Aeschlimann

Department of Physics,  
University of Kaiserslautern,  
Kaiserslautern, Germany

# Laser-Induced Femtosecond Magnetic Recording

A scientific essay in the  
Natural Sciences, Mathematics and Computer Science

Doctoral thesis

to obtain the degree of doctor  
from Radboud University Nijmegen  
on the authority of the Rector Magnificus prof. dr. S.C.J.J. Kortmann,  
according to the decision of the Council of Deans  
to be defended in public on Friday, 3 October 2008  
at precisely 12:00 hours

by

Claudiu Daniel Stanciu

born on 20 December 1979  
in Pitesti, Romania



**Doctoral supervisor:** Prof. dr. Th. Rasing

**Co-supervisors:** Dr. A. V. Kimel  
Dr. A. Kirilyuk

**Doctoral Thesis Committee:**

Prof. dr. M. Katsnelson

Prof. dr. R. W. Chantrell  
Department of Physics,  
University of York,  
York, U.K.

Prof. dr. M. Aeschlimann  
Department of Physics,  
University of Kaiserslautern,  
Kaiserslautern, Germany

The work described in this thesis was financially supported by the **European RTN Network DYNAMICS**, de Nederlandse Organisatie voor Wetenschappelijk Onderzoek (NWO), de Stichting voor Fundamenteel Onderzoek der Materie (FOM), as well as the Dutch nanotechnology initiative NanoNed.

*Iubitei mele soții,  
Mihaela*



## Preface

After 4 years of adventures on the waves of magnetism, this thesis is ready. In 2004 when I arrived in Nijmegen to start my PhD, I received a temporarily desk and a PhD thesis to read. It was something about magnetization dynamics. But I couldn't understand almost anything not even the pictures. This made me understand what a big challenge represents a PhD, i.e. to understand a research field well enough to be able to write a thesis and more importantly to have what to write about. Fortunately, soon after I started my PhD I realized that I am not alone and that science is a team work. And so, I had the chance to work with many people who made my PhD a very pleasant experience both socially and scientifically, and without the help of whom this thesis would not have been possible. It is a pleasure to thank now all of them.

As a foreigner arriving in the Netherlands I discovered that I must study not only physics but also law, and that with the help of the Immigration and Naturalisation Service (IND). Thank you Marilou for all your time spent to help me go through the immigration bureaucracy. I would also like to thank to both Marilou and Riki for helping me with all kind of administrative issues during my stay in Nijmegen.

I fell very privileged as I have been conducting my PhD research under the supervision of some of the best scientists in the field of magnetization dynamics: Prof. Theo Rasing, Dr. Alexey Kimel and Dr. Andrei Kirilyuk.

Dear Theo, thank you for having confidence in me and for giving me the opportunity to work in your lab during these four years. I very much enjoyed and appreciated your optimism and permanent positive attitude. For me, this represented a vast source of motivation even in those moments when the journal referees proved to be more politicians than scientists. I also strongly valued your many comments and constructive criticism to my manuscripts and presentations. I thank Theo for being not only a great thesis supervisor but also such a kind person.

Dear Alexey, I was always amazed by your scientific accuracy and your constant strong interest for the experiments. I truly admire your endless energy for doing experiments. Thank you for all your help during my PhD and for your permanent extensive feedback to my manuscripts!

Dear Andrei, first thank you for fishing me out from the many applicants for a PhD position in this group. I had the chance to benefit from your guidance which felt so complementary with Alexey's and Theo's. The many discussions that we had have been very inspiring. Not less inspiring were the experiences such as testing the Alsatian wines during our research visit in Strasbourg.

As an experimentalist I spent a significant amount of my PhD working in the lab. This was a real pleasure as I have been working in a great environment which combined highly specialized technicians and some of the most modern ultrafast laser systems. Here, I would like to thank Albert van Etteger, Tonnie Toonen and Wiesiek Szweryn for their great technical help. Especially, I would like to thank Albert for

sharing with me his vast knowledge on lasers and optics, and for the maintenance of the lasers to very good operational standards.

The work presented in this thesis would have not been possible without our Japanese friends and collaborators: Dr. Arata Tsukamoto and Prof. Achioshi Itoh. I would like to thank them here for providing me with great samples. I also wish to thank them for the very nice time in Tokyo and the unforgettable sushi diner arranged by Prof. Itoh. Dear Arata, thank you for sharing with me your large experience in the field of magneto-optics. With your regular visits to Nijmegen, our collaboration extended to more than a scientific collaboration. I will always remember with pleasure our many chats about the Japanese and the Romanian culture, and your great and unique style of telling stories.

During these four years of PhD I had the chance to visit, work and learn from some of the best scientists in magnetism. I have enjoyed working in the labs of one of the pioneering groups in the field of ultrafast magnetization dynamics. Dear Prof. Jean-Yves Bigot, thank you for offering me this opportunity. I very much enjoyed the time spend in the lab with you and Dr. Mircea Vomir. Dear Mircea thank you very much for your kindness and your time spent to show me Strasbourg.

The most memorable experience outside Nijmegen labs was a short but intensive internship at Seagate's labs in Pittsburg, USA. For this amazing period during the Summer of 2007 I wish to thank Dr. Julius Hohlfeld and Dr. Sharat Batra who had to spend a long time filling in a huge amount of official papers in order to make my visit possible. Here I have been working with Dr. Julius Hohlfeld and Dr. Adnan Rebei, two great people and scientists. Dear Julius, dear Adnan, I will always remember with much pleasure the many long and inspiring discussions that we had during the coffee brakes, about life, about switching spins and everything else. During this one month of working together with you I felt like working with two good friends.

Throughout these 4 years of PhD in Nijmegen, many people have left and even more have joined the group. I would like to thank here my first two roommates Ventsislav Valev and Kürşat Bal who after my arrival in Nijmegen have been kindly answering to my infinite number of questions such as: How do I do this? From where do I get that? How do I call that? . . . Ventsi and Biliana, thank you for your help such as drawing me the map and the schedule of some shops in Nijmegen. Also thanks for the nice time that we had together.

During my first day as a PhD student, I was glad to hear that another Romanian recently started his PhD in our group. Soon after this news, a guy came to my office and asked me: "*Vorbești românește?*" (Do you speak Romanian?) - These were the words that started a very nice friendship with Lucian Jdira. *Dragă Lucian (Gigel), mulțumesc pentru prietenia pe care mi-ai acordat-o și pentru timpul lung în care ascultai toate amănuntele problemelor mele de la lucru . . . Chiar Gigel, când mergem la pește?*

Since I have started to work on magnetization dynamics, I got a lot of help from Fredrik Hansteen. While attending many conferences together, our collaboration extended to a nice friendship which I very much enjoyed and which lead to many nice memories. It is good to look back and see that our ambitious plans to switch magnetization by light, prepared during the conference MMM 2005, has succeeded just half a year later. Thank you Fredrik for all our nice chats and for always being open to listen to my long and stuffy stories about the experiments!

I very much enjoyed working in the lab and discussing with scientist visiting our group such as Prof. R.V.Pisarev, Dr. V.V. Pavlov and Dr. P.A. Usachev, from Iofee Institute, St Petersburg, Russia, Prof. E.D. Mishina from Moscow State Institute of Radioengineering, Russia; and with the visiting PhD students Alex Reid from Oxford University, UK; Ji-Wan Kim and Jae-Woo Jeong, KAIST, Korea.

The daily life would have not been so pleasant and interesting without my room-mates: Chris - the guy always happy to help everybody no matter how hard will be, the quiet and mysterious Dimitry, Joost always fighting with his computer, Michiel and Tom. Beyond doubt, working in a very large and international group, including two other Romanians, has been motivating and inspiring. I really enjoyed playing guitar with Roman, going fishing with Lucian, Ventsi, Arata and Roman, having barbeques and drinking beer until late in the night at Muzenplaats with Lucian, Roman, Sergiy, Loïc and Fredrik, going to conferences and workshops with Fredrik, Loïc, Sasha and Jan, drinking glue wine as only Oleg knows to prepare, and all the diners, barbeques and interesting chats with Kürşat, Ventsi, Wiesiek, Fred, Jing, Gabi, Marina, Weizhe and Yanyan, Duncan, Chris, Kadir, Johan and the enthusiastic Serhiy.

Although a PhD can take almost all the time, my life succeeded to extend outside the university too. And here the Romanian community in Nijmegen had a very important role. *Dragii mei Lucian și Henriette, Lucian și Alice, Călin și Delia, Ana și Cătă, Nicu și Roberta, Simona și Sacco, Angelica, Cosmina, mulțumesc pentru toate momentele frumoase pe care le-am petrecut împreună. Luiza, Dan și Costel mulțumesc pentru mititei, ciorba de burtă si voia bună! Marius (Prâslea) și Diana, success în noua viață printre olandezi!*

I also wish to express my gratitude to the faculty members of the West University, Timisoara, Romania who directly contributed to my scientific education. Especially, I would like to thank Conf. dr. I. Mălăescu, Lect. dr. Marin Cătălin and Prof. dr. Z. Schlett for their support. *De asemenea, doresc să amintesc aici numele a doi profesori din timpul liceului care au avut un impact puternic pozitiv asupra dezvoltării cunoștințelor mele în acele momente: Prof. D. Rudeanu din cadrul Liceului de Chimie Industrială Nr. 4 și Prof. de fizică F. Ghinescu.*

I would like to thank my beloved family for their permanent support and love: *Draga mea mamă, folosesc această cale pentru a-ți mulțumi din toată inima pentru toată dragostea pe care mi-ai acordat-o de-a lungul vieții și pentru neîntreruptul sprijin moral și financiar cu care ai fost întodeauna lângă mine. Tată, mulțumesc pentru*

*susținera financiară pe timpul facultății. Dragul meu frațior Mariusică, mulțumesc pentru prietenia și tot ajutorul pe care mi l-ai acordat mereu, în special în timpul facultății, dar și pentru cadourile frumoase pe care mi le cumpărai întodeauna de ziua mea. Dragii mei tata și mama s, vă mulțumesc mult pentru toată afecțiunea cu care m-ați acceptat ca pe fiul dumneavoastră și pentru toate zilele frumoase pe care le petrecem împreună de fiecare dată când ne întoarcem în România. Deasemenea, mulțumesc celor doi Cristi ai familiei pentru prietenia pe care o împărtășim.*

Days, nights and weekends of experiments, literature research and writing and rewriting articles are bound together in this thesis. Definitely, without the love, support, trust and the huge patience of my gorgeous wife Mihaela during all this time, this thesis would not have been possible. My lovely wife, THANK YOU for being part of my life! You always give me strength and motivation to go forward. *Draga mea, minunata mea și iubita mea soție Mihaela, te iubesc mult, mult de tot. Fără ajutorul tău nimic din ceea ce am realizat în acești ani n-ar fi fost cu putință. Mulțumesc pentru că ești!*

Finally, I wish to add that looking back through the experimental data, I realize that all the first observations of the effects reported in this thesis have an interesting thing in common: all happened during the weekend!

Nijmegen  
August 2008

*Daniel Stanciu*

---

## Contents

---

<b>1</b>	<b>Introduction</b>	<b>1</b>
1.1	Magnetic Data Storage and its Speed . . . . .	1
1.2	Optical Excitation of Magnetic Metals . . . . .	5
1.3	Laser-Induced Ultrafast Demagnetization . . . . .	6
1.4	Precessional Magnetization Dynamics . . . . .	11
1.5	Magnetization Reversal . . . . .	15
1.5.1	Reversal in an Applied Magnetic Field . . . . .	15
1.5.2	Reversal by Spin Injection . . . . .	18
1.5.3	All-Optical Switching . . . . .	19
1.6	Overview of This Thesis . . . . .	22
	References . . . . .	23
<b>2</b>	<b>Rare Earth - Transition Metal Amorphous Alloys</b>	<b>27</b>
2.1	Introduction . . . . .	27
2.2	Magnetic Properties . . . . .	28
2.3	Optical and Magneto-Optical Properties . . . . .	32
2.4	Growth . . . . .	33
2.5	RE-TM Alloys Studied in This Work: GdFeCo . . . . .	34
2.6	Summary . . . . .	36
	References . . . . .	37
<b>3</b>	<b>Experimental Techniques</b>	<b>39</b>
3.1	Introduction . . . . .	39
3.2	Linear Magneto-Optics . . . . .	41



3.3	The Femtosecond Laser System . . . . .	44
3.4	The Magneto-Optical Pump-Probe Set-up . . . . .	46
3.5	The Magneto-Optical Imaging Set-up . . . . .	51
	References . . . . .	52
<b>4</b>	<b>The Role of Angular Momentum Compensation</b>	<b>55</b>
4.1	Thermal-induced Magnetization Dynamics in GdFeCo . . . . .	56
4.1.1	Introduction . . . . .	56
4.1.2	Experimental Details . . . . .	57
4.1.3	Magnetization Dynamics in a Two-Sublattice Magnetic Systems	59
4.1.4	Magnetization Precession Excitation Mechanism . . . . .	62
4.1.5	Coherent Magnetization Precession as a Function of the Mag- netic Field Amplitude: Ferromagnetic Resonance . . . . .	64
4.1.6	Magnetization Precession as a Function of Temperature: Ferri- magnetic Resonance . . . . .	67
4.1.7	Conclusions . . . . .	76
4.2	Sub-picosecond Magnetization Reversal across Ferrimagnetic Compen- sation Points . . . . .	77
4.2.1	Introduction . . . . .	77
4.2.2	Experimental Details . . . . .	78
4.2.3	Results and Discussion: Pump Fluence Dependence . . . . .	78
4.2.4	Intrinsic Switching Speed . . . . .	83
4.2.5	Femtosecond Optical Excitation of Localized Magnetic Moment in Gd . . . . .	85
4.2.6	Conclusions . . . . .	88
4.3	Summary . . . . .	88
	References . . . . .	89
<b>5</b>	<b>The Role of Photon Angular Momentum</b>	<b>95</b>
5.1	Ultrafast Interaction of the Angular Momentum of Photons with Spins in GdFeCo . . . . .	97
5.1.1	Introduction . . . . .	97
5.1.2	Experimental Details . . . . .	98
5.1.3	Averaging Out the Laser Induced Heating Effects . . . . .	99
5.1.4	Observation of an Opto-Magnetic Effect in GdFeCo . . . . .	100
5.1.5	A Possible Mechanism: The Inverse Faraday Effect . . . . .	103
5.1.6	Conclusion . . . . .	105
5.2	All-Optical Magnetic Recording with Circularly Polarized Light . . . .	106
5.2.1	Introduction . . . . .	106
5.2.2	Experimental Details . . . . .	106
5.2.3	Demonstration of All-Optical Magnetization Reversal . . . . .	107

CONTENTS

---

5.2.4	Magnetization Reversal with Single 40-fs Circular Polarized Laser Pulses . . . . .	111
5.2.5	Conclusion . . . . .	113
5.3	Summary . . . . .	113
	References . . . . .	114
	<b>Summary and Outlook</b>	<b>119</b>
	<b>Samenvatting en Vooruitblik</b>	<b>123</b>
	<b>Rezumat</b>	<b>127</b>
	<b>List of Publications</b>	<b>133</b>
	<b>Curriculum Vitae</b>	<b>135</b>



# CHAPTER 1

---

## Introduction

---

**M**agnetism is certainly one of the cornerstones of what we today call *the information technology era*. Following the huge development of electronic devices such as the personal computer, this era has been strongly driven by the growing demand to increase the density and the speed of writing and retrieving data in memory devices. Today, the demand for information storage is enormous and expected to increase even further as new technologies such as high-definition video and on-demand TV are established in the market. In this quest, driven by the two words "smaller and faster", *magnetic recording remains the dominant data storage technology*. The reason for this is the unmatched combination offered by magnetic recording: large storage capacity, small physical size, random and fast access to data, non-volatility, radiation hardness and low cost. Consequently, the science and technology of magnetic materials is strongly fuelled by the global market for magnetic storage devices, which was estimated at \$20 billion in 2005, and is expected to grow to \$40 billion in 2010. Some examples of storage devices that are based on magnetism such as hard disk drive (HDD), magneto-optical disk and magnetic random access memory (MRAM), are shown in Figure 1.1.

### 1.1 Magnetic Data Storage and its Speed

In magnetic memory devices, logical bits ("ones" and "zeros") are stored by setting the magnetization vector of individual magnetic domains either 'up' or 'down'. The

size of these domains is what defines the density of information in a memory device. In other words, the smaller the bit size is, the higher is the storage capacity of data storage media. The evolution of the bit size has been impressive since 1955, when IBM built the first hard disk drive<sup>1</sup> featuring a storage capacity of about 5MB (5 million 8-bit characters) with areal recording density of 2 kbit/in<sup>2</sup>.<sup>2</sup> This corresponded to a bit size of  $\sim 0.55\text{mm} \times 0.55\text{mm}$ . The barrier of 100 Gbit/in<sup>2</sup> has already been passed in 2002. Today there are new technologies such as Seagate's Heat Assisted Magnetic Recording (HAMR) that promises recording densities beyond 1 Tbit/in<sup>2</sup>, *i.e.* bit sizes of  $\sim 10\text{nm} \times 65\text{nm}$ . As the bit size becomes smaller, the information recording speed must also become faster. The current disk drives are operating at an internal data transfer rate of approximately 200 MB/s, which corresponds to a channel data rate of about 1.6 Gbit/s [2, 3]. Therefore, the writing time for a single bit, or in other words the magnetization reversal time in a bit, is not far below 1 nanosecond. Although today a recording speed in the nanosecond range might be considered high enough with respect to the available densities, there is no doubt that the future Tbit/in<sup>2</sup> will ask for a much higher recording speed of the information, that is a faster magnetization reversal time.

Besides to disk storage, a tremendous research effort has been devoted in recent years to MRAM. This magnetic memory has the potential to store data at a relatively high density, high speed, and to have a low power consumption. Although currently Flash memory still offers higher areal density, MRAM has a potentially infinite endurance compared with  $\sim 10^5$  cycles for a Flash. Such characteristics together with its non-volatility makes MRAM an "ideal memory". Generally speaking, the most common design for MRAM uses a magnetic tunnel junction: two ferromagnetic thin films as electrodes and a thin tunneling barrier separating them. The resistance of the tunneling junction is modified as the magnetic moments of the two ferromagnetic layers change their relative orientation. The difference in junction resistance corresponding to the stable parallel and anti-parallel orientations, respectively, allows the definition of binary memory states. In July 2006, Freescale started selling the first commercial MRAM chip, with 4Mbit of memory while recently Toshiba and NEC have announced a 16 Mbit MRAM chip, with 34 ns read and write cycles [4]. Obviously, there is a large space here for improving the speed of manipulating data if appropriate new technological concepts are introduced.

Traditionally, in order to reverse the magnetization, and thus write or rewrite the information, an external magnetic field pulse is applied. The operation time for this magnetization reversal mechanism lies in the nanosecond regime. Increasing the strength of the magnetic field, the magnetization reversal time can be pushed into the

---

<sup>1</sup>This first HDD called RAMAC (Random Access Method of Accounting and Control) consisted out of 50 disks, each with a diameter of 24 inch (61 cm).

<sup>2</sup>The capacity of a HDD is in general referred to as the number of bits (or bytes - series of 8 bits) that can be squeezed on a square inch of a storage medium.

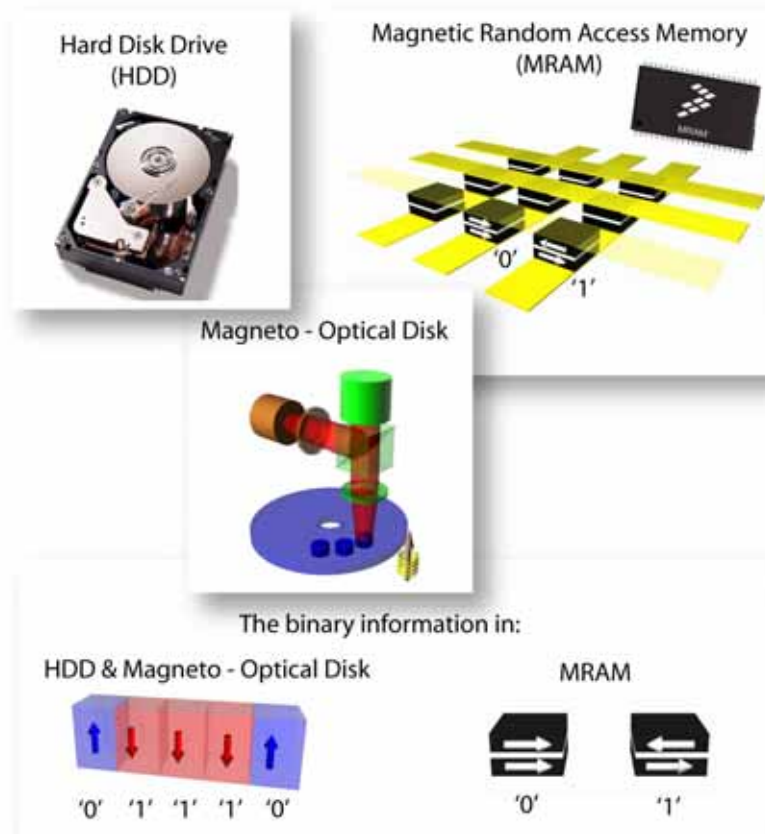


**Figure 1.1:** Illustration of various memory devices based on magnetism. In a Hard Disk Drive the binary state of the storage element is represented by magnetic domains with magnetization vector oriented either "up" or "down" corresponding to the values "1" or "0". On the other hand, in MRAM (magnetic random access memory) the values "1" or "0" are recorded in the two opposite orientations of the magnetization in one of the magnetic layers of magnetic tunnel junctions, which are connected to the crossing points of the two perpendicular arrays of parallel conducting lines. Here, the information is written by current pulses sent through one line of each array. Only at the crossing point of these lines the resulting magnetic field is high enough to reorient the magnetization in one of the two magnetic layers - called the *free layer*. The information can be read out by exploiting the GMR (giant magnetoresistance) or TMR (tunneling magnetoresistance) effect [1].

picosecond range. However, by trying to do this new challenges appear. In particular, the write poles approach their limits in achieving strong and short field pulses for HDD. In addition, it must be noted that the increase in the density of the recorded information is achieved by using materials with very high magnetic anisotropy. In these conditions, the strength of the writing field must increase even more. There are more challenges regarding the actual writing process in which a coil is used. For example, in order to not affect the neighboring data the writing field distribution must be scaled down as the density of information increases. On top of all these challenges, it has been recently predicted that no matter how short and strong the magnetic-field pulse, magnetic recording cannot be made ever faster than about 2 picoseconds ( $2 \cdot 10^{-12}$  s) [5]. Having all this in mind, it becomes clear that the actual magnetic storage technology is fast approaching its speed limitations.

Ultrafast<sup>3</sup> laser pulses could present the key to access a new ground for the magnetic data storage technology. In fact, the laser has already proven to be able to solve some of the above mentioned problems. In particular, the need to use materials with high magnetic anisotropy, converted the conventional magnetic recording into a hybrid magnetic recording - HAMR - in which a laser beam is used to locally heat the storage medium and thus decrease its anisotropy, while the data is simultaneously written magnetically with the traditional scheme. However in this scheme the laser is only used to heat the material while, as will be shown in this thesis, its potential for data processing goes beyond simple heating.

With the recent developments of ultrafast femtosecond lasers<sup>4</sup>, the study of ultrafast magnetization dynamics has become one of the most active fields of magnetism fuelled by both scientific and technological interest. In this quest, the ultrafast optical manipulation of the magnetization promises to become a real alternative to the magnetic field pulses. Note that the time-scale offered by femtosecond laser pulses for manipulating the magnetization is orders of magnitude shorter than the magnetization reversal time in actual memory devices. Indeed, the first experimental studies on magnetization dynamics using femtosecond lasers uncovered a sub-picosecond demagnetization of magnetic metals [6]. Following this experiment, a wave of exciting results appeared: excitation of coherent spin waves via optically changing the magnetic anisotropy fields [7, 8]; optical excitation of high frequency spin oscillations ( $\sim 400$  GHz) in antiferromagnets [9, 10] and even their control via the opto-magnetic inverse Faraday effect [11]; small-angle ultrafast switching of magnetization in garnets via the opto-magnetic inverse Faraday effect [12] and laser-induced coherent spin dynamics at a frequency of several THz [13, 14]. In all these experiments, though fast, the laser excitation only brings the spins out of equilibrium (about several degrees) for a certain amount of time but does not accomplish a complete ultrafast magnetization reversal, as required for data storage. *Consequently, one of the biggest challenge in*

---

<sup>3</sup>As it was recently defined [1], ultrafast is everything what is happen on a time-scale shorter than 100 picoseconds (0.000 000 000 1 seconds).

*the field of ultrafast magnetization dynamics is to find ways to ultrafast induce (180°) magnetization reversal.*

## 1.2 Optical Excitation of Magnetic Metals

The interaction of photons with metallic systems is in general seen as a many steps process, steps that may overlap in time. As a first step, photons are absorbed by the metallic system and their energy is transferred to the electron system, creating highly energetic electrons-hole pairs ( $\sim 1$  eV). Next, these electron-hole pairs thermalize to a hot Fermi-Dirac distribution, via mechanisms such as electron-electron interactions. Since the electron heat capacity is typically one to two orders of magnitude smaller compared to that of the lattice, the excitation might lead to electron temperatures of a 1000 K ( $\sim 0.1$  eV) while the lattice temperature is still low. Subsequent exchange of the electrons energy with the phonons leads to an increase of the lattice temperature (e.g.  $\sim 100$  K) that later propagates into the environment.

This absorption of the photons is described by the Beer-Lambert-Bouguer law

$$I(d) = I_0 \exp[-\alpha(\omega)d]. \quad (1.1)$$

This gives an exponential spatial profile of the intensity in the material. Here  $\alpha$  is the optical absorption (extinction) coefficient. The optical penetration depth, defined as

$$\delta = \frac{\lambda}{4\pi k} = \alpha^{-1}, \quad (1.2)$$

represents the spatial extend over which the light is absorbed, where  $\lambda$  is the light wavelength and  $k$  is the imaginary part of the complex refractive index  $\tilde{n} = n + ik$ . In the case of metals excited by lasers with a wavelength in the visible spectra range, the optical penetration depth usually varies between 10 - 30 nm. Thus, in the experiments, in order to ensure fast and homogeneous deposition of energy within a laser pulse, the magnetic samples are typically films of nanoscale thickness.

Using photon energies in the visible range (1.5 - 3 eV) the characteristic excitation time due to the absorption of a photon with energy  $\hbar\omega$  is of order of  $\tau \sim 1/\omega \sim 1$  fs. This time is shorter than the typical laser pulse length of  $\approx 40$ -100 fs, used in the experiments. Thus, it can be stated that *the laser pulse energy is deposited in the material as electron-hole pairs on the time-scale equal to the pulse length.*

Besides the electrons and the phonons, *the presence of magnetic ordering introduces another degree of freedom in the system: the spin (or magnetization) reservoir.* For ferromagnetic materials, it is known that the increased sample temperature causes the destruction of the ferromagnetic order as shown in Figure 1.2 [1]. It follows that

<sup>4</sup>Currently, ultrafast lasers are generating pulses with a typical duration of  $10^{-13}$  to  $10^{-14}$  s, that represent some of the shortest man-made events.



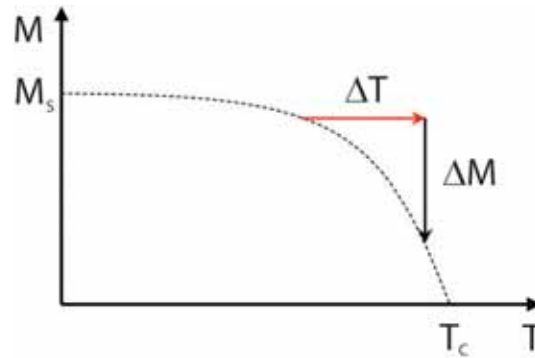


**Figure 1.2:** Schematic view of the temperature dependence of saturation magnetization  $M_s$  in a ferromagnet up to Curie temperature  $T_c$ , where the ferromagnetic order is lost. An increase of the temperature  $\Delta T$  leads to a partial demagnetization of the sample,  $\Delta M$ .

the increase in the sample temperature induced by the the optically excited electrons will also affect locally the magnetization of a metallic magnet.

### 1.3 Laser-Induced Ultrafast Demagnetization

#### Three-temperature model

Based on the above discussion it can be stated that in a metallic *ferromagnet*, the energy supplied by the photons can be stored on different time-scales in three different forms: the energy of electrons, the change of magnetization (spins) and the energy of phonons (lattice) (see Fig. 1.3). To describe the evolution in time of such system, a three-temperature model has been developed [6, 15] in which an independent temperature has been assigned to each of these reservoirs: the electron temperature  $T_e$ , the spin temperature  $T_s$  and the lattice temperature  $T_l$ . Of most importance for magnetization dynamics is the magnetization and therefore the spin reservoir. In the three-temperature model, the magnetization  $M_s$  of the metallic magnet is governed by the spin temperature  $T_s$ . However as previously discussed, the energy from the photons is deposited first, on the timescale of the laser pulse, as highly energetic electrons. Since optical transitions in general preserve the spin (in the electric dipole approximation spin-flip transitions are forbidden and thus it can be assumed that the light accesses mainly the orbital part of the electronic wave-function), only the electron system is first excited. After the electron thermalization ( $<100$  fs), the electron system reaches temperatures that are often far above the Curie temperature ( $T_c$ ) of

the ferromagnetic metal. However, they cool down below  $T_c$  very quickly by transferring the excess energy to the phonons (lattice vibration) via the electron-phonon coupling [15] and to the spin reservoir. The channels through which the spin reservoir can be reached, and the demagnetization can occur, are the electron-spin interaction and/or the spin-lattice interaction. Note that since the essence of magnetization is angular momentum, a change of magnetization will also involve a flow of angular momentum to and from the spin reservoir. A demagnetization taking place via the electron-spin interaction (*e.g.* via quasi-elastic spin-flip scattering) has the potential to be very fast (*i.e.* few 100 fs) since it has a purely electronic character. On the other hand, a demagnetization taking place via the spin-lattice interaction is expected to be a slower process (*i.e.* picosecond time-scale). This is because the energy and the angular momentum will first be transferred to the lattice via the electron-phonon coupling and later excite the spins via the spin-lattice coupling. Consequently, in order to understand the laser-induced demagnetization process we must address the following questions:

- To what extent is the spin system affected by the optically excited electron population?
- What is the dominating channel for the energy and angular momentum transfer from the electron to the spin bath and what is the characteristic time-scale for the energy equilibration between these two baths?

#### Prior work

The first experimental studies on laser-induced demagnetization of a ferromagnetic material following laser excitation were performed by Agranat *et al.* on a Ni film, with picosecond laser pulses [16]. These experiments concluded that the demagnetization process took place on a nanosecond time-scale. At the beginning of the 1990s Vaterlaus *et al.* employing more sophisticated pump-probe experiments could observe a spin relaxation time of about  $100 \pm 80$  ps for Gd [17] whereas in Fe this mechanism was deduced to take place on a time-scale between 30 ps and 20 ns [18]. Furthermore, a theoretical analysis by Hübner and Bennemann [19], on Gd demagnetization, provided a spin relaxation time of 48 ps, in good agreement with the experimental results that were also attributed to spin-lattice relaxation. As a result, around 1995, it was believed that the laser-induced demagnetization evolved mainly via the spin-lattice channel and took place on a typical time-scale of 0.1 - 1 ns.

Striking results on laser-induced demagnetization were published in 1996 by Beaurepaire *et al.* [6]. Using a time-resolved pump-probe MOKE set-up (magneto-optical Kerr effect)<sup>5</sup>, the research group at the University of Strassbourg demonstrated for the first time ultrafast demagnetization in a Ni thin film, induced by 60 fs laser pulses.

<sup>5</sup>Magneto-optical effects and pump-probe set-up are detailed in Chapter 3.

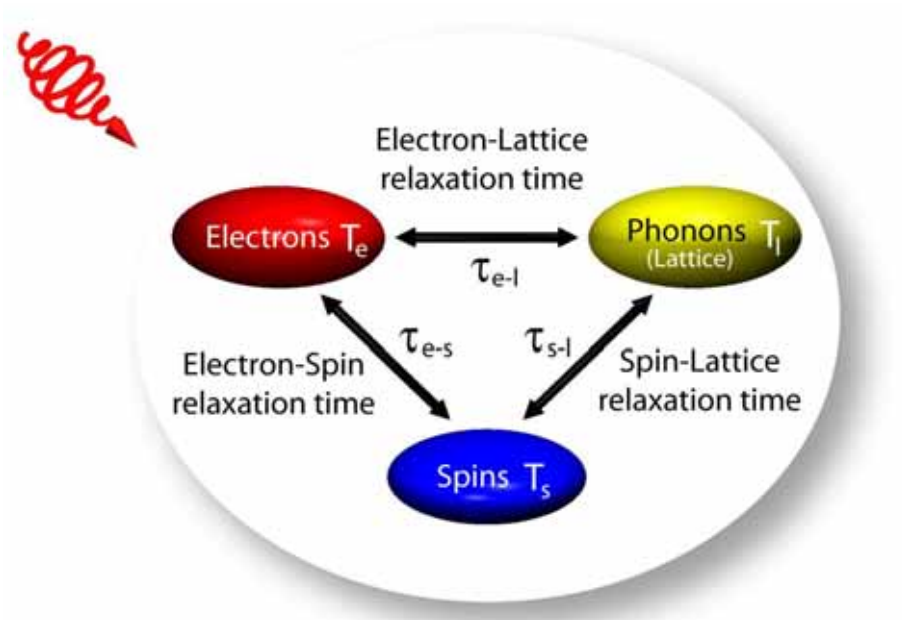


**Figure 1.3:** Schematic illustration of the heat reservoirs in a ferromagnetic material and the possible channels that can lead to changes in magnetization following laser excitation, as it is currently understood. For each reservoir a temperature has been assigned ( $T_e$ ,  $T_s$  and  $T_l$ ). Note that just after the laser excitation these temperatures may not be found in equilibrium. The equilibration of one reservoir with the other has a characteristic time  $\tau$ .

In this experiment a spin temperature  $T_s$  was introduced and found to reach a maximum after about 2 picoseconds, that was orders of magnitude faster as previously observed. This experiment was described by the three temperature model (see Fig. 1.4), where the electron-spin coupling was considered dominant over the spin-lattice relaxation in order to explain such ultrafast demagnetization. Thus, the ultrafast demagnetization was attributed to the hot nonequilibrium electron gas created by the femtosecond laser pulses that leads to an efficient electron-spin scattering process.

This demonstration of ultrafast magnetization reduction in ferromagnetic materials rapidly gained the interest of researchers across the world. This was partly fuelled by the strong scientific interest in understanding these ultrafast phenomena and partly by the tremendous impact of magnetization dynamics on the advancement of mag-

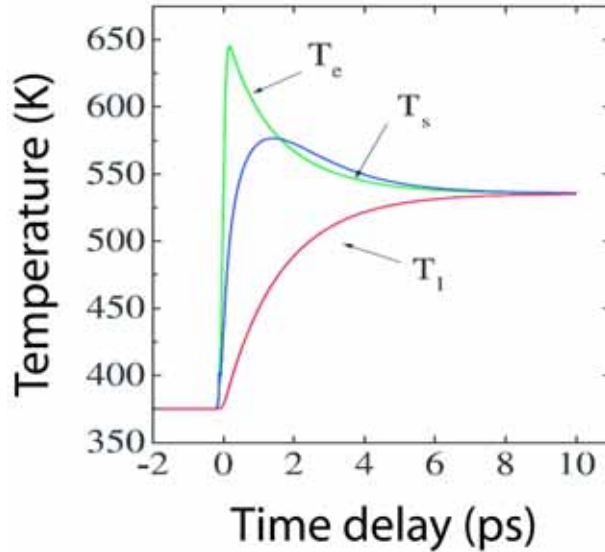


**Figure 1.4:** Temperature transients for a Ni film excited by an ultrashort laser pulses simulated by G. Zhang *et al.* in [20]. This three-temperature model favors a mechanism that transfers energy efficiently from the electrons to the spins without any major contribution from the lattice.

netic recording technologies. Hence, an avalanche of results followed the experiments of Beaupaire *et al.* Hohlfeld *et al.*, experimentally demonstrated a much faster demagnetization on the timescale of the laser pulse duration (150 fs). Furthermore, the authors showed that the classical  $M(T)$  curve can be reproduced for delay times longer than the electron thermalization time of about 280 fs, even when electrons and lattice have not reached thermal equilibrium [21]. The ultrafast drop of magnetization was also observed by Scholl *et al.* with spin-resolved two-photon photoemission on Ni films [22] and by Beaupaire *et al.* on CoPt<sub>3</sub> [23]. Using a higher time resolution (40 fs), Hohlfeld *et al.* again demonstrated an instantaneous drop of magnetization (in Ni and Co) during the pulse duration without any delay between the electron and spin dynamics, within the experimental time resolution [24]. On the other hand, some doubts about quasi-instantaneous response of the magnetization following photo-excitation, were addressed by Regensburger *et al.* [25] and Koopmans *et al.* [26]. Koopmans *et al.* argued that neither photons, nor electrons, nor phonons are responsible for the observed ultrafast demagnetization [27]. The authors concluded that because of state-filling effects, during the first picosecond the magneto-optical response does not properly reflect  $M(t)$  and thus the fast initial drop of the magneto-optical signal

observed in the previous experiments could not be unambiguously attributed to ultrafast demagnetization [26, 27]. However, a systematic experimental analysis of the MOKE response in CoPt<sub>3</sub> performed by Guidoni *et al.*, established again an almost instantaneous response of the spin system following laser excitation, where the delay between the electronic excitation and the magnetic breakdown was in the range of 50 fs [28, 29]. More recently, in order to unify all the previous observations on ultrafast demagnetization, Koopmans *et al.* have proposed a microscopic model where the electron-phonon scattering with spin flip can be considered as an additional and significant mechanism responsible for the ultrafast demagnetization [30]. The model is also supported by the experimental results of Cinchetti *et al.* [31].

Note that in all the above experiments, the attention has been mainly focussed on the laser induced heating, originating in the photon energy. The photon angular momentum is usually disregarded in the metallic magnets. Indeed, as will be demonstrated in the present work, the ultrafast demagnetization picture as currently known neglects processes that are taking place on the femtosecond time-scale during and/or following the optical excitation such as the ultrafast interaction of the photon angular momentum with the spins.

Another example of a process taking place on the femtosecond time and unknown until recently is the spin-lattice interaction, usually considered to be too weak to account for subpicosecond processes. Surprisingly enough, it has been recently demonstrated that the spin angular momentum can be quenched in  $\sim 100$  fs, following optical excitation by femtosecond laser pulses [32]. In this case, the angular momentum conservation requires a transfer of the spin angular momentum from the spin reservoir to another reservoir. The key interaction that ensures the flow of the angular momentum out of the spin system is the spin-lattice interaction. As a result, a spin-lattice relaxation time has been deduced that is orders of magnitude shorter than previously known ( $\sim 100$  ps [18, 19]). This efficient novel channel for angular momentum dissipation to the lattice is thought to originate in a *laser-enhanced spin-orbit coupling* that can be induced during the femtosecond laser excitation of a ferromagnet.

Therefore, although a large amount of work has been devoted to the field of magnetization dynamics, the main mechanisms leading to the photo-induced ultrafast demagnetization are only partially understood and still a matter of debate. In other words, it is not yet clarified how the magnetic moment of a ferromagnet can be quenched in about 100 fs, while its total angular momentum is conserved. Nevertheless, here are some conclusions that are emerging from the previous works on ultrafast magnetization dynamics and generally accepted:

- The laser-induced ultrafast demagnetization takes place on the femtosecond time-scale; a demagnetization time of about 100 - 300 fs is commonly accepted.
- The interaction of the light pulse with the ferromagnetic material can be phenomenologically described within the so-called three temperature model. In this

model the energy from the photons is deposited as *hot* electrons that rapidly thermalize via the electron-electron interaction. During this time the demagnetization occurs via interaction of the spin system with the electrons, the lattice or a combination of these two systems. After this thermalization time, the spin and electron temperatures are in equilibrium ( $T_s=T_e$ ). On a longer time-scale ( $\sim 1$  ps), the electron-phonon interactions brings the lattice and electrons to an equilibrium ( $T_e=T_l$ ). On a longer time-scale the energy relaxation is governed by the thermal diffusion.

## 1.4 Precessional Magnetization Dynamics

On a longer time-scale the demagnetization process may be followed by a directional change of the magnetization, via a precessional motion. To explain the onset of such a precession, let us first discuss the motion of a single spin in an external magnetic field.

If a spin  $\mathbf{S}$  form a nonzero angle with the direction of a magnetic field  $\mathbf{H}$ , a torque  $\mathbf{T} = -|\gamma|\mathbf{S} \times \mathbf{H}$  will act on its magnetic moment.  $\mathbf{T}$  is an axial vector perpendicular to  $\mathbf{S}$  and  $\mathbf{H}$ . The dynamic response of a magnetic moment to a torque is determined by the ratio of the magnetic moment to the angular momentum, called the gyromagnetic ratio  $\gamma$ . Based on the fundamental law of conservation of angular momentum, the change in angular momentum with time must equal the torque. Thus, one can obtain an equation for the spin motion in external magnetic field

$$\frac{d\mathbf{S}}{dt} = -|\gamma|(\mathbf{S} \times \mathbf{H}) \quad (1.3)$$

which describes a precessional motion of the spin around the magnetic field. Here  $\gamma = 2\pi g\mu_B/h$  is the gyromagnetic ratio determined by the spectroscopic splitting factor  $g$  (Lande factor or  $g$ -factor) where  $\mu_B$  is the Bohr magneton ( $\mu_B = 9.2740154 \times 10^{-24}$  J·T<sup>-1</sup>) and  $h$  is Planck's constant ( $h = 6.6260755 \times 10^{-34}$  J·s). For a single electron, where  $g = 2$  and represents only the spin of the electron, the gyromagnetic ratio is  $\approx 2\pi(28 \text{ GHz/T})$ . Thus, the electron spin precesses in a 1T field by 1 rad =  $360^\circ/2\pi = 57.3^\circ$  in 5.68 ps. In other words, *for an applied field of 1 T, an electron spin makes one full precession in 36 ps*. Here, the precession frequency is given by

$$\omega = |\gamma|\mathbf{H}. \quad (1.4)$$

On the other hand, at equilibrium, the change in angular momentum is zero and thus the torque is zero.

In ferro- and ferrimagnetic materials the magnetic moments of the single spins<sup>6</sup>  $\mathbf{S}_i$  add up to form the magnetization vector  $\mathbf{M}$ . Here  $\mathbf{M} = -|\gamma|\mathbf{A}$ , where  $\mathbf{A}$  is the total angular momentum of the system. Note, that the gyromagnetic ratio for an electron is negative and shows that *the magnetic moment and the angular momentum are antiparallel to each other*. However, as will be shown in Chapter 2, in the case of ferrimagnets the magnetic and the angular momentum may also be found parallel to each other in a certain temperature range.

Before being excited, the magnetization vector  $\mathbf{M}$  rests along a direction that is determined by the balance of all the internal and external energies acting on it. Thus, the equilibrium direction is defined by the initial effective magnetic field which is the vectorial sum of the internal anisotropy field, demagnetizing field and eventually an external applied magnetic field<sup>7</sup>. On the other hand, in a magnetic material the exchange interaction aligns the spins parallel or anti-parallel to each other. Therefore, the exchange interaction is isotropic with no preferential direction with respect to a specific axis. Consequently, it is not taken into account since usually it does not contribute to the torque on  $\mathbf{M}$ . If an external stimulus (such as a magnetic field or laser pulse) disturbs one of the above effective field constituents, on a time-scale shorter than the response time of the system, due to the torque exerted the magnetization will start to precess around the new effective field  $\mathbf{H}_{\text{eff}}$ .

The motion of the magnetization  $\mathbf{M}$  in an external magnetic field  $\mathbf{H}$  can be written in a similar way as Eq. 1.3. Yet, because the magnetization experiences not only the external magnetic field, but is also affected by magneto-crystalline anisotropy, shape anisotropy, etc., the equation of motion is expressed in terms of the effective field  $\mathbf{H}_{\text{eff}}$  comprising all these contributions

$$\frac{d\mathbf{M}}{dt} = -|\gamma|(\mathbf{M} \times \mathbf{H}_{\text{eff}}). \quad (1.5)$$

Eq. 1.5 indicates that an instantaneous application/change of a magnetic field will cause the magnetization to precess around the new effective field  $\mathbf{H}'_{\text{eff}}$ , as shown in Figure 1.5 (a).

However without any restoring force, in other words without damping, the magnetization will never align with the new effective field. This is in strong contrast with what experience tells us: depending on the strength of the applied field, the magnetic moments will eventually become aligned to this field, as is shown in Figure 1.5 (b). In fact, this phenomenon can be simply observed in a hysteresis loop where beyond some value of an externally applied field, the magnetic sample can be considered saturated. Since the precession alone will not allow the magnetization to reach that

<sup>6</sup>Orbital moments are neglected here, as they are assumed to be quenched by the ligand field. This assumption is mostly true for 3d metals and less true for rare earth ions with 4f orbitals (with the exception of Gd).

<sup>7</sup>The energies determining the orientation of the magnetization are detailed in Chapter 4.

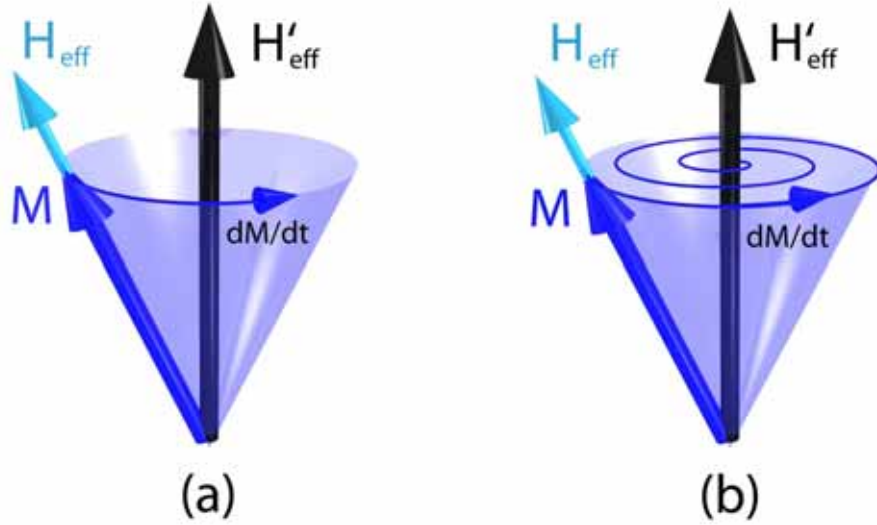


**Figure 1.5:** A schematic illustration of the magnetization precession following a sudden change of the initial effective magnetic field  $\mathbf{H}_{\text{eff}} \rightarrow \mathbf{H}'_{\text{eff}}$ . a) Constant precession without damping. b) In a real system however, due to the presence of damping, the magnetization will eventually align with the new effective magnetic field  $\mathbf{H}'_{\text{eff}}$ . The search of the magnetization for  $\mathbf{H}'_{\text{eff}}$  is in general a spiral trajectory.

limit, Eq. 1.5 must also include an extra term, a *damping term*, that will force after some time the alignment of magnetization with the applied field, via a spiral path. This damped precessional dynamics can be described by the Landau-Lifshitz-Gilbert (LLG) equation of motion [33–35]

$$\frac{d\mathbf{M}}{dt} = -|\gamma|(\mathbf{M} \times \mathbf{H}_{\text{eff}}) + \frac{\alpha}{M_s}(\mathbf{M} \times \frac{d\mathbf{M}}{dt}). \quad (1.6)$$

Here  $\alpha$  is the so-called Gilbert damping parameter (a dimensionless parameter), that stands for unspecified dissipative phenomena. For  $\alpha \ll 1$  the magnetization relaxes exponentially to its equilibrium orientation on a typical time-scale  $\tau$  given by

$$\tau = \frac{1}{\alpha\omega}. \quad (1.7)$$

During the damping process, the magnetization spirals around the field direction, this process corresponding to a variation of the angular momentum. Therefore, the angular momentum conservation implies that during this process the angular momentum must be transferred to another reservoir. Indeed, the angular momentum flows



out from the spin system ending up in the lattice, intermediated by the spin-orbit coupling. Consequently, the latter usually presents a bottleneck in the equilibration of  $M$  with the rest of the system and determines the time-scale of this process. Finally, the angular momentum is transferred to the surrounding environment.

In conclusion, the LLG equation describing the magnetization motion indicates that *a suddenly applied magnetic field exerts a torque on the magnetization vector that may result in a precession taking place on a picosecond time-scale. This precession is one of the fastest known ways of changing the magnetization direction* [1].

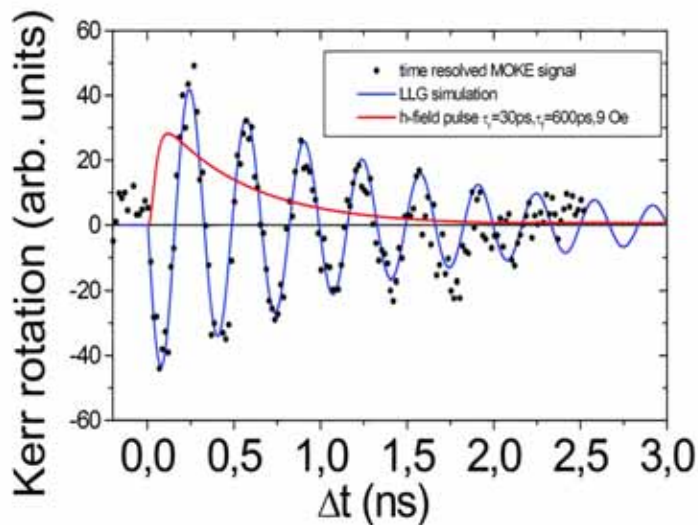


**Figure 1.6:** Precession of the magnetization of a ferromagnetic NiFe thin film triggered by a magnetic field pulse, as measured with a time-resolved pump-probe set-up employing magneto-optical effects [37].

Since the precession is taking place on the picosecond time-scale, the visualization of the entire precessional and damping process requires an experimental pump-probe set-up with a time resolution of  $10^{-12}$ s such as used in [37, 38]. A typical trace of the magnetization precession measured with a magneto-optical pump-probe set-up is shown in Figure 1.6. Such an experimental set-up, used also in the present work and detailed in Chapter 3, involves femtosecond laser pulses that may even be used to map the precession of magnetization in real space via magneto-optical effects [39]. The observation of this GHz precessional motion has been only recently accom-

plished [7, 8, 40]. With the visualization of magnetization precession made possible, coherent control of the precession on a time-scale of a few hundred picoseconds has been demonstrated by different methods based either on the shaping of magnetic field pulses [41–43] or on nonthermal photomagnetic effects [12, 44].

## 1.5 Magnetization Reversal

We will now concentrate on the magnetization reversal process. Magnetization reversal, or switching, represents the process that leads to a  $180^\circ$  reorientation of the magnetization vector with respect to its initial direction, from one stable orientation to the opposite one along the *easy axis*<sup>8</sup>. Technologically, this is one of the most important processes in magnetism that is linked to the magnetic data storage process. As we have previously discussed, the speed of storing data into a memory device is decided by how fast one can switch the magnetization. However, it is very important to stress here that *the time defining the speed of storing the information is the time required to initialize a magnetization reversal that will lead to its complete switching into the new desired direction*. In this view, as long as the magnetization reversal process is reliable, it is acceptable to have a longer settling down process such as the magnetization recovery process following laser heating [1]. As it is known today, there are only few possible ways to reverse the magnetization of a metallic magnet: *reversal in an applied magnetic field* and *reversal by spin injection*. Only theoretically demonstrated until now, *all-optical switching* is also sometimes regarded as a possible way to switch the magnetization [1].

### 1.5.1 Reversal in an Applied Magnetic Field

The conventional way to switch magnetization is by an external magnetic field (Fig. 1.7). In order to switch the magnetization, in general, the magnetic field is applied opposite to the initial magnetization orientation. However, the speed of this relatively slow process, taking place on a nanosecond timescale, is dominated in thin films either by domain nucleation processes or by domain wall propagation [45].

Using precession, the magnetization can be simply switched during half a precession by applying the external magnetic field perpendicular to the initial magnetization direction ( $\mathbf{H} \perp \mathbf{M}$ ), as shown in Figure 1.8 [36, 43, 46]. This makes *precessional magnetization switching* or *ballistic switching* very attractive because it is faster by one

---

<sup>8</sup>The so-called easy axis, is the axis along which the magnetization rests in a minimum energy state. Its origins are in the magnetic anisotropy. Thus, depending on the materials magnetic properties, the orientation of the easy axis with respect to the sample plain might vary for different magnetic materials. For data storage purposes, the perpendicular orientation is preferred today because it allows for higher data storage densities.

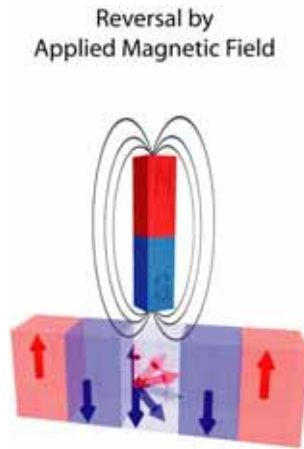


**Figure 1.7:** A schematic illustration of the field-driven reversal of perpendicular magnetic bits.

to two orders of magnitude and uses less energy to reverse the magnetization  $\mathbf{M}$  compared to the traditional methods of switching in use today [36]. Furthermore, in this scheme  $\mathbf{M}$  may be switched "back" (by rotating another  $180^\circ$  in the same direction) without changing the polarity of the magnetic field pulse but simply by applying the switching pulse again. Therefore, the only ingredients required to control the precessional switching are the strength and the duration of the field pulses. However, when approaching the time-scale of a few hundreds picoseconds, generation of sufficiently short and strong field pulses becomes extremely difficult. In general, the magnetic field pulses are generated either by electrical coils, Schottky-diodes [47] or via optical switches (so-called Auston switch) that can generate relatively short pulses [48]. Although the rise-time of a field pulse generated by an optical switch can be a few picoseconds, the decay time is  $\sim 100$  ps. In addition, the strength of such pulses is low, of the order of 0.01 T pulse-peak [41], while the reversal of magnetization in magnetic data storage media requires a field strength that exceeds 0.1 T. Consequently, although the shape of the field pulses can be adjusted using a second optical switch [37, 41], the realization of both short and high-amplitude field pulses remains a difficult task. Nevertheless, very short and strong field pulses can be generated. For example, using relativistic bunches of electrons supplied by the 3 km long Stanford Linear Accelerator in California (SLAC), magnetic field pulses as short as 2.3 ps with a maximum strength of about 3 T have been generated and employed in the study of magnetic samples [1, 56]. Yet, such magnetic field pulse generators are far too exotic from the point of view of applications.

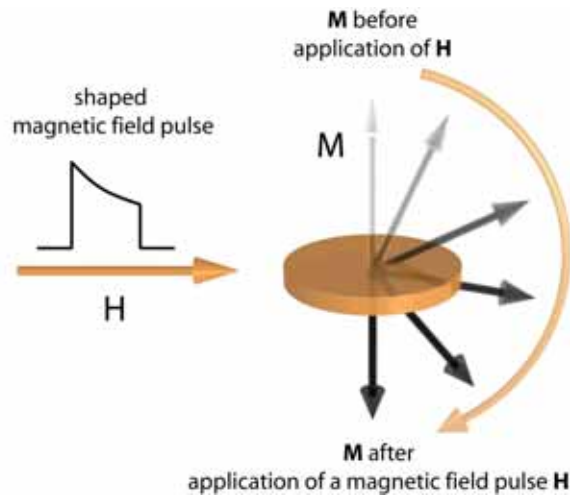


**Figure 1.8:** Schematic illustration of the precessional magnetization switching. Ultrafast switching may occur when the magnetic field  $H$  is applied perpendicular on the magnetization  $M$ . If the magnetic field  $H$  is pulsed and precisely timed  $M$  may be switched in a time equal to half a precession. Alternatively, when the field pulse lasts too long,  $M$  may be switched back to the initial direction. A method for shaping in time the magnetic field pulses, to obtain  $180^\circ$  magnetization reversal, is described in Ref. [41].

New ultrafast field-driven alternatives to the precessional switching are also currently being developed that might one day reach the sub-picosecond time-scale. For example, ultrafast magnetic switching of a vortex core has recently been demonstrated [49]. Micromagnetic simulations demonstrated that such vortex core reversal is mediated by a rapid sequence of vortex-antivortex pair creation and annihilation subprocesses. This exchange field driven switching took about 40 ps, which is about 5 times faster than the current attainable time in precessional switching, and opens a new way for ultrafast field-driven magnetization reversal.

In hard magnetic materials, where the available field strength alone might not be able to reverse the magnetization, a laser beam is employed to help the switching in an applied field, by delivering localized heating to the material [50]. It is anticipated that this *heat assisted magnetization reversal* (HAMR) combined with patterned media approaches such as self-organized magnetic arrays will push the magnetic recording density beyond 50 Tb/in<sup>2</sup> [51]. Finally, to further lower the field strength required to switch magnetization the thermally assisted technique can be also combined with schemes such as *exchange springs* [52–55].

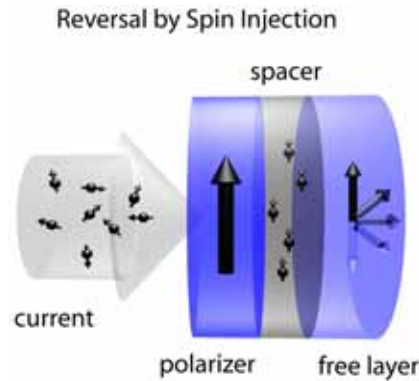


**Figure 1.9:** Magnetization reversal by spin injection.

### 1.5.2 Reversal by Spin Injection

Spin-polarized currents provide a new method for manipulating magnetic systems at the nanoscale level without the application of magnetic fields, utilizing the short range and strong electronic exchange interaction. A schematic representation of a spin injection structure is shown in Figure 1.9. Here, a charge current of random spin polarization is injected through a pillar composed of different thin layers. A ferromagnetic layer with fixed magnetization direction, the polarizer (in practice fixed by exchange bias), creates a spin polarized current as the injected current is passing through this layer. Next, the spin polarized current enters the free layer and generates a torque on the magnetization of this second ferromagnetic film. At sufficiently high current densities the spin current is capable of switching the magnetization of the free layer. Note that the two magnetic layers, the polarizer and the free layer are magnetically independent, separated by a non-magnetic interlayer (*e.g.* copper). If the direction of the injected random spin polarization current is reversed, now entering through the free layer, a spin accumulation builds up in front of the polarizer by reflection of spins from the polarizer. These spins are oriented opposite to the transmitted spins and being reflected they travel back through the free layer and can switch its magnetization back to the original state. This new magnetization reversal technique is expected to lead to future data-storage and information-processing applications [57].

In theory, the switching speed of this technique is determined only by the duration and amplitude of the current pulse [1] because the transfer of the angular momentum from the spin polarized pulse to the magnetic moments of the sample would be direct, avoiding the spin-lattice relaxation bottleneck. On the other hand, in practice such a

switching has been only demonstrated on the hundreds of picoseconds time-scale, for current densities above a few  $10^6$  A cm<sup>-2</sup> [58, 59]. Furthermore, since faster switching implies shorter current pulses and thus higher amplitude currents, this technique may run into power limitations.

### 1.5.3 All-Optical Switching

Although in this thesis, all-optical switching of metallic magnets is demonstrated as one of the possible ways of reversing the magnetization, it must be stressed that until very recently this was considered only a hypothetical method [1].

Generally called all-optical switching, this technique refers to a method of reversing magnetization in a ferromagnet simply by circularly polarized light (see Fig. 1.10), where the magnetization direction is controlled by the light helicity. In particular, the direction of the angular momentum of the photons would set the magnetization direction. In fact, this process could be seen as similar to magnetization reversal by spin injection. The only difference is that now, the angular momentum is supplied by the circularly polarized photons instead of the polarized electrons.

It was first proposed by Hübner and Zhang that an ultrafast laser-induced magnetic response (within 10 fs), such as observed in the experiments on Ni (detailed in Section 1.3), can be explained by the dephasing induced by the cooperative effect of spin-orbit coupling and the external laser field [60]. On theoretical grounds, the authors showed that such effect may even lead to a femtosecond all-optical magnetization reversal that would be based on the application of a shaped ultrashort laser pulse of certain frequency, duration and polarization [61]. However, in this computation unrealistic high laser fields were involved. Simple estimates of Koopmans *et al.* [26, 27] show that the number of photons in real experiments on metallic magnets is far too low to be of any significance and thus it was concluded that a direct photoinduced mechanism can not explain the ultrafast demagnetization observed in ferromagnets. In particular, the calculation was performed for a ferromagnetic nickel in an epitaxial Cu/Ni(13 nm)/Cu structure. Previous experiment performed on this sample indicates a 5 % demagnetization of the Ni sample due to laser excitation at a photon energy of about 1.7 eV [26]. In this experiment 1.6 nJ pulse energy was focused to a 10  $\mu$ m diameter spot. Since ferromagnetic Ni carries  $0.6 \mu_B$  per atom the observed demagnetization represented a loss of magnetic moment of  $0.03 \mu_B$  per atom. Based on the above mentioned experimental conditions one can obtain the number of photons in the laser pulse ( $\sim 0.5 \cdot 10^{10}$  photons) and the number of the atoms that can be found in the irradiated volume ( $\sim 10^{11}$  atoms). This indicates about 0.05 photons available in the laser pulse for every Ni atom. Taking also into account a 20 % absorption of the photons in the film leads to 0.01 photons per atom. Furthermore, in the ferromagnetic transition metals, the quenching of the orbital momentum by the crystal field leads to a dichroism of the order of 0.01. This effect added

### All-Optical Magnetization Reversal by Circularly Polarized Light

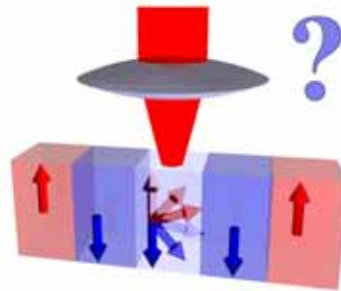


**Figure 1.10:** All-optical magnetization reversal scheme. Here, the direction of the magnetization of a magnetic bit is controlled via the helicity of light. Note that this is a technique that was subject of debate in the past years and generally believed being impossible.

to the above result indicates a demagnetization due to the angular momentum of the photons of only  $0.0001 \mu_B$  per atom, which is two orders of magnitude smaller than that observed in the experiment. Therefore, if a photon transfers a full quantum of angular momentum to or from the system, the above result shows that the all-optical switching must be a very weak effect.

In addition, an extra obstacle for the reliability of the all-optical magnetization reversal might be represented by the electron-electron scattering events that follow the laser excitation in metals. In particular, the electron states in solids have a finite life time due to the transitions induced by the electron-electron scattering. For example, the lifetime for states at about 1 eV above the Fermi energy in Co is only a few fs [62], much shorter than the typical pulse duration of  $\sim 50$  fs used in the experiments. It is expected that the relaxation of the excited states in electron-electron scattering must lead to the destruction of the spin coherence. This would make the coherent manipulation of magnetization by  $\sim 100$  fs laser pulses difficult if not impossible [1].

Summarizing the above presented issues one can formulate some conclusions that represent the state of the art of all-optical switching of only few years ago:

- In real experiments on ferromagnets, there are not enough photons to lead to a significant change of the magnetization [26];
- The all optical switching is quite difficult in metals, where electron-electron scattering appears to make coherent manipulation of the magnetization difficult if not impossible [1].

Thus, an important role for the photon angular momentum was generally considered highly unlikely in metallic magnets, and the switching of magnets by light on tens of femtoseconds time-scales remained a challenge: "...*completely coherent control of magnetization by optical means would be worthwhile dreaming of.*" [27]. But, is the photon transferring only energy to the metallic magnet or is there also a nonthermal action of the angular momentum of the photons on the spin system? A clear answer to this question is given in Chapter 5 of this thesis.

In fact, the possibility of all-optical switching by femtosecond laser pulses is entirely excluded if we also take into account the previously mentioned SLAC experiment, indicating that deterministic magnetization reversal has a natural limit on the picosecond time-scale [5, 56]. This experiment employed some of the shortest and most powerful magnetic field pulses available on Earth, with a strength of about 3 Tesla and a duration of about 2 ps, generated by a tightly packed bunch of electrons. These field pulses were used to excite a 14-nm-thick film of perpendicular magnetic recording media of the CoCrPt-type. Since the sample was magnetized perpendicular, the in-plane generated field pulses were oriented perpendicular to  $\mathbf{M}$ . In these experimental conditions, with the correctly timed pulses, it was expected that the first magnetic field pulse will switch  $\mathbf{M}$  to the opposite direction, via precessional switching, while every second pulse will switch  $\mathbf{M}$  back to its initial state. In order to analyze the effects of such strong and short magnetic field pulses on the magnetization, the sample was exposed to successive electron bunches. Later, the pattern of magnetic domains produced by the field pulses was imaged by magneto-optical microscopy. The results were not as expected. Instead of sharp magnetic domains oriented up or down depending on the number of the field pulses, the results were showing a deterioration in the sharpness of the boundaries that were separating the domains. The deterioration was increasing with the number of the field pulses to which the sample was exposed. Obviously, this non-uniformity that evolves with the number of pulses is highly undesirable in data storage applications, where the switching must happen in the same way regardless of the number of the writing cycle. This chaotic switching was attributed to the non-uniform precessional modes excited by the very strong magnetic field pulses used in the experiment. As a result, since 2004, a few picoseconds was believed to be the speed limit of magnetic recording devices, beyond which the reversal mechanism becomes a non-deterministic process [5, 63–66]. As a consequence, fundamental questions were born from here: Have we really found the natural (or practical) limit for the magnetization reversal? Can we not switch magnetization faster than a picosecond? Besides its fundamental importance, the answer to these questions will have a tremendous impact on the future of the magnetic data storage technology. A clear answer to these questions is given in this thesis.



## 1.6 Overview of This Thesis

We have seen that today the magnetization dynamics on ultrafast time-scales is one of the most exciting issues in magnetism. Driven by strong fundamental and technological interest this field advanced dramatically in recent years, from the nanosecond to the picosecond and even further to the femtosecond time-scale, leaving far behind the time-scale of processing information in the today's electronics. However, as we have seen in this introductory chapter, with this fast advancement, elementary questions now arise with crucial impact on the understanding of this new field of ultrafast magnetization dynamics.

As stated above, one of the most important question in the field of ultrafast magnetization dynamics is: *Can we ever switch the magnetization on a sub-picosecond time-scale, in a deterministic way? And if so, how?*

In this thesis *two different ways* of reversing the magnetization faster than picoseconds are experimentally demonstrated, thus breaking through the previously imposed magnetic recording speed limit.

The experiments were performed on ferrimagnetic rare-earth-transition-metal amorphous alloys, materials widely used as data storage media in magnetic memory devices. The magnetic and magneto-optical properties of these metallic magnets are detailed in Chapter 2. The main experimental techniques used to investigate and control the magnetization dynamics on the picosecond and femtosecond time-scales are presented in Chapter 3.

The experimental results are presented in the last two chapters of this thesis. More specifically, Chapter 4 first presents the crucial role of the angular momentum compensation point of a ferrimagnet for obtaining high-speed and strongly damped spin dynamics. In the second part of Chapter 4 we go one step further and use the knowledge accumulated about the angular momentum compensation. In particular, by ultrafast heating the ferrimagnet across its compensation points, under an applied magnetic field, a sub-picosecond magnetization reversal is experimentally demonstrated for the first time.

In Chapter 5 it is first demonstrated that in a metallic magnet there is an ultrafast nonthermal coupling between the spins and the angular momentum of the photons. In other words, it is shown that the circularly polarized photons act on the magnetization as an effective magnetic field. Although the observed effect was relatively weak, under the proper conditions, it could be fully exploited. As a result, in the second part of Chapter 5 we experimentally demonstrate deterministic all-optical magnetic recording by femtosecond circularly polarized pulses. In contrast to the ultrafast magnetization reversal demonstrated in Chapter 4, this sub-picosecond magnetization reversal is induced simply by light and does not require the application of a magnetic field.

## References

- [1] J. Stöhr, H. C. Siegmann, *Magnetism. From fundamentals to Nanoscale Dynamics* (Springer-Verlag, Berlin, 2006).
- [2] A. Taratrin, S. Yuan, and V. Nikitin, *J. Appl. Phys.* **93**, 6444, (2003).
- [3] S. W. Yuan, E. Lee, W. Hsiao, H. Santini, H. Lam, G. Sui, T. Lam, Y. Luo, M. Madison, V. Nikitin, B. Webb, Y. Shen, M. Ramasubramanian, J. Jarratt, R. Hsiao, T. Harris, S. Sahami, N. Robertson, D. Freitas, Y. Freitas, Y. Hsu, M. Williams, A. Taratrin, J. Heidemann, R. Simmons, and J. Smyth, *IEEE Trans. Magn.* **38**, 1873, 2002.
- [4] <http://www.mram-info.com/history>
- [5] C. H. Back and D. Pescia, *Nature* **428**, 808 (2004).
- [6] E. Beaurepaire, J.-C. Merle, A. Daunois, and J.-Y. Bigot, *Phys. Rev. Lett.* **76**, 4250 (1996).
- [7] G. Ju, A. V. Nurmikko, R. F. C. Farrow, R. F. Marks, M. J. Carey, and B. A. Gurney, *Phys. Rev. Lett.* **82**, 3705 (1999).
- [8] M. van Kampen, C. Jozsa, J. T. Kohlhepp, P. LeClair, L. Lagae, W. J. M. de Jonge, and B. Koopmans, *Phys. Rev. Lett.* **88**, 227201 (2002).
- [9] A. V. Kimel, A. Kirilyuk, A. Tsvetkov, R. V. Pisarev, and Th. Rasing, *Nature* **429**, 850 (2004).
- [10] A. V. Kimel, C. D. Stanciu, P. A. Usachev, R. V. Pisarev, V. N. Gridnev, A. Kirilyuk, and Th. Rasing, *Phys. Rev. B* **74**, 060403(R) (2006).
- [11] A. V. Kimel, A. Kirilyuk, P. A. Usachev, R. V. Pisarev, A. M. Balbashov, and Th. Rasing, *Nature* **435**, 655 (2005).
- [12] F. Hansteen, A. Kimel, A. Kirilyuk, and Th. Rasing, *Phys. Rev. Lett.* **95**, 047402 (2005).
- [13] A. Melnikov, I. Radu, U. Bovensiepen, O. Krupin, K. Starke, E. Matthias, and M. Wolf, *Phys. Rev. Lett.* **91**, 227403 (2003).
- [14] I. Radu, Ph.D. thesis, Berlin, Germany, 2006.
- [15] Guoping Zhang, Wolfgang Hübner, Eric Beaurepaire, and Jean-Yves Bigot, *Topics of Applied Physics: Spin Dynamics in Confined Magnetic Structures I*, edited by B. Hillebrands and K. Ounadjela (Springer-Verlag Berlin Heidelberg 2002), pp. 245-290.

- 
- [16] M. Agranat, S. Ashikov, A. Granovskii, and G. Rukmann, *Sov. Phys. JETP* **59**, 804 (1984).
- [17] A. Vaterlaus, T. Beutler, F. Meier, *Phys. Rev. Lett.* **67**, 3314 (1991).
- [18] A. Vaterlaus, T. Beutler, D. Guarisco, M. Lutz, F. Meier, *Phys. Rev. B* **46**, 5280 (1992).
- [19] W. Hübner, K. H. Bennemann, *Phys. Rev. B* **53**, 3422 (1996).
- [20] B. Hillebrands and K. Ounadjela (editors), *Topics of Applied Physics: Spin Dynamics in Confined Magnetic Structures I*, (Springer-Verlag Berlin Heidelberg 2002).
- [21] J. Hohlfeld, E. Matthias, R. Knorren, and K. H. Bennemann, *Phys. Rev. Lett.* **78**, 4861 (1997).
- [22] A. Scholl, L. Baumgarten, R. Jacquemin, and W. Eberhardt, *Phys. Rev. Lett.* **79**, 5146 (1997).
- [23] E. Beaurepaire, M. Maret, V. Halté, J.-C. Merle, A. Daunois, J.-Y. Bigot, *Phys. Rev.* **58**, 12134 (1998).
- [24] J. Hohlfeld, J. Gädde, U. Conrad, O. Dühr, G. Korn, E. Matthias, *Applied Physics B Lasers and Optics* **68**, 505 (1999).
- [25] H. Regensburger, R. Vollmer, J. Kirschner, *Phys. Rev. B* **61**, 14716 (2000).
- [26] B. Koopmans, M. van Kampen, J.T. Kohlhepp, W. J. M. de Jonge, *Phys. Rev. Lett.* **85**, 844 (2000).
- [27] B. Koopmans in *Topics of Applied Physics: Spin Dynamics in Confined Magnetic Structures II*, edited by B. Hillebrands and K. Ounadjela (Springer-Verlag Berlin Heidelberg 2003).
- [28] Luca Guidoni, Eric Beaurepaire, and Jean-Yves Bigot, *Phys. Rev. Lett.* **89**, 017401, (2002).
- [29] J.-Y. Bigot, L. Guidoni, E. Beaurepaire, and P. N. Saeta, *Phys. Rev. Lett.* **93**, 77401, (2004)
- [30] B. Koopmans, J. J. M. Ruigrok, F. Dalla Longa, and W. J. M. de Jonge, *Phys. Rev. Lett.* **95**, 267207 (2005).
- [31] M. Cinchetti, M. Sánchez Albaneda, D. Hoffmann, T. Roth, J.-P. Wüstenberg, M. Krauß, O. Andreyev, H. C. Schneider, M. Bauer, and M. Aeschlimann, *Phys. Rev. Lett.* **97**, 177201 (2006).

- 
- [32] C. Stamm, T. Kachel, N. Pontius, R. Mitzner, T. Quast, K. Holldack, S. Khan, C. Lupulescu, E. F. Aziz, M. Wietstruk, H. A. Dürr and W. Eberhardt, *Nature Materials* **6**, 740 (2007).
- [33] L. Landau and E. Lifshitz, *Phys. Z. Sowjetunion.* **8**, 153 (1935).
- [34] T. L. Gilbert, *Phys. Rev.* **100**, 1243, (1955).
- [35] Thomas L. Gilbert, *IEEE Trans. Magn.* **40**, 3443 (2004).
- [36] B. Hillebrands and K. Ounadjela (editors), *Topics of Applied Physics: Spin Dynamics in Confined Magnetic Structures II*, (Springer-Verlag Berlin Heidelberg 2003).
- [37] T. Gerrits, Ph.D. thesis, Nijmegen, The Netherlands, 2004.
- [38] F. Hansteen, Ph.D. thesis, Nijmegen, The Netherlands, 2006.
- [39] M. Vomir, L. H. F. Andrade, L. Guidoni, E. Beaurepaire, and J.-Y. Bigot, *Phys. Rev. Lett.* **94**, 237601 (2005).
- [40] B. C. Choi, M. Belov, W. K. Hiebert, G. E. Ballentine, and M. R. Freeman, *Phys. Rev. Lett.* **86**, 728 (2001).
- [41] T. Gerrits, H. A. M. van den Berg, J. Hohlfeld, L. Bär, and Th. Rasing, *Nature (London)* **418**, 509 (2002).
- [42] S. Kaka and S. E. Russek, *Appl. Phys. Lett.* **80**, 2958 (2002).
- [43] H. W. Schumacher, C. Chappert, P. Crozat, R. C. Sousa, P. P. Freitas, J. Militat, J. Fassbender, and B. Hillebrands, *Phys. Rev. Lett.* **90**, 017201 (2003).
- [44] F. Hansteen, A. Kimel, A. Kirilyuk, and Th. Rasing, *Phys. Rev. B* **73**, 014421 (2006).
- [45] J. Pommier, P. Meyer, G. Pénissard, J. Ferré, P. Bruno, and D. Renard, *Phys. Rev. Lett.* **65**, 2054 (1990).
- [46] C. H. Back, D. Weller, J. Heidmann, D. Mauri, D. Guarisco, E. L. Garwin, and H. C. Siegmann, *Phys. Rev. Lett.* **81**, 3251 (1998).
- [47] Y. Acreman, C. H. Back, M. Buess, D. Pescia, and V. Pokrovsky, *Appl. Phys. Lett.* **79**, 2228 (2001).
- [48] D. H. Auston, *IEEE J. Quantum Electron.* **QE-19**, 639 (1983).
- [49] R. Hertel, S. Gliga, M. Fähnle, and C. M. Schneider, *Phys. Rev. Lett.* **98**, 117201 (2007).

- [50] Terry W McDaniel, *J. Phys.: Condens. Matter* **17**, R315 (2005).
- [51] M. H. Kryder, talk at FAST, Monterey 2002.
- [52] E. F. Kneller and R. Hawig, *IEEE Trans. Magn.* **27**, 3588 (1991).
- [53] O. Hellwig, J. B. Kortright, K. Takano, and E. E. Fullerton, *Phys. Rev. B* **62**, 11694 (2000).
- [54] E. E. Fullerton, J. S. Jiang, M. Grimsditch, C. H. Sowers, and S. D. Bader, *Phys. Rev. B* **58**, 12193 (1998).
- [55] Jan-Ulrich Thiele, Stefan Maat, and Eric E. Fullerton, *Appl. Phys. Lett.* **82**, 2859 (2003).
- [56] I. Tudosa, C. Stamm, A. B. Kashuba, F. King, H. C. Siegmann, J. Stohr, G. Ju, B. Lu, D. Weller, *Nature* **428**, 831 (2004).
- [57] Claude Chappert, Albert Fert, and Frédéric Nguyen van Dau, *Nature Materials* **6**, 813 (2007).
- [58] A. A. Tulapurkar, T. Devolder, K. Yagami, P. Crozat, C. Chappert, A. Fukushima, Y. Suzuki, *Appl. Phys. Lett.* **85**, 5358 (2004).
- [59] M. Nakayama, T. Kai, N. Shimomura, M. Amano, E. Kitagawa, T. Nagase, M. Yoshikawa, T. Kishi, S. Ikegawa, and H. Yoda, *J. Appl. Phys.* **103**, 07A710 (2008).
- [60] G.P. Zhang, W. Hübner, *Phys. Rev. Lett.* **85**, 3025 (1999).
- [61] R. Gomez-Abal, O. Ney, K. Satitkovitchai, and W. Hübner, *Phys. Rev. Lett.* **92**, 227402 (2004).
- [62] M. Aeschlimann, M. Bauer, S. Pawlik, W. Weber, R. Burgermeister, D. Oberli, and H. C. Siegmann, *Phys. Rev. Lett.* **79**, 5158 (1997).
- [63] [http : //physicsworld.com/cws/article/news/19401](http://physicsworld.com/cws/article/news/19401)
- [64] [http : //www.innovations-report.com/html/reports/physics\\_astronomy/report-28436.html](http://www.innovations-report.com/html/reports/physics_astronomy/report-28436.html)
- [65] [http : //www.newscientist.com/article.ns?id=dn4905](http://www.newscientist.com/article.ns?id=dn4905)
- [66] [http : //www.sciencedaily.com/releases/2004/04/040426054807.htm](http://www.sciencedaily.com/releases/2004/04/040426054807.htm)

## CHAPTER 2

---

### Rare Earth - Transition Metal Amorphous Alloys

---

#### 2.1 Introduction

**D**uring the last 30 years, rare earth - transition metal (RE-TM) amorphous alloys have been the subject of extensive research from both a fundamental and an application point of view [1–35]. The main reason for this intensive study has been the high relevance of these materials for the magnetic and magneto-optical recording technology. Although developments indicated that also other materials are suitable for magneto-optical (MO) recording, the first MO commercial system incorporated media based on RE-TM alloy thin films. The special magnetic and magneto-optical properties of these amorphous alloys have been discovered in 1972 by a team of researchers at IBM, lead by R. J. Gambino [1]. To underline the high importance of this discovery for technology, in 1995 this research team was awarded the National Medal of Technology of the USA. Generating a worldwide \$2 billion market for erasable optical storage, these magnetic materials made possible today's magneto-optical disk storage industry.

RE-TM alloys advanced even more in the recent years, moving towards the Magnetic Random Access Memory (MRAM) technology. MRAM called "the ideal memory" or the "holy-grail of memory" is a new memory concept that promises to provide non-volatile, low-power, high speed and low-cost memory. Here, a free layer consisting of RE-TM alloys promises a constructive impact on the power consumption and cost of the memory, bringing MRAM to a competitive level [30, 32, 35].

## 2.2 Magnetic Properties

The magnetic properties of RE-TM alloys strongly vary depending on the RE component and its concentration. The magnetic moment of an RE atom is nearly completely built up by the localized  $f$ -electrons. Depending on these electrons, the magnetic moment of the RE component can couple ferromagnetically or antiferromagnetically with the TM. In particular, the so called light RE atoms (La, Ce, Pr, Nd, Pm, Sm and Eu), with less than half-filled  $f$ -electrons, couple ferromagnetically with TM atoms such as Fe, Co or Ni. These light RE-TM alloys are therefore used in permanent magnets. On the other hand, the heavy RE atoms (Gd, Tb, Dy, Ho, Er, Tm, Yb and Lu), with more than half filled  $f$ -electrons, couple antiferromagnetically with the TM atoms. The ferromagnetic or antiferromagnetic coupling can be understood from Hund's rule. Hund's rule states that for less than half filled shells the orbital moment and spin moment couple antiparallel ( $J=L-S$ ) while they couple parallel ( $J=L+S$ ) in the second half of the series [21]. Since the orbital moment is always greater than the spin moment for the light RE elements, the total moment ends up antiparallel to the spin moment. Because the  $4f$  spin moment couples antiparallel to the TM moment (mediated through positive intra-atomic  $4f-5d$  and negative inter-atomic  $5d-3d$  exchange [23]) the total moment of the RE couples parallel to the TM moment for the light REs and antiparallel for the heavy REs. As the magnetic moment magnitude of the two different magnetic sublattices (RE and TM) is different, the antiferromagnetic coupling gives rise to a *ferrimagnetic* structure. Along with several other properties, the ferrimagnetic structure is one of the essential characteristics of these alloys for magneto-optical recording, which at the same time is the source for a wide variety of interesting magnetic phenomena [17, 21, 33, 35]. This is one of the reasons why in this thesis we focus our attention on the ferrimagnetic RE-TM alloys.

As is the case for most of the RE-TM alloys studied in this thesis, at low temperatures the magnetization of the RE magnetic sublattice is far larger than that of the TM sublattice, as shown in Figure 2.1. When the sublattices of a ferrimagnet are strongly coupled to each other, they all have the same Curie temperature  $T_c$  which means that the phase transition between the ferrimagnetic and paramagnetic state occurs at the same temperature for both sublattices. However, due to the different origin of the magnetic moment of the two sublattices (the magnetic moment of the TM sublattice originates in the itinerant  $3d$  electronic shell while the magnetic moment of the RE sublattices is given mainly by the localized  $4f$  shell), there is a difference in the temperature dependence of the RE and TM component,  $M_{RE}$  and  $M_{TM}$ . In RE, the localization of the  $4f$  moments causes  $M_{RE}$  to decrease faster than  $M_{TM}$  with increasing temperature, because there is a reduced exchange with the neighbors for the RE sublattice. This is also the reason why at room temperature all pure RE materials are paramagnetic. The different temperature dependence of the two sublattices may lead at a certain temperature to an equivalence of the two sublattices

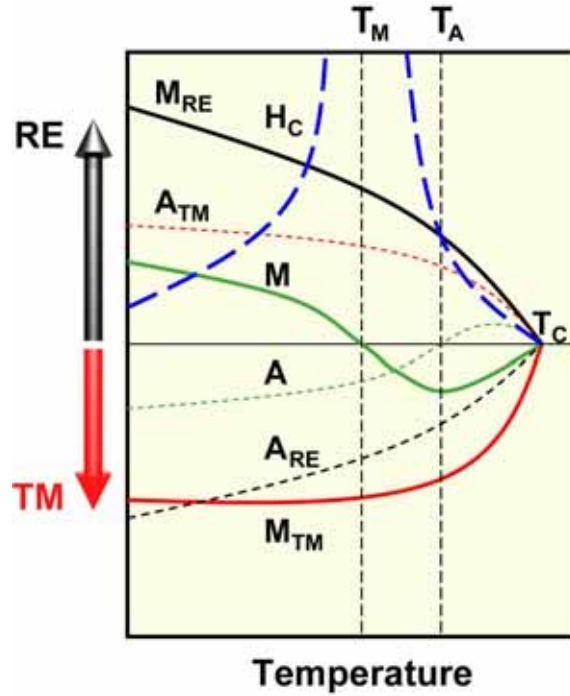


**Figure 2.1:** A qualitative description of the temperature dependence of: Magnetization ( $M$ ) and angular momentum ( $A$ ) of the sublattices versus temperature in a ferrimagnetic RE-TM alloy with magnetization compensation temperature ( $T_M$ ) and angular momentum compensation temperature ( $T_A$ ). Here ( $H_c$ ) represent the coercive field.

magnetizations, therefore to a cancellation of the net magnetic moment

$$M(T_M) = M_{RE}(T_M) + M_{TM}(T_M) = 0. \quad (2.1)$$

This feature, present in some ferrimagnets leads to the so called *magnetization compensation temperature*,  $T_M$ . At this temperature the strength of the magnetic field required to switch the magnetization (coercive field -  $H_c$ ) shows a divergence (Fig. 2.1). The reason for the occurrence of this divergence is that in RE-TM, the intrinsic magnetic anisotropy  $K_u$  (that is a measure of how strong the spins are locked to a specific lattice direction)<sup>1</sup> is only weakly dependent on temperature over the  $T_M$ , while the net magnetic moment  $M_s$  is strongly reduced [3]. Note that the strength

<sup>1</sup>The magnetic anisotropy is discussed in more details in Subsection 4.1.4.



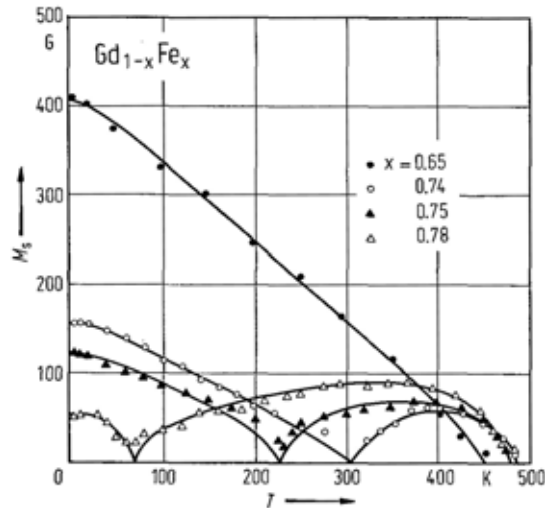


**Figure 2.2:** Saturation magnetization vs. temperature for the amorphous alloy GdFe with various compositions (from [24]). Note that the addition of Gd increases the temperature of magnetization compensation while reducing the Curie temperature (due to reduced Fe-Fe exchange interaction).

of the coercive field is proportional to  $2K_u/M_s$  [25]. In other words, at  $T_M$  there is no magnetic moment that can be reversed by the applied magnetic field since the net magnetic moment vanishes.

The magnetization compensation point, represents a real advantage of these materials. Since at this point the strength of the field required to switch magnetization diverges, the recorded data stored around this temperature is protected from stray magnetic fields and unwanted erasure. In addition, this feature preserves uniform magnetic alignment in the perpendicular direction by preventing the magnetization from breaking into magnetic domains. The variation with temperature of the sublattices magnetization,  $M_{RE}$  and  $M_{TM}$  in Figure 2.1, suggests that  $T_M$  may be set to any required value by varying the RE and TM concentrations, and thus  $M_{RE}$  and  $M_{TM}$ . Therefore, the great advantage of these materials is that by simply changing the composition of the RE and TM components, one can vary this compensation temperature. This effect is clearly seen in Figure 2.2. In this way  $T_M$  can be brought in the vicinity of ambient temperature by a proper choice of the composition, as required for safe data storage. While achieving sufficient stability of the magnetic bits at room

temperature, the strongly decreasing  $H_c$  with temperature offers the possibility of reversing the magnetization at elevated temperatures by means of a moderate field strength.

As mentioned in Section 1.4, the magnetic system is also characterized by angular momentum that is coupled antiparallel with the magnetization, due to the negative charge of the electron. Similarly to the magnetization compensation point, in ferrimagnetic RE-TM (with  $T_M$ ), there is also an *angular momentum compensation temperature* ( $T_A$ ) where the angular momentum of the two sublattices,  $A_{RE}$  and  $A_{TM}$ , cancel each other, resulting therefore in a vanishing net angular momentum

$$\mathbf{A}(T_A) = \mathbf{A}_{RE}(T_A) + \mathbf{A}_{TM}(T_A) = 0. \quad (2.2)$$

The difference in temperature between  $T_M$  and  $T_A$ , as shown in Figure 2.1, is a result of the difference between the gyromagnetic ratios (the ratio of the magnetization to the angular momentum) of the RE and TM sublattice. As the difference between the two gyromagnetic ratios increases, also the splitting in temperature between the two compensation temperatures increases. Therefore, by changing the RE and TM elements or by doping the RE-TM alloy with other elements,  $T_A$  can be changed with respect to  $T_M$ . This flexibility is important since, as will be shown in the present work (Chapter 4), the angular momentum compensation temperature is a crucial point for achieving high speed writing and thus information writing in data storage devices based on RE-TM alloys.

For a certain composition range, thin-films of amorphous RE-TM alloys exhibit positive perpendicular magnetic anisotropy ( $K_{\perp}$ ) [13]. In other words, the low net magnetization  $M_s$  resulting from the ferrimagnetic structure and the relatively strong positive uniaxial magnetic anisotropy ( $K_u$ ) lead to a quality factor  $Q > 1$ , where  $Q = K_u/2\pi M_s^2$ . Here  $Q > 1$  indicates a dominant  $K_u$  over the demagnetizing energy that tries to pull the magnetization in the plane of the thin film. Therefore the film magnetization prefers to lie normal to the film plane were

$$K_{\perp} = K_u - 2\pi M_s. \quad (2.3)$$

As will be shown in Section 2.5, the high magnetic anisotropy and low  $M_s$  also gives rectangular hysteresis loops (in the applied magnetic field perpendicular to the film plane) that implies good switching characteristics: the remanent magnetization and the saturation magnetization are nearly equal. Consequently, once the magnetization has been saturated in one direction, removing or reducing the applied magnetic field does not lead to the reduction of the magnetic moment. All these great properties, that are very suitable for magnetic recording, can be found in RE-TM alloys such as GdFeCo, TbFeCo, DyFeCo and others.

### 2.3 Optical and Magneto-Optical Properties

The perpendicular magnetic anisotropy and large magneto-optical effect that characterizes many of the RE-TM alloys makes them particularly useful for Faraday (or polar Kerr) effect readout, while the amorphous nature of the films eliminates a significant source of noise existent in polycrystalline films due to roughness and grain-boundary noise.

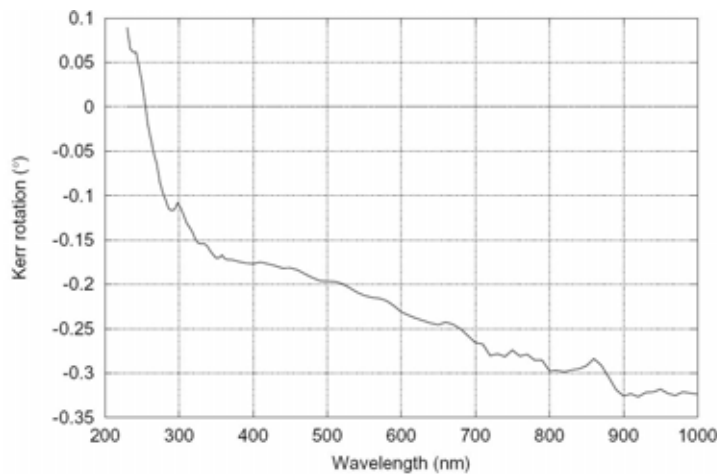


**Figure 2.3:** Kerr rotation spectra of the amorphous RE-TM alloy GdFeCo at room temperature.<sup>2</sup>

Similar to the magnetic properties of amorphous RE-TM, the magneto-optical properties can be tailored by selecting the appropriate preparation conditions and composition. Because of the amorphous structure of these alloys, there is no well defined band structure [23]. The spectral dependence of the Kerr rotation shows almost no structure (see Fig. 2.3).

For the RE-TM alloys such as GdFe or TbFe that are of interest in the storage industry, the polar Faraday rotation at room temperature in the visible wavelength is about  $0.3^\circ$ . The magneto-optical effect at this wavelength is attributed to the polarization of  $3d$  electrons, thus representing mainly the TM magnetic sublattice, while the transitions between the  $4f$  and  $5d$  states of the RE atoms become dominant at shorter wavelengths (below 300 nm) [7, 10, 13, 29]. Indeed, the magnetic electrons of transition metals such as Fe and Co are located in the  $3d$  electronic shell which build the outer layer of the ion since the  $4s$  electrons become part of the conduction

<sup>2</sup>Manuel Bilderbeek, master thesis, Nijmegen, The Netherlands, 2001.

electron sea. On the other hand, the  $4f$  electrons that are the main suppliers for the magnetism in the RE are deeply buried under the  $5s$ ,  $5p$  and  $5d$  shells. This is why photons in the visible wavelength with a relatively low energy are not able to probe the  $4f$  electrons. Therefore, the interaction of the low energy photons with only the outermost electrons is the reason why the red or near-infrared photons carry information mainly about the TM sublattice. Actually, this is a great advantage for the reading out of the magnetic domains stored near the magnetization compensation point, as it leads to large magneto-optical effects although near  $T_M$  the net magnetic moment of the ferrimagnetic system is strongly reduced. This is also an advantage for the present work, allowing the study of magnetization dynamics in the vicinity of  $T_M$ .

The enhancement of the magneto-optical effect at room temperature can be achieved by proper selection of the TM components. It has been found that the addition of Co to RE-TM alloys containing Fe enhances the Faraday rotation at room temperature. Note that this increase is valid only for a certain range of Co content [18]. Moreover, this is true only for the alloys where the TM magnetic sublattice is dominant at room temperature and is due to the raising of the Curie point by the additional transition metal [7].

For data storage purposes, a further increase of the magneto-optical Kerr effect signal is achieved via multiple reflections, by depositing the RE-TM thin film on top of a high reflecting aluminium layer [21].

## 2.4 Growth

The RE-TM films are deposited by sputtering either from an alloy target, or from multiple element targets. Sputtering techniques are preferred because they lead to denser films. Among these techniques, magnetron sputtering is the most used, since the films sputtered in this way exhibit a better morphology. The final magnetic properties of the RE-TM alloy strongly depend on the fabrication process [21]. Thus the type of the sputtering gas (argon, krypton, etc.), the pressure of the gas during the sputtering process, the deposition rate, the temperature of the substrate and the type of substrate have an important impact on the short-range order of the resulting magnetic thin film and its properties. The sputtering conditions can also have a strong impact on the structural characteristics of the RE-TM alloys and may lead to the occurrence of an appreciable columnar structure [12].

The usual MO disks are deposited as a multilayer structure as shown in Figure 2.4. Nevertheless, the MO media can be also deposited in various multilayer structure where the information reading process is performed with the laser beam passing through the substrate. In this case, the substrate must be a rigid material and provide a very good optically flat surface. Ideally, the substrate should have a number of characteristics such as optical transparency, uniform refractive index, free from

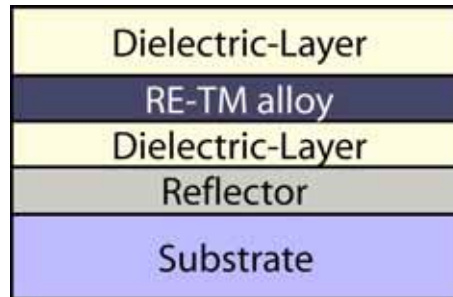


**Figure 2.4:** Typical multilayer film structure used for MO recording media.

birefringence, isotropic expansion with temperature and low thermal conductivity. However, no single material is able to meet all these requirements. Therefore, one of the widely used substrates is glass because of its great rigidity and accuracy of the surface control.

A reflector layer is deposited on top of the substrate. Besides the role to enhance the magneto-optical effect the reflector, that can be an aluminium layer, is also used as a heat sink. The amorphous ferrimagnetic RE-TM alloy is deposited on top of this layer sandwiched between two dielectric layers that have a protective role. This protection by the dielectric layers is crucial, since the magnetic rare earth elements are known to react strongly with oxygen and form non-magnetic oxides, which will lead to a change in the magnetic properties and a finite life time of the storage media. AlN and SiN have proven to be a good choice and lead to suitable protective layers by magnetron sputtering [9] while having also the role of anti-reflective coating. Long term stability has been also achieved by adding Be or In to the RE-TM alloy during the deposition process [11, 14] and controlling the structural characteristics of the alloy [12].

## 2.5 RE-TM Alloys Studied in This Work: GdFeCo

Because of the strength and approximately random orientation of the local magnetic anisotropy field of the RE ions, which tends to pull the local magnetic moment away from a collinear arrangement, the directions of RE moments are randomly canted from the direction anti-parallel to the TM moments, and conically distributed around the easy axis of magnetization [2, 4, 23]. However, the specific electronic configuration of gadolinium, which presents a half filled  $4f$  shell and thus an isotropic S-state character, gives the Gd-TM alloys a unique ferrimagnetic structure with collinear magnetic moment alignment [28].

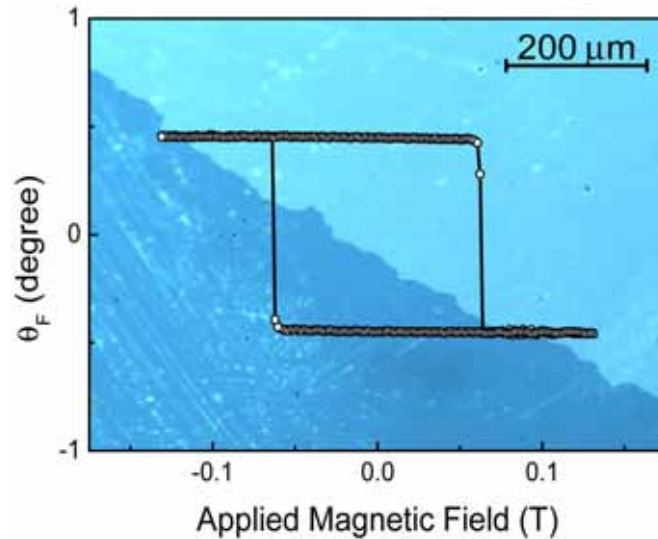


**Figure 2.5:** Hysteresis loop measured in amorphous  $\text{Gd}_{22}\text{Fe}_{74.6}\text{Co}_{3.4}$  thin film at room temperature. Background: Magneto-optical image of magnetic domains observable in a polarizing microscope. Light and dark domains represent regions in the sample with magnetization 'up' or 'down'.

Gd is probably the most interesting member of the lanthanide series because its ground-state electronic configuration is  $4f^7(5d6s)^3$ , with the highest possible number of majority-spin electrons and no minority-spin electron at its  $4f$  state, according to Hund's rule. Its combination with transition metals such as Fe, results in an antiferromagnetic coupling that originates in a hybridization between the Gd  $5d$ -states and the FeCo  $3d$ -states, mediated by the  $5d$  state via the  $4f$ - $5d$  intra-atomic exchange [23].

This collinear arrangement that leads to a simple ferrimagnetic structure represents one of the reasons why here we choose to study a Gd-TM amorphous alloy. Furthermore, its isotropic S-state character leads to a relatively soft magnetic anisotropy compared with the non-S-state RE ions. This is an advantage for some of the experiments presented here, since the coercivity of some of these materials lies in a range below the maximum magnetic field strength available in our experiments.

The RE-TM alloy studied in this work is the ferrimagnetic amorphous alloy GdFeCo<sup>3</sup>. As mentioned above, the small content of Co that was added to the

<sup>3</sup>Samples were grown by Dr. A. Tsukamoto and Prof. Dr. A. Itoh at the College of Science and

GdFe alloy has the role to enhance the Faraday effect at room temperature. The samples were grown by magnetron sputtering in the following multilayer structure: glass|AlTi(10nm)|SiN(5nm)|GdFeCo| SiN(60nm), where the GdFeCo layers had the following composition and thickness:  $\text{Gd}_{22}\text{Fe}_{74.6}\text{Co}_{3.4}$  (20nm),  $\text{Gd}_{23}\text{Fe}_{73.64}\text{Co}_{3.36}$  (20nm),  $\text{Gd}_{23}\text{Fe}_{73.64}\text{Co}_{3.36}$  (30nm). The AlTi layer serves as a reflector and heat sink and the dielectric layer SiN as buffer and capping layer respectively. Such ferrimagnetic materials are widely used in magneto-optical recording [26]. These films exhibit strong perpendicular magnetic anisotropy, a square hysteresis loop and large magnetic domains which are easily observable in a polarizing microscope (see Fig. 2.5). As previously discussed, the saturation magnetization of the films strongly varies with temperature and composition. For the GdFeCo sample shown in Fig. 2.5 the saturation magnetization at room temperature was about  $4\pi M_s = 1000$  Gauss.

## 2.6 Summary

Summarizing the above presented properties of the amorphous RE-TM alloys one can formulate the advantages of these materials:

1. *the amorphous structure* of these materials provides a freedom in choosing the alloy composition;
2. *the ferrimagnetic structure* is a very important feature that leads to:
  - the existence of *magnetization and angular momentum compensation* points that are crucial for a safe storing and a fast manipulation of the magnetic bits of information;
  - *weak magnetization* above room temperature implying a low demagnetization field that prevents the formation of domains;
  - *good control of the Curie temperature*;
  - *a strong temperature dependence of the coercive field* - this allows the magnetization direction to be controlled by moderate magnetic field strength at temperatures relatively close to room temperature;
3. *high and perpendicular anisotropy* that, in combination with a low demagnetizing field, yields stable perpendicular magnetic domains.

Above all, these great properties can be simply controlled by choosing the proper composition of the RE and TM components. The only, but important, disadvantage these alloys have is that they are highly subject to corrosion. Nevertheless, this drawback can be corrected by an optimized multi-layer structure.

---

Technology, Nihon University, Chiba, Japan.

## References

- [1] P. Chaudhari, J. J. Cuomo, and R. J. Gambino, *Appl. Phys. Lett.* **22**, 337 (1973).
- [2] J. M. D. Coey, *Phys. Rev. Lett.* **36**, 1061 (1976).
- [3] R. C. Taylor and A. Gangulee, *J. Appl. Phys.* **47**, 4666 (1976); **48**, 358 (1977).
- [4] J. M. D. Coey, *J. Appl. Phys.* **49**, 1646 (1978).
- [5] T. Mizoguchi and G. S. Cargill III, *J. Appl. Phys.* **50**, 3570 (1979).
- [6] R. Malmhäll and T. Chen, *J. Appl. Phys.* **53**, 7843 (1982).
- [7] S. Tsunashima, S. Masui, T. Kobayashi, and S. Uchiyama, *J. Appl. Phys.* **53**, 8175 (1982).
- [8] M. Mansuripur, G. A. N. Connell and J. W. Goodman, *J. Appl. Phys.* **53**, 4485 (1982).
- [9] T. K. Hatwar, S.-C. Shin, D. G. Stinson, *IEEE Trans. Mag.* **22**, 946 (1986).
- [10] T. R. McGuire, R. J. Gambino, T. S. Plaskett, and W. Reim, *J. Appl. Phys.* **61**, 3352 (1987).
- [11] T. Iijima and I. Hatakeyama, *IEEE Trans. Mag.* **23**, 2626 (1987).
- [12] M. Naoe, N. Kitamura, and H. Ito, *J. Appl. Phys.* **63**, 3850 (1988).
- [13] P. Hansen, C. Clausen, G. Much, M. Rosenkranz, and K. Witter, *J. Appl. Phys.* **66**, 756 (1989).
- [14] T. Tokushima, N. Horiai, and T. Fujii, *IEEE Trans. Mag.* **25**, 687 (1989).
- [15] M. Aeschlimann, A. Vaterlaus, M. Lutz, M. Stampanoni, and F. Meier, *J. Appl. Phys.* **67**, 4438 (1990).
- [16] Y. Mizusawa and K. Ichihara, *Jpn. J. Appl. Phys. Part 1* **30**, 484 (1991).
- [17] M. Aeschlimann, A. Vaterlaus, M. Lutz, M. Stampanoni, F. Meier, and H. C. Siegmann, *Appl. Phys. Lett.*, **59** (17), 2189 (1991).
- [18] Z.Y. Lee, X.S. Miao, P. Zhu, Y.S. Hu, D.F. Wan, D.W. Dai, S.B. Chen and G.Q. Lin *J. Magn. Mater.* **115**, 44 (1992).
- [19] Robert S. Weng and Mark H. Kryder, *IEEE Trans. Magn.* **29**, 2177 (1993).
- [20] J. Daval and B. Bechevet, *J. Magn. Mater.*, **129**, 98 (1994).



- 
- [21] M. Mansuripur, *The Physical Principles of Magneto-Optical Recording* (Cambridge University Press, Cambridge, 1995).
- [22] R. Carey, D. M. Newman and B. W. J. Thomas, *J. Phys. D: Appl. Phys.* **28**, 2207 (1995).
- [23] J. A. Fernandez-Baca and Wai-Yim Ching, *The Magnetism of Amorphous Metals and Alloys* (World Scientific Publishing Co. Pte. Ltd., Singapore, 1995).
- [24] P. Hansen. *Crytalline and amorphous films with rare earth and 3d transition elements.*, Landolt-Bornstein, Group III, Vol. **19g**, 165 (Springer, Berlin, 1988).
- [25] J. D. Livingston, *J. Appl. Phys.* **52**, 2544 (1981).
- [26] H. Awano, S. Ohnuki, H. Shirai, N. Ohta, A. Yamaguchi, S. Sumi, and K. Torazawa, *Appl. Phys. Lett.*, **69** (27), 4257 (1996).
- [27] J. Hohlfeld, Th. Gerrits, M. Bilderbeek, Th. Rasing, H. Awano, and N. Ohta, *Phys. Rev. B* **65**, 012413 (2002).
- [28] O. S. Anilturk and A. R. Koymen, *Phys. Rev. B* **68**, 024430 (2003).
- [29] Joo Yull Rhee, *Journal of the Korean Physical Society*, **43**, 792 (2003).
- [30] Christian Kaiser, Alex F. Panchula, and Stuart S. P. Parkin, *Phys. Rev. Lett.* **95**, 047202 (2005).
- [31] T. Kobayashi, H. Hayashi, Y. Fujiwara, and S. Shiomi, *IEEE Trans. Magn.* **41**, 2848 (2005).
- [32] Christian Kaiser and Stuart S. P. Parkin, *Appl. Phys. Lett.* **88**, 112511 (2006).
- [33] C. D. Stanciu, A. V. Kimel, F. Hansteen, A. Tsukamoto, A. Itoh, A. Kiriliiuk, and Th. Rasing, *Phys. Rev. B* **73**, 220402(R) (2006).
- [34] M. Binder, A. Weber, O. Mosendz, G. Woltersdorf, M. Izquierdo, I. Neudecker, J. R. Dahn, T. D. Hatchard, J.-U. Thiele, C. H. Back, and M. R. Scheinfein, *Phys. Rev. B* **74**, 134404 (2006).
- [35] Xin Jiang, Li Gao, Jonathan Z. Sun, and Stuart S. P. Parkin, *Phys. Rev. Lett.* **97**, 217202 (2006).

## CHAPTER 3

---

**Experimental Techniques**

---

**3.1 Introduction**

**T**he past decades have witnessed significant advancement in instrumentation for the characterization of magnetic materials [1]. There are techniques developed that can measure the global magnetic response of a sample to an applied magnetic field, such as Superconducting Quantum Interference Device (SQUID), Vibrating Sample Magnetometer (VSM) and Alternating Gradient Force Magnetometer (AGFM) and techniques that can give access to local magnetic properties of materials on microscopic/nanoscale scales, such as magneto-optical microscopy, Magnetic Force Microscopy (MFM), Transmission/Scanning Electron Microscopy (TEM/SEM) with magnetic contrast and Spin-Polarized Scanning Tunneling Microscopy (SPSTM). All these techniques, however, probe static magnetic properties. The development of femtosecond (fs) laser sources has opened the way to create measurement techniques that can locally probe the evolution of magnetization on a sub-picosecond timescale. The availability and accessibility of commercial laser systems with pulses shorter than fundamental timescales such as spinlattice relaxation times and spin precession times, has resulted in many exciting experimental results, shaping the field of spin dynamics into one of the most exciting field of modern magnetism. With this, a new adventure has begun, *ultrafast magnetization dynamics*, that allows to probe the fundamentals of magnetic anisotropy, atomic spin-orbit energy, interatomic exchange energy and beyond.

Due to the well known magneto-optical (MO) effects such as Faraday or Kerr effect, the use of ultrafast laser pulses allows us not only to deposit energy and thus excite a magnetic system but also to study how these systems behave away from or towards equilibrium, in response to a sudden perturbation. Electronic devices that are available on the market today cannot measure fast enough those events that are taking place on a time scale much shorter than a nanosecond. Therefore, new techniques had to be developed in order to study the ultrafast processes following femtosecond laser excitation.

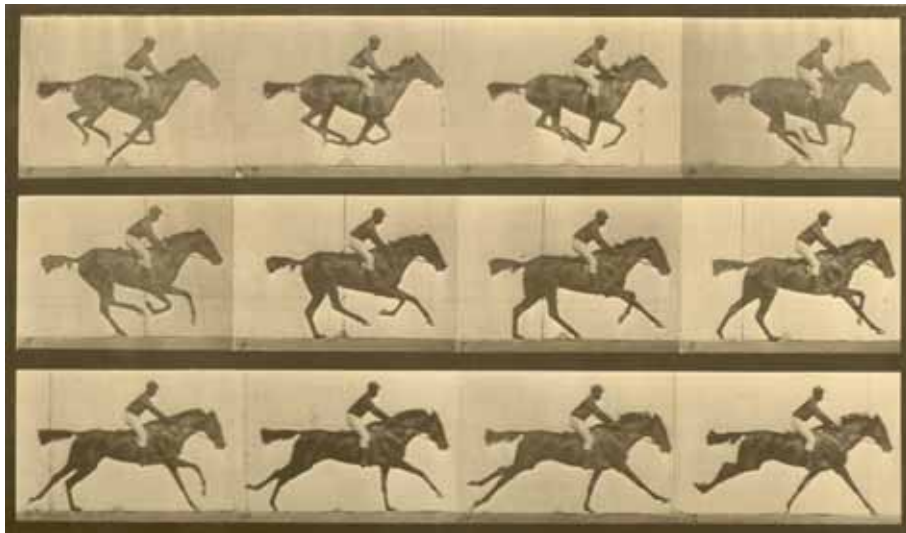


**Figure 3.1:** The Horse in Motion. One of the first motion photograph that splits the second - by Eadweard Muybridge.<sup>1</sup>

One of the ways to visualize fast processes is to use a very short flashing light that will freeze the process at the required time. A sequence of these images acquired at different moments in time will lead to a complete image of the dynamics of the process. Using such a technique, the San Francisco photographer Eadweard Muybridge was the first to photograph a motion. In 1872, at the request of Leland Stanford who wanted to know whether during a horse's trot, all four hooves were ever off the ground at the same time, Muybridge set up 12 still cameras along a racetrack, each with a string-activated shutter. The strings were held taut across the infield and when the horse passed it broke each string in succession, triggering a sequence of images (see

<sup>1</sup>Collections of the University of Pennsylvania Archives. This image is used with the permission of the University of Pennsylvania Archives and Records Center.

Fig. 3.1). This is how the forerunner of modern stroboscopes was born.

Based on a stroboscopic approach, to some extent similar to that of Muybridge, so called pump-probe techniques have been employed in studying magnetization dynamics. Here, in general, an ultrashort stimulus (in general an optical, magnetic field or current pulse) is used to trigger the dynamics of the magnetic system of interest while a much weaker laser pulse (probe) is used to "picture" the dynamics of this system at the chosen moment, via one of the MO effects. The first application of such approach for ultrafast pump-probe studies of spin dynamics was used by Awschalom et al. in 1985 [2]. The advantages of the pump probe technique is that it is non-destructive and allows one to probe the magnetic ordering in ferromagnets, antiferromagnets and complex magnetic nanostructures with high spatial resolution (sub-micrometer) and extreme temporal resolution (sub-picosecond). However, it must be stressed that in contrast to Muybridge's experiment, such stroboscopic technique is based on the repetitiveness of the process that is being observed. This is because while in his experiments Muybridge uses many cameras to obtain the dynamics of a single event, in a pump-probe set-up only such a "camera" is used (in a pump-probe set-up a camera is the equivalent of an ultrafast laser system and a detection scheme). Using a single laser system, an ultrafast event can be observed at only one moment during its motion. In order to resolve the whole dynamics, the same event must be triggered many times and observed at different moments. Consequently, for a reliable result, the repetition rate of the stimuli that triggers the dynamics of the system should be slower than the actual relaxation time of the studied process and the system should always relax to its original state such that every new stimulus finds the system recovered in the same state.

The present chapter introduces the main experimental techniques used in this Ph.D. work for the characterization and manipulation of magnetization in ferrimagnetic RE-TM amorphous alloys, namely *the pump-probe technique* combined with linear magneto-optical effects and MO-microscopy.

## 3.2 Linear Magneto-Optics

In a general but not very specific way magneto-optics is defined as the interaction of electromagnetic radiation with a material located in a magnetic field [3]. In the case of magnetically ordered matter (ferromagnets, ferrimagnets, etc.), MO effects may appear in the absence of an external magnetic field as well. It follows that magneto-optics is a relatively large area of physics. Although the magneto-optical effects are usually associated with visible light, they may be seen in the whole spectrum of electromagnetic radiation. Thus, depending on the electromagnetic spectrum, various MO effects can be found. However, in all the experiments presented in this thesis, the detection of the static and dynamic magnetization was based on the linear MO effects that occur in the near infrared and the visible part of the electromagnetic spectrum.

Interband transitions are those responsible for the MO effects occurring in this range of the electromagnetic spectrum. These are excitations from the valence band to the conduction band or, in conducting materials such as metals, also from the conduction band to empty higher-level states.

The oldest MO effect, the Faraday effect, is named after his discoverer M. Faraday (1845). It is also described as circular magnetic birefringence because it originates from a splitting of the index of refraction for left-handed ( $\sigma^-$ ) and right-handed ( $\sigma^+$ ) circularly polarized light. Due to this optical anisotropy, when plane-polarized light is transmitted through a magnetized material, the polarization plane of transmitted light is changed. The sampling depth is determined by the optical absorption depth which, as discussed in Chapter 1, is about 20 nm for the strongly light absorbing ferromagnetic metals. In other words, in materials such as metals, light can travel a few tens of nanometers as the penetration depth of light is given by the inverse value of the absorption constant, which is about to  $10^6 \text{ cm}^{-1}$  for metals in the visible spectrum range. Therefore, in films which are only several nanometer thick, it is still possible to transmit light in order to measure the Faraday effect. Nevertheless, the optical anisotropy of a magnetized medium manifests itself also in reflection of light from the medium surface. This effect, which was discovered by the Scottish physicist John Kerr in 1877, is known as the magneto-optical Kerr effect (MOKE) and allows to study thick opaque materials or thin films on opaque substrates. Both, the Faraday and Kerr effect are similar phenomena, being proportional to the magnetization of the media and scaling with the optical penetration of the investigated medium.

Magneto-optical effects are best described in terms of the dielectric permittivity tensor  $\epsilon$  of the medium in which the interaction between the light and the magnetization takes place. In an optically isotropic material the three diagonal elements of this tensor are identical. Considering the case of interest here where the light interacts with a ferromagnetic material and where both the incident light and the magnetization are parallel to the  $z$ -axis, there is a non-zero off-diagonal element which couples the  $x$ - and  $y$ -components of the optical E-field. A quantum mechanical treatment relates this non-diagonal element to magnetic perturbations which are linear spin functions such as the spin-orbit coupling, the Zeeman effect (the splitting of the energy levels in an external magnetic field) and to optical transition probabilities [4]. Consequently, the dielectric tensor for this case reads <sup>2</sup>

$$\epsilon = \begin{pmatrix} \epsilon_{xx} & i\epsilon_{xy} & 0 \\ -i\epsilon_{xy} & \epsilon_{xx} & 0 \\ 0 & 0 & \epsilon_{xx} \end{pmatrix}. \quad (3.1)$$

In linear approximation, the off-diagonal elements  $\pm\epsilon_{xy}$  are the only ones dependent on the magnetization [4], and lead to a magnetization-dependent rotation of the

<sup>2</sup>Note that  $\epsilon$  is wavelength-dependent.

transmitted or reflected polarization. Since the symmetry is broken in a ferromagnetic material, the optical eigenmodes are circularly polarized waves, and one should use those for a correct description of the magneto-optical effects. Consequently, the refractive indices  $n_-$  and  $n_+$  become different for the  $\sigma^-$  and  $\sigma^+$  light, leading to the phenomenological description of the Faraday effect. Because they "see" a different medium with a different refractive index,  $\sigma^-$  and  $\sigma^+$  propagate with different velocities  $c/n_-$  and  $c/n_+$  through the magnetized medium. In this case, since linear polarized light can be represented as a superposition of the  $\sigma^-$  and  $\sigma^+$  waves, the plane of polarization of the incident linear polarized light rotates over an angle. In cylindrical system of coordinates, the linearly polarized light may be written as  $\hat{x} = 1/\sqrt{2}(\hat{e}_+ + \hat{e}_-)$  where  $\hat{e}_+$  and  $\hat{e}_-$  represent the two circularly polarized waves  $\sigma^+$  and  $\sigma^-$  that can be written as

$$\begin{aligned}\hat{e}_- &= \frac{1}{\sqrt{2}}(\hat{x} - i\hat{y}), \\ \hat{e}_+ &= \frac{1}{\sqrt{2}}(\hat{x} + i\hat{y}), \\ \hat{e}_z &= \hat{z}.\end{aligned}\tag{3.2}$$

In this cylindrical system of coordinates, the dielectric tensor  $\epsilon$  has the form

$$\epsilon_c = \begin{pmatrix} \epsilon_{xx} - i\epsilon_{xy} & 0 & 0 \\ 0 & \epsilon_{xx} + i\epsilon_{xy} & 0 \\ 0 & 0 & \epsilon_{xx} \end{pmatrix}.\tag{3.3}$$

From the formulae 3.2 and 3.3 we can define nonequal dielectric constants for  $\sigma^+$  and  $\sigma^-$ , namely

$$\epsilon_{\pm} = \epsilon_{xx} \pm i\epsilon_{xy}.\tag{3.4}$$

Thus, analyzing the difference between the transmission of left- and right-handed polarized light one is sensitive to the magnetization of a material through the magnetization dependence of  $\epsilon_{xy}$ . Because of this, linearly polarized light will experience rotation of its polarization axis and will gain an ellipticity upon propagation through such material. These two effects are quantified by the ellipticity  $\eta$  and rotation  $\theta$  contributions to the complex rotation angle:  $\Phi = \theta + i\eta$ . In terms of dielectric tensor components, for a magnetized medium in the polar geometry ( $k \parallel \mathbf{M} \parallel \hat{z}$ ) one obtains

$$\Phi \sim \epsilon_{xy}/\epsilon_{xx} \sim \mathbf{M}.\tag{3.5}$$

Therefore, measuring the polarization change of the light along the direction of the magnetization ( $z$ -direction in the above case) yields a complex rotation  $\Phi$  proportional to the out-of-plane component of the magnetization,  $M_z$ . In fact, the small linear MO effects represent the magnitude of the magnetization-induced off-diagonal components of the dielectric tensor in comparison to the diagonal ones ( $\sim \varepsilon_{xy}/\varepsilon_{xx}$ ).

Because of the simplicity and good spatial resolution (below  $1 \mu\text{m}$ ), MO effects such as Faraday rotation or polar Kerr rotation find application in magneto-optical recording where linearly polarized light is used to read-out the orientation of perpendicular magnetic bits [6]. For thin films these MO effects are relatively small; for example for Fe, Co or Ni, in the visible range of the spectrum the rotation angle is less than one degree. However, for the case of these MO effects the sign of the rotation depends only on the direction of the magnetic field (or magnetization) being independent of the light direction. Therefore,  $\theta$  will not change sign when the light travels in the opposite direction (the MO effect breaks time-reversal invariance). This has consequences for technical applications. In particular, for metallic thin films or non-absorbing magnetic materials is it possible to amplify the effect by letting the light travel multiple times through the material [6].

### 3.3 The Femtosecond Laser System <sup>3</sup>

The magnetization dynamics studies presented in this work were performed with the help of a Spectra-Physics commercial laser system consisting of

- a Tsunami mode-locked Titanium-doped sapphire ( $\text{Ti}^{3+}:\text{Al}_2\text{O}_3$ ) laser;
- a Spitfire pulsed Ti:sapphire regenerative amplifier;
- an Optical Parametric Amplifier (OPA 800).

The femtosecond laser system is schematically shown in Figure 3.2. The seed laser is the Tsunami (Spectra-Physics). This mode-locked femtosecond laser system was pumped by a 5 Watt continuous (CW) solid-state diode-pumped Nd:YVO<sub>4</sub> laser, at a 532 nm wavelength. While the absorption band of the Ti:sapphire crystal lies in the visible range (between 400 nm and 600 nm), its emission spectrum is shifted towards the near-infrared. The broad emission spectrum allows a continuous tunability of the laser pulses between  $\sim 700$  nm and  $\sim 1000$  nm [7]. In our experiments the laser system was operating at a central wavelength of  $\sim 805$  nm. The output consists of pulses with a Gaussian temporal profile with a width (FWHM) of about 60 fs. The train of 60 fs pulses is provided at a repetition rate of 82 MHz. The pulse energy provided by the Tsunami is up to several nJ [7].

<sup>3</sup>Note that part of the experiments presented in this thesis were performed using a similar but newer version of the Spectra-Physics laser system described here, with 40 fs laser pulse duration.

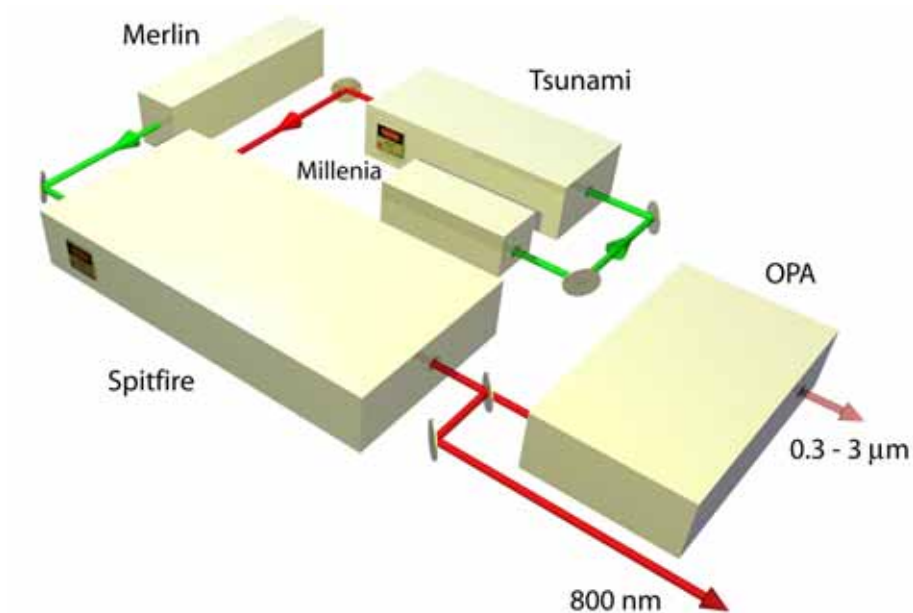


**Figure 3.2:** The femtosecond laser system: the Tsunami Ti:sapphire cavity pumped by a Millenia diode pumped Nd:YVO<sub>4</sub> laser, the regenerative amplifier Spitfire pumped by a Merlin Nd:YLF laser while seeded by the 60 fs pulses from the Tsunami. The output from the amplifier can be used to pump the Optical Parametric Amplifier (OPA) which helps to vary the wavelength of the laser pulses between 300 nm and 3 μm.

To obtain a higher pulse energy, the Ti:sapphire laser pulses are amplified using a Spectra-Physics Spitfire regenerative amplifier. The regenerative amplification resulted from pumping a gain medium such as Ti:sapphire. The amplifier is pumped by a pulsed Nd:YLF laser (Merlin) at  $\lambda=527$  nm and seeded by the Ti:sapphire laser. The average output power of the pump laser is 10 W at a repetition rate of 1 kHz. This pumped energy is stored while the fs seed pulse to be amplified is injected in the cavity that contains the gain medium. The synchronization of the timing between the seed and pump pulse is insured by a Pockels cell which opens for a short time giving the pulse access to the cavity. The seed pulse undergoes several round trips in the cavity (a few tens) being amplified to higher energies. After the pulse has gained the maximum energy, a second Pockels cell is activated and the pulse is let out of the cavity. However, if the pulse would be amplified directly to a higher energy (such as 500 μJ/pulse), the intra-cavity peak intensity would become extremely high and damage



the optics. Consequently, before amplification the seed pulse has to be first stretched to a much longer duration, amplified, and then compressed back. This process is called chirped pulse amplification. According to Fourier transformation, a Gaussian light pulse with a temporal width  $\Delta t$  is built up out of a continuous distribution of frequency components with bandwidth  $\Delta\omega \approx 1/\Delta t$ . Thus, by temporarily delaying certain frequencies the pulse can be stretched and conversely, compressed. The pulse stretching and compressing can be achieved with diffraction gratings or prisms. The compressor allows retrieving a temporal duration close to the one of the input pulse. The output of the amplifier consists of pulses with an energy of about  $500 \mu\text{J}/\text{pulse}$  for a pulse duration of about 100 fs at a repetition rate of 1 kHz. Optionally, the laser pulses from the Spitfire can be used as pump for an Optical Parametric Amplifier (OPA800). This leads to laser pulses which wavelength can be continuously tuned between 300 nm and  $3 \mu\text{m}$ .

### 3.4 The Magneto-Optical Pump-Probe Set-up

The magnetization dynamics in GdFeCo samples was induced and investigated using a time-resolved all-optical pump-probe set-up. The schematic drawing of this time-resolved set-up is depicted in Figure 3.3. The amplified 100 fs laser pulses emitted by the amplified Ti:Sapphire laser, were split into two beams of different intensities by a beam splitter, at a ratio of about 90:10. The most intense pulses, the pump pulses, were used to trigger the magnetization dynamics (as shown in Chapter 4). The linear polarization of the pump beam was insured by a polarizer. A synchronized chopper, working at half the frequency of the Spitfire repetition rate, is used to modulate this beam such that every second pump pulse is blocked. As it will be explained in this section, this modulation is crucial for a good signal-to-noise ratio in the lock-in based detection technique. A quarter-wave plate placed in the pump beam allows to change the light polarization from linear to elliptically or circularly polarized light. The pump beam is then focused on the sample. The focus diameter in the present work was relatively large, about  $200 \mu\text{m}$ . Note that the amplified femtosecond system is able to supply the 100 fs pulses at a pulse energy of  $500 \mu\text{J}$ . Such high energy focused to  $200 \mu\text{m}$  is far above the damage threshold of our metallic RE-TM samples. In order to avoid permanent damage of the sample surface, the optical power of the pump beam is reduced before being focused on a sample. The attenuation was achieved by using neutral density optical filters. Alternatively, for a more sensitive control of the beam intensity a half-wave plate can be used, placed before the polarizer. The laser fluence used in the experiments presented here ranged between  $\sim 1 \text{ mJ}/\text{cm}^2$  -  $\sim 15 \text{ mJ}/\text{cm}^2$ .

The less intense pulses were used to examine the changes of the magnetic state of the sample via the changes in the magneto-optical effect. The thickness of the samples studied here (20 nm or 30 nm) allows the sample to be studied in the transmission geometry (Faraday effect), a more convenient geometry from the experimental point of

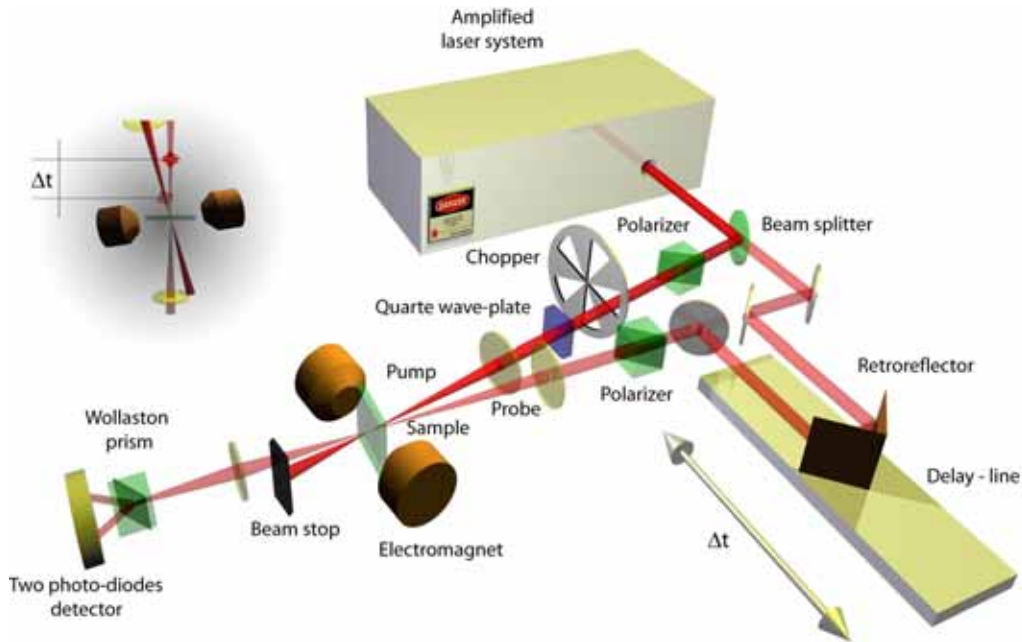


**Figure 3.3:** Schematic drawing of the time-resolved pump-probe experimental set-up used to study ultrafast magnetization dynamics. Amplified femtosecond laser pulses split in two beams: an intense laser beam - *pump beam*, used to trigger the magnetization dynamics and a much weaker laser beam - *probe beam*, used to monitor the magnetization dynamics via the magneto-optical Faraday effect. The Faraday effect is detected by a detector made of a Wollaston prism and two photo-diodes. The time resolution of this experiments is assured by a computer controllable variable delay-line that moves the retroreflector and thus delays the probe pulses with respect to the pump pulses as shown in the inset of the figure.

view. In order not to influence the evolution of the magnetization dynamics initiated by the pump pulses, the probe beam intensity has been attenuated ( $I_{\text{pump}}/I_{\text{probe}} > 100$ ). The monitoring of the magnetization dynamics in time is achieved by using a motorized linear stage (the delay line) with a length of 60 cm. The temporal delay between the pump and probe pulses is modified via a change of their relative pathway. In this way, the 60 cm-long delay line represents a maximum delay between pump and probe of 4 ns. The resolution of this delay line is  $0.1 \mu\text{m}$  that corresponds to a time resolution of  $2 \times 0.33 \text{ fs}$ . To make use of the motor-driven translation stage, a retroreflector was mounted on it. The beam falling on to the retroreflector is reflected

parallel to the direction of incidence. Due to this retroreflector, once the alignment of the delay line is done, the probe beam can be focused on the sample on a place that will not change with the shortening/lengthening of the probe optical path. In fact this alignment is a very important issue for the all-optical pump-probe set-up since the aim is to obtain an overlap between pump and probe that is not changing in space with the optical path change. In order to gain access to near all of the 4-ns-delay-time given by the delay-line, the so called "zero delay" (the time overlap of the pump and probe pulses) was placed near the end of the delay-line. As it will be further shown, depending on the type of the experiment performed, the probe beam was focused to an equal or much smaller spot than the pump beam.

Both pump and probe beams were focused on to the sample at nearly normal incidence. The magneto-optical Faraday effect is proportional to the projection of the magnetization in the sample along the k-vector of the probe beam (here, out-of-plane component of the magnetization,  $\mathbf{M}_z$ ). Thus, the evolution of the magnetization in time is simply measured by analyzing the polarization state of the transmitted probe pulses. In particular, a pump pulse triggers the precession of the magnetization while the probe pulse arriving at a later time ( $\Delta t$ ) acquires the projection of the magnetization on the k-vector at that specific time. Generally speaking, every pump and probe pair represents a data point ( $\Delta \mathbf{M}_z, \Delta t$ ). For the case in which the magnetization is precessing with an out-of-plane component, a sequence of such pump-probe events acquired for different  $\Delta t$  leads to the observation of an oscillating behavior of the Faraday angle in time.

To analyze the rotation of the probe polarization after its transmission through the RE-TM alloy, we have used a detection scheme that consists out of a Wollaston prism and two photo-diodes [8]. The incident light transmitted through this prism, is split in two orthogonally polarized beams that exit with a beam deviation from normal. The intensities of these two beams are detected by the two different photo-diodes leading to two separate signals  $I_A$  and  $I_B$ . Before a measurement, the intensities on the two photo-diodes are balanced such that  $I_A=I_B$ . In this way, any following change of the probe beam polarization plane (due to the change of the sample magnetization direction or magnitude) can be detected by simply monitoring the difference  $I_A-I_B$ , because the intensity on one photo-diode increases while decreasing on the other. Depending on the polarization plane angle of the probe beam  $\theta$  with respect to the transmission axis of a polarizer, the signal on the two diodes,  $I_A$  and  $I_B$ , can be written as  $I_A = I_0 \cos^2 \theta$  and  $I_B = I_0 \sin^2 \theta$ , where  $I_0$  is the initial intensity of the beam. Thus, for  $\theta=45^\circ$  the detector is balanced so that  $I_A-I_B=0$ . It can be shown that a change  $\theta_F$  in the polarization of the transmitted beam can be detected as a differential signal that is  $I_A - I_B \approx 2I_0\theta_F$  [8–11]. It can be also shown that a change in the ellipticity leads to a similar change in both diodes and thus is not visible in the signal [9]. Yet, the ellipticity can be still measured if a quarter-wave-plate is placed in the transmitted beam in order to convert the ellipticity into a rotation. This

differential detection scheme is a very good method for analyzing the small magneto-optical effects, giving a very good signal-to-noise ratio due to the compensation of the laser instabilities in intensity, a general issue for ultrafast lasers.

Some of the experiments presented in Chapter 4 and Chapter 5 have been performed in air while other experiments have been performed in an optical cryostat in order to gain access to a wider range of temperature. This was a cold finger cryostat where the temperature could be stabilized in the range of 10-400 K with a precision better than 0.5 K. As will be discussed in Chapter 4, some of the experiments required application of an external magnetic field. In order to do this, a commercial electromagnet has been used. The electromagnet is placed on a plate, which allows the magnetic field to be applied up to  $\sim 30^\circ$  out-of-plane of the sample, in every direction around the sample holder. The maximum applied magnetic field was about 0.3 T.

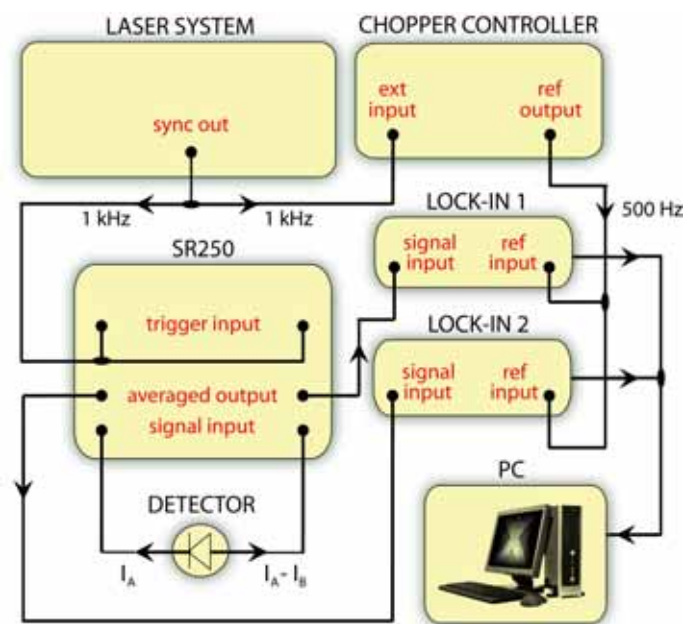


**Figure 3.4:** A block diagram showing the main electronic devices used in connection with the time-resolved pump-probe set-up shown in Fig. 3.3.

As discussed in section 3.1, the electronics available today has a much slower response time when compared to the ultrafast laser pulses such as those used in our experiments. For example, the response of the detector used in the present work to a

femtosecond optical pulse, is broadened to about  $25 \mu\text{s}$ . Nevertheless, this response time is short enough when compared to 1 ms, the time between two pulses supplied by the 1 kHz amplified laser system. To increase the signal-to-noise ratio, a SR250 Gated Integrator and Boxcar Averager from Stanford Research has been used, that allows to integrate all the signal within a specific time window (gate) while ignoring all the rest. More specifically, the signal received from the detector has been supplied to the SR250 triggered by the 1 kHz reference frequency from the Spitfire (see Figure 3.4. Visualizing on an oscilloscope, the signal from the detector can be gated for only the response time of the detectors ( $\geq 25 \mu\text{s}$ ). In this way, noise is avoided. The integrated signal is then supplied to the output for 1 ms with the help of a sample-and-hold circuit. As a result, the output of the SR250 will consist in only the "real" signal that represents the process of interest. This averaged signal is sent to a Lock-in amplifier. To further increase the signal-to-noise ratio, the pump beam is chopped by a synchronized chopper working at half the frequency of the Spitfire (500 Hz). Consequently, every second pump pulse is blocked such that the subsequent probe beam is monitoring the magnetic system in a non-excited state. The 500 Hz frequency is used as reference for the Lock-in. This alternating pump-on and pump-off condition reduces the noise by excluding any non-magnetic background effects that might be present in the detected signal. The Lock-in is averaging over several tens of excitation events (*e.g.* 50). This is another reason why, before every new pump pulse exciting the sample, the magnetic system has to be relaxed back to the initial state. Finally, it must be mentioned here that although more noisy, the pump-probe experiments can be also performed without the chopping technique and the boxcar integrator (where the signal from the photodiodes is directly supplied to the Lock-in, using as an external reference the 1 kHz *sync out* signal from the amplified laser system).

In all the above experiments an extra Lock-in amplifier is used in order to record the signal only from a single photo-diode (*e.g.*  $I_A$ ). The reason for this is that the laser pump pulses temporarily affect not only the magnetic properties but also the optical properties of the sample. These changes are reflected in the sample transmittivity and thus affect the probe intensity  $I_0$ . Since  $I_A - I_B \approx 2I_0\theta_F$ , the differential signal is also influenced by an intensity change. Therefore, in order to observe solely the magneto-optical effect the differential signal must be normalized to the signal from a single photo-diode (that represents optical effects).

In conclusion, the pump-probe set-up described above can be employed only for the study of periodic processes such as the magnetization precession. Nevertheless, by including into the experimental set-up a pulsed magnetic field that can initialize the magnetization direction before the arrival of each pump pulse, one can also study the time evolution of non-periodic processes such as the magnetic switching [12].

### 3.5 The Magneto-Optical Imaging Set-up

The magneto-optical imaging set-up that has been build within the pump probe set-up is schematically illustrated in Figure 3.5. The aim of this set-up was to observe the result of exciting the RE-TM alloys with circularly and linearly polarized light while no external magnetic field was applied. Here in order to excite the sample we have used an amplified Spectra-Physics commercial laser system supplying 40 fs laser pulses at a central wavelength of 800 nm. The magneto-optical images have been obtained by illuminating the magnetic sample with a polarized white-light source. The light

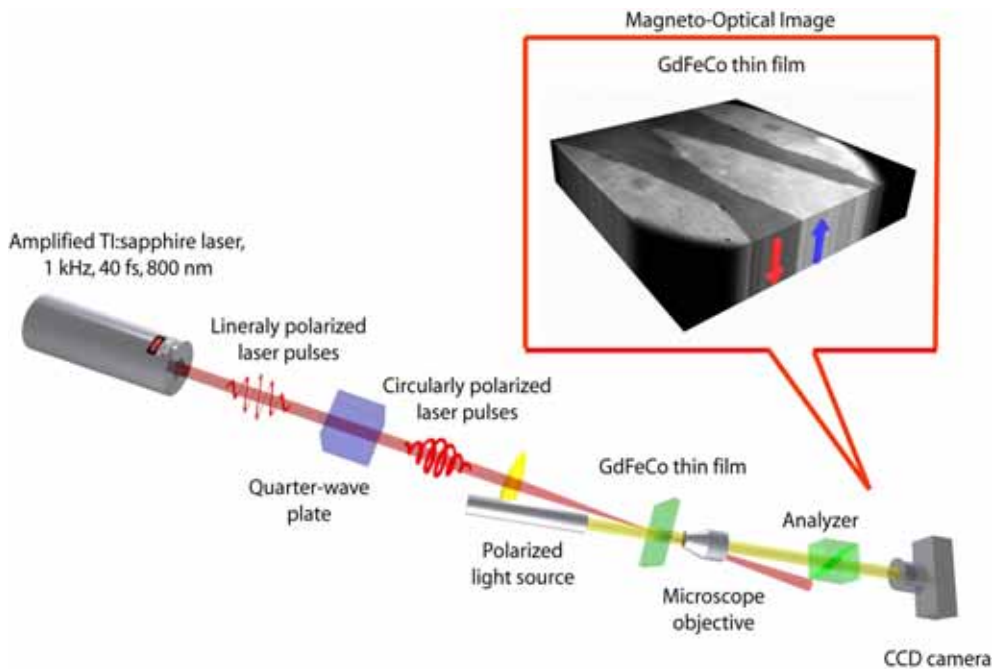


**Figure 3.5:** Schematic illustration describing the magneto-optical imaging set-up. 40 fs laser pulses are used to excite the RE-TM alloy. A quarter-wave plate allows to control the polarization of the pulses. The magneto optical-images of the sample are produced using a polarizing microscope, where the polarized light shining on the sample is captured by a microscope objective and directed on to a CDD camera while passing through an analyzer. By nearly crossing the analyzer with the incoming light polarization, a magneto-optical image of the sample becomes visible such as that shown above. Here, the black and white domains represent magnetic domains with magnetization down and up, respectively.

in the region of interest at the sample was collected using a microscope objective and guided onto a CCD (charged coupled devices) camera through an analyzer. The axis of the analyzer has been set to be nearly crossed with the polarization of the light beam. A magneto-optical image observable through such set-up is shown in Fig. 3.5. Here, black and white regions represent magnetic domains with magnetization down and up respectively (sample has perpendicular magnetic anisotropy). This image is the result of the Faraday effect. In order to protect the camera from the (800 nm) intense laser pulses used to excite the sample, an optical filter with bandpass range of about 400-500 nm has been mounted in front of the analyzer. Using this simple set-up one can acquire images either after or during the excitation process.

Compared with other techniques that involve the study of the sample in a static regime, after excitation with ultrashort pulses [13–16], the advantage of this set-up is that the results can be followed during the excitation process, though still at a static level. Furthermore, in contrast to the pump-probe experiments where, to acquire a data point, the pump/probe cycle must be repeated several times, the simple set-up presented here enables us to perform single shot experiments such as the experiments at SLAC (see Subsection 1.5.3). In addition, although the results are not discussed here, we have recently developed an experimental set-up, where the imaging technique was incorporated into the pump-probe set-up. This set-up is currently further developed in our lab, in order to observe the time evolution of all-optical switching.

## References

- [1] Yimei Zhu, *Modern techniques for characterizing magnetic materials* (Kluwer Academic Publishers, London, 2005).
- [2] D. D. Awschalom, J.-M. Halbout, S. von Molnar, T. Siegrist, and F. Holtzberg, *Phys. Rev. Lett.* **55**, 1128 (1985).
- [3] A. K. Zvezdin and V. A. Kotov, *Modern Magneto-optics and Magneto-optical Materials* (Institute of Physics Publishing, London, 1997).
- [4] Victor Antonov, Bruce Harmon, and Alexander Yaresko, *Electronic Structure and Magneto-Optical Properties of Solids* (Kluwer Academic Publishers, Dordrecht, 2004).
- [5] M. Vomir, L. H. F. Andrade, L. Guidoni, E. Beaurepaire, and J.-Y. Bigot, *Phys. Rev. Lett.* **94**, 237601 (2005).
- [6] M. Mansuripur, *The Physical Principles of Magneto-Optical Recording* (Cambridge University Press, Cambridge, 1995).

- 
- [7] Spectra-Physics, *Tsunami: Mode-locked Ti:sapphire Laser, User's Manual*, 2002.
  - [8] B. Koopmans in *Topics of Applied Physics: Spin Dynamics in Confined Magnetic Structures II*, edited by B. Hillebrands and K. Ounadjela (Springer, New York, 2003), pp. 265.
  - [9] Thomas Gerrits, Ph.D. thesis, Nijmegen, The Netherlands, 2004.
  - [10] Fredrik Hansteen, Ph.D. thesis, Nijmegen, The Netherlands, 2006.
  - [11] Mircea Vomir, Ph.D. thesis, Strasbourg, France, 2006.
  - [12] J. Hohlfeld, Th. Gerrits, M. Bilderbeek, Th. Rasing, H. Awano, and N. Ohta, *Phys. Rev. B* **65**, 012413 (2002).
  - [13] C. H. Back, R. Allenspach, W. Weber, S. S. P. Parkin, D. Weller, E. L. Garwin, H. C. Siegmann, *Science* **285**, 864 (1999).
  - [14] C. H. Back, D. Weller, J. Heidmann, D. Mauri, D. Guarisco, E. L. Garwin, and H. C. Siegmann, *Phys. Rev. Lett.* **81**, 3251 (1998).
  - [15] I. Tudosa, C. Stamm, A. B. Kashuba, F. King, H. C. Siegmann, J. Stohr, G. Ju, B. Lu, D. Weller, *Nature* **428**, 831 (2004).
  - [16] J. Stohr and H. C. Siegmann, *Magnetism: From Fundamentals to Nanoscale Dynamics* (Springer Verlag, New York, 2006).





## CHAPTER 4

---

## The Role of Angular Momentum Compensation <sup>1</sup>

---

**T**he magnetization in solids reacts to external stimuli such as a change in temperature or magnetic fields. In general, the motion of the magnetization towards its new equilibrium happens along a spiral trajectory, as shown in Section 1.4. This is the magnetization precession, which is one of the fastest known ways of changing the magnetization direction. Consequently, the precession frequency and the damping of this precession are the ingredients defining the speed of the precessional magnetization reversal. Hence, identification of physical mechanisms that can facilitate the control of these parameters is highly desirable. For example, in certain devices, it is essential to suppress the "ringing" of the magnetization after its reversal while in others such as MRAM low damping is desired in order to switch the magnetization of the free-layer using the lowest possible currents [1]. Consequently, the magnetization precession frequency and its damping are subjects of strong research interest due to their relevance for the speed of data processing in magnetic memory devices.

This chapter presents time-resolved experimental studies on ultrafast laser induced spin dynamics and magnetization reversal in the rare earth-transition metal ferrimagnetic alloy GdFeCo, in an applied magnetic field. For this study an all optical pump and probe set-up is used, such as described in Section 3.4. The results presented here are divided into two main sections. The first section of this chapter, "*Thermal-induced*

---

<sup>1</sup>Adapted from: C. D. Stanciu, A. V. Kimel, F. Hansteen, A. Tsukamoto, A. Itoh, A. Kiriliyuk, and Th. Rasing, *Phys. Rev. B* **73**, 220402(R) (2006), and C. D. Stanciu, A. Tsukamoto, A. V. Kimel, F. Hansteen, A. Kiriliyuk, A. Itoh, and Th. Rasing, *Phys. Rev. Lett.* **99**, 217204 (2007).

*Magnetization Dynamics in GdFeCo*”, focuses on how the precessional motion (precession frequency and damping) of the magnetization in a ferrimagnet is affected on the ps time scale by the strength of the applied magnetic field, the sample temperature and the RE-TM concentrations. The highlight of this study is the observation of the magnetization dynamics near the ferrimagnetic compensation points in the amorphous RE-TM alloy. More specifically, it is shown that the angular momentum compensation temperature strongly affects the magnetization dynamics leading to a high-speed and strongly damped precession. In the second section of this chapter entitled *”Sub-picosecond Magnetization Reversal Across Ferrimagnetic Compensation Points”* it is shown how the angular momentum compensation can indeed lead to ultrafast magnetization reversal, demonstrating experimentally for the first time a time-resolved observation of sub-picosecond magnetization reversal.

## 4.1 Thermal-induced Magnetization Dynamics in GdFeCo

### 4.1.1 Introduction

As also detailed in the second chapter, the rare earth - 3d transition metal (RE-TM) ferrimagnetic compounds are widely used materials for magneto-optical (MO) recording. Depending on their composition, RE-TM ferrimagnets can exhibit a magnetization compensation temperature  $T_M$  where the magnetizations of the RE and TM sublattices cancel each other and similarly, an angular momentum compensation temperature  $T_A$  where the net angular momentum of the sublattices vanishes. The theory of ferrimagnetic resonance [2, 3] predicts a strong temperature dependence of the dynamic behavior in such systems. In particular, the frequency of the homogeneous spin precession as well as the Gilbert damping parameter  $\alpha$ , are expected to diverge at the temperature  $T_A$  [21]. However, so far there are no experimental results to substantiate these claims in ferrimagnets such as RE-TM amorphous alloys. Experimental confirmation of these theoretical predictions is important for magnetic recording, since the combination of a high frequency and large damping of the spin precession would provide ultrafast and ringing-free magnetization reversal via precessional motion [5]. In addition, knowledge of the temperature behavior of the frequency and damping of the spin precession is crucial for the calculation of the domain wall velocity [6] and thus of great importance for magneto-optical recording. The knowledge of damping in RE-TM alloys is also important for applications in Magnetic Random Access Memory. In this case it is important to find the low damping regime of these materials in order to reduce the spin current required to switch the RE-TM free layer. Although of fundamental and technological interest, the temperature dependence of the Gilbert damping and of the magnetization precession frequency over the compensation points in multi-sublattice magnetic systems such as ferrimagnetic RE-TM alloys were not well known until now.

In this section the study of ultrafast laser induced spin dynamics in the RE-TM ferrimagnetic alloy GdFeCo is presented under various experimental conditions: different applied magnetic fields, different sample temperatures and various sample concentrations. In contrast to other techniques that use magnetic field pulses to excite the magnetic system, in the all-optical technique used here the magnetization is excited by laser pulses while a DC magnetic field is applied. In this case a ferrimagnet can be excited even near the compensation points where there is no net magnetic moment. As a result, it is demonstrated experimentally that both Gilbert damping and spin precession frequency increase significantly when the temperature of the sample approaches the point of angular momentum compensation  $T_A$ . These results indicate thus the crucial role of the angular momentum compensation for controlling the fast magnetization switching process. Moreover, our approach also allowed to observe the exchange resonance mode: as it softens near  $T_A$ , it is found to dominate the ferromagnetic resonance mode.

#### 4.1.2 Experimental Details

The magnetic material studied in this work is the ferrimagnetic rare earth-transition metal (RE-TM) amorphous alloy GdFeCo. The samples were grown by magnetron sputtering in the following multilayer structure: glass|AlTi(10nm)|SiN(5nm)|GdFeCo|SiN(60nm), where the GdFeCo layers analyzed in this work had the following composition and thickness:  $Gd_{22}Fe_{74.6}Co_{3.4}$ (20nm),  $Gd_{23}Fe_{73.64}Co_{3.36}$ (20nm),  $Gd_{23}Fe_{73.64}Co_{3.36}$ (30nm). The AlTi layer serves as a heat sink and SiNi as buffer and capping layer respectively. Such ferrimagnetic materials are widely used in magneto-optical recording [7] and known for their strong magneto-optical effects [8].

It was shown that in RE-TM amorphous alloys the magnetization compensation temperature  $T_M$  can be simply changed by tuning the composition of the ferrimagnet [9]. This effect can be clearly seen in the samples used for this study. Figure 4.1 demonstrates that two different compositions of the GdFeCo alloy show the divergence of the coercive field  $H_c$  at totally different temperatures. The coercive field has been extracted from the measured hysteresis loops at different temperatures. From the divergences of  $H_c$  we have identified the magnetization compensation points for the samples studied here as follows:  $T_M \sim 160$  K for  $Gd_{22}Fe_{74.6}Co_{3.4}$ (20nm),  $T_M \sim 370$  K for  $Gd_{23}Fe_{73.64}Co_{3.36}$ (20nm) and  $T_M \sim 390$  K for  $Gd_{23}Fe_{73.64}Co_{3.36}$ (30nm). Therefore, a variation not only of composition but also of the sample thickness results in a change of the magnetization compensation temperature. This effect, reflecting a change in the magnetic properties of the sample, is believed to be due to the preferred oxidation of the RE near the film boundaries causing a relative increase of the TM with respect to RE concentration by decreasing the film thickness [10, 11]. From the vanishing of the observed hysteresis towards high temperatures, the Curie temperature of the samples has been identified as  $T_c \sim 500$  K for  $Gd_{22}Fe_{74.6}Co_{3.4}$ (20nm),  $T_c \sim 525$  K

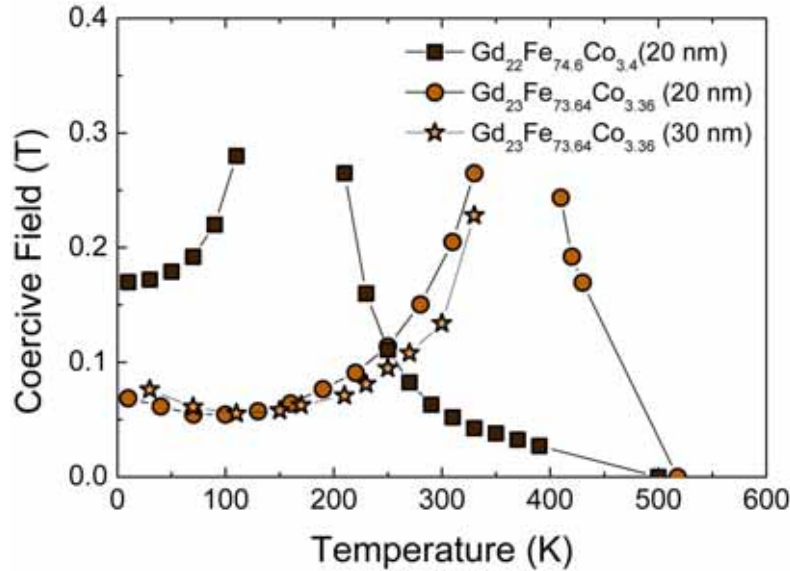


**Figure 4.1:** Temperature dependence of the coercive field  $H_c$  in ferrimagnetic amorphous alloy  $\text{Gd}_x\text{Fe}_y\text{Co}_z$  for samples with different composition and different thickness. The divergence of  $H_c$  indicates the magnetization compensation point  $T_M$ . Note that the coercive field was measured for an external magnetic field applied at an angle  $\theta_{\text{ext}} = 60^\circ$  from the easy axis of anisotropy.

for  $\text{Gd}_{23}\text{Fe}_{73.64}\text{Co}_{3.36}$  (20nm) and  $T_c \sim 525$  K for  $\text{Gd}_{23}\text{Fe}_{73.64}\text{Co}_{3.36}$  (30nm).

The magnetization dynamics in GdFeCo samples was induced and investigated using a time-resolved all-optical pump-probe set-up. Amplified 100 fs laser pulses at a central wavelength of 805 nm and a repetition rate of 1 kHz, emitted by a commercial Ti:Sapphire laser, were split into two beams of different intensities. The most intense (pump) pulses ( $I_{\text{pump}}/I_{\text{probe}} > 100$ ), were used to trigger the magnetization dynamics. The less intense (probe) pulses, delayed in time by a delay line, were used to probe the changes of the magnetic state of the sample as a function of time via the changes in the magneto-optical Faraday rotation. The Faraday rotation is proportional to the component of the magnetization vector  $\mathbf{M}$  along the wave vector  $\mathbf{k}$  of the light ( $\theta_F \propto \mathbf{M} \cdot \mathbf{k}$ ). Both linearly polarized beams were focused on to the sample to a spot of  $200 \mu\text{m}$  diameter for the pump and  $40 \mu\text{m}$  for the probe beam, at nearly normal incidence. Thus, the present geometry is sensitive to the variation in the out-of-plane component of the magnetization,  $\mathbf{M}_z$ . The measurements were carried out in a cold finger cryostat.

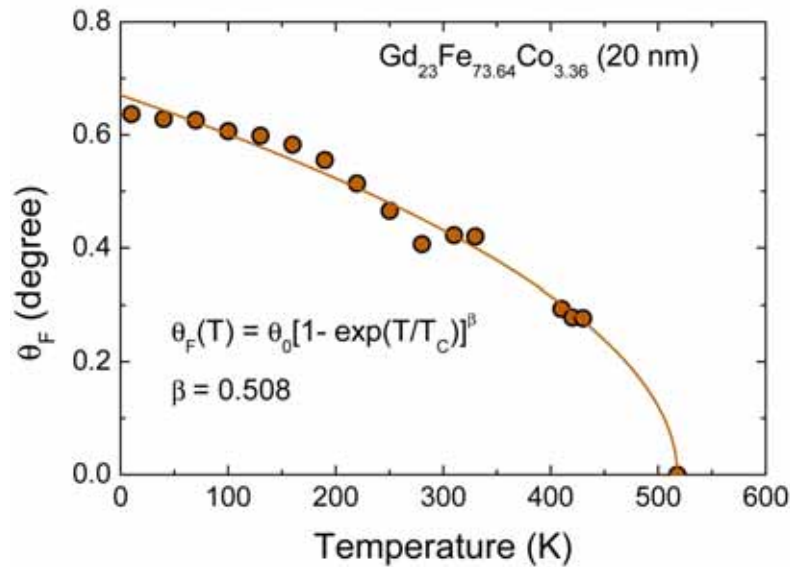


**Figure 4.2:** Measured Faraday rotation  $\theta_F$  at  $\lambda = 805$  nm as a function of temperature in  $\text{Gd}_{23}\text{Fe}_{73.64}\text{Co}_{3.36}$  (20nm). The solid line represents the fitting with the inset equation.

As discussed in Chapter 2, the laser wavelength of 805 nm used in the present experiments, representing a photon energy of 1.54 eV, probes mainly the FeCo sublattice [12–14]. This feature is a real advantage for the optical study of ferrimagnetic alloys with magnetization compensation points, since near this point the Faraday rotation remains strong although the net magnetic moment is vanishing. The Faraday rotation measured in  $\text{Gd}_{23}\text{Fe}_{73.64}\text{Co}_{3.36}$  (20nm), representing the magnetization of the FeCo sublattice is shown Figure 4.2 as a function of temperature. Here,  $M(T)$  exhibits a second order phase transition at  $T_c \sim 525$  K, with a critical exponent  $\beta = 0.508$ .

### 4.1.3 Magnetization Dynamics in a Two-Sublattice Magnetic Systems

Phenomenologically, the dynamics of the magnetization  $\mathbf{M}$  precessing in a magnetic field  $\mathbf{H}$  is routinely described by the Landau-Lifshitz-Gilbert equation (LLG) [15–17]. This equation can also well describe the magnetization dynamics in a ferrimagnetic system as our RE-TM alloy, but now the LLG must be written for a two sublattice

system as [2]

$$\frac{d\mathbf{M}_1}{dt} = -|\gamma_1|[\mathbf{M}_1 \times (\mathbf{H}_1 - \lambda_{\text{ex}}\mathbf{M}_2)] + \frac{\alpha_1}{M_1}(\mathbf{M}_1 \times \frac{d\mathbf{M}_1}{dt}) \quad (4.1)$$

and

$$\frac{d\mathbf{M}_2}{dt} = -|\gamma_2|[\mathbf{M}_2 \times (\mathbf{H}_2 - \lambda_{\text{ex}}\mathbf{M}_1)] + \frac{\alpha_2}{M_2}(\mathbf{M}_2 \times \frac{d\mathbf{M}_2}{dt}), \quad (4.2)$$

where 1 and 2 represent the RE and TM sublattices respectively, with the gyromagnetic ratio

$$|\gamma_i| = g_i \frac{\mu_B}{\hbar} \quad (4.3)$$

and the Gilbert damping parameter  $\alpha_i$  given by:

$$\alpha_i = \frac{\lambda_i}{|\gamma_i|M_i} \quad (4.4)$$

where  $i=1,2$ . Here  $\lambda$  is the Landau-Lifshitz damping parameter [15]. These equations are coupled by the presence of the exchange fields  $-\lambda_{\text{ex}}\mathbf{M}_1$  acting on  $\mathbf{M}_2$  and  $-\lambda_{\text{ex}}\mathbf{M}_2$  acting on  $\mathbf{M}_1$ , and as we will see in the following, give rise to two resonance modes. Here  $\lambda_{\text{ex}}$  is the exchange constant.

### The ferromagnetic mode

Assuming an applied magnetic field sufficiently low, far from the compensation points, the ferrimagnetic system behaves as a simple ferromagnetic system with its motion described by a single LLG equation

$$\frac{d\mathbf{M}}{dt} = -|\gamma_{\text{eff}}|(\mathbf{M} \times \mathbf{H}_{\text{eff}}) + \frac{\alpha_{\text{eff}}}{M}(\mathbf{M} \times \frac{d\mathbf{M}}{dt}), \quad (4.5)$$

but now employing an effective gyromagnetic ratio  $\gamma_{\text{eff}}$  [2, 18]:

$$\gamma_{\text{eff}}(T) = \frac{M_1(T) - M_2(T)}{M_1(T)/|\gamma_1| - M_2(T)/|\gamma_2|} = \frac{M(T)}{A(T)} \quad (4.6)$$

and an effective Gilbert damping parameter  $\alpha_{\text{eff}}$  [20, 33]

$$\alpha_{\text{eff}}(T) = \frac{\lambda_1/|\gamma_1|^2 + \lambda_2/|\gamma_2|^2}{M_1(T)/|\gamma_1| - M_2(T)/|\gamma_2|} = \frac{A_0}{A(T)} \quad (4.7)$$

where  $A(T)$  is the net angular momentum of the ferrimagnetic system;  $A_0$  is a constant under the assumption of the Landau-Lifshitz damping parameter being independent on temperature [21]. The validity of this assumption was confirmed over a wide temperature interval by FMR measurements in 3d-TM [22].

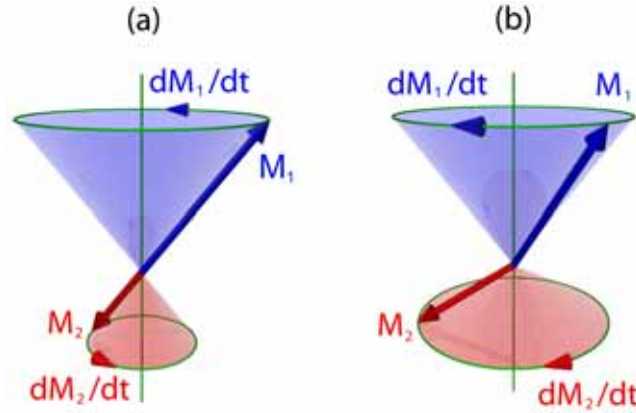


**Figure 4.3:** Schematic illustration of the two resonance modes present in the ferrimagnetic resonance [27, 33]: a) the ferromagnetic mode  $\omega_{\text{FMR}}$  where the two sublattices remain parallel; b) the exchange mode  $\omega_{\text{ex}}$  where the angle between  $\mathbf{M}_1$  and  $\mathbf{M}_2$  is changed during the precession. While far from compensation points the system precesses in a magnetic field as shown in panel (a), near the angular momentum compensation the resonance of the ferrimagnetic system may become a mixture of the two modes.

Thus, Eq. 4.5 describes the *ferromagnetic* resonance (FMR) mode,

$$\omega_{\text{FMR}}(T) = \gamma_{\text{eff}}(T) \mathbf{H}_{\text{eff}}(T), \quad (4.8)$$

This is the resonance mode where the sublattices remain almost perfectly antiparallel to each other as they precess around the effective field  $\mathbf{H}_{\text{eff}}$  [see Fig. 4.3 a)]. This effective field acting on the net magnetic moment  $\mathbf{M}$ , where  $\mathbf{M} = \mathbf{M}_1 + \mathbf{M}_2$ , is determined by the applied magnetic field  $\mathbf{H}_{\text{ext}}$ , the magneto-crystalline anisotropy field  $\mathbf{H}_{\text{a}}$  and the shape anisotropy field  $\mathbf{H}_{\text{s}}$ . The precession direction of the FMR mode is given by the sign of  $\gamma_{\text{eff}}$  resulting usually in a positive  $\omega_{\text{FMR}}$  (counterclockwise precession), with the exception of the region between  $T_{\text{M}}$  and  $T_{\text{A}}$  where  $\gamma_{\text{eff}}$  changes sign because of the parallel alignment of  $M$  and  $A$  [3].

### The exchange mode

In addition to the ferromagnetic mode  $\omega_{\text{FMR}}$ , spins in a ferrimagnetic system may oscillate with the *exchange* (Kaplan and Kittel) resonance frequency [26, 27]

$$\begin{aligned} \omega_{\text{ex}}(T) &= \lambda_{\text{ex}}(|\gamma_2| M_1 - |\gamma_1| M_2) \\ &= \lambda_{\text{ex}} |\gamma_1| |\gamma_2| A(T). \end{aligned} \quad (4.9)$$



The number of exchange modes present in a ferrimagnet is  $N-1$ , where  $N$  is the number of sublattices. Thus, in GdFeCo only one such mode exists. This resonance mode is a result of the distortion of the coupling between the two sublattices [see Fig. 4.3 b)]. The motion of a magnetic sublattice is determined here by the exchange field generated by the opposite sublattice. At low applied magnetic field, such as that used in general in the experiments, the frequency  $\omega_{\text{ex}}$  lies usually in the infrared (THz) region [28] but approaching the compensation points it can appear in the microwave (GHz) region [29, 30, 33].

Eqs. 4.6 and 4.7 indicate a divergence of both the precession frequency and Gilbert damping parameter of the FMR mode at the temperature  $T_A$  where  $A$  goes to zero. On the other hand, Eq. 4.6 also indicates that the FMR frequency strongly decreases towards  $T_M$ . However, since  $\omega_{\text{FMR}}$  is affected by both  $\gamma_{\text{eff}}$  and  $\mathbf{H}_{\text{eff}}$ , Eq. 4.6 alone cannot fully describe the FMR frequency near  $T_M$ . In order to explain the temperature dependence of  $\gamma_{\text{eff}}$  near this point, the magneto-crystalline anisotropy (that is a part of  $\mathbf{H}_{\text{eff}}$ ) should be also taken into account [33]. This issue will be further discussed in subsection 4.1.6. Next, from Eq. 4.9, one can notice that the exchange resonance branch softens at the angular momentum compensation temperature  $T_A$  [29], and thus may also become observable in our experiments.

It should be mentioned here, that because GdFeCo contains  $S$ -state RE ions and orbital-momentum-quenched  $3d$  ions, it is in general referred to as a ferrimagnetic system that possesses equivalent gyromagnetic ratios for the two sublattices. However such a system where  $\gamma_1 = \gamma_2$  would result in a  $\gamma_{\text{eff}}$  that would not depend on temperature. On the other hand previous experiments on similar RE-TM (i.e. Gd-Fe) thin films [23] and the present experiments reveal a clear temperature dependence of  $\gamma_{\text{eff}}$ , thus indicating that the assumption  $\gamma_1 = \gamma_2$  in GdFeCo is not applicable.

#### 4.1.4 Magnetization Precession Excitation Mechanism

The scenario for the excitation of the spin waves in GdFeCo is as follows: Initially, the magnetization  $\mathbf{M}$  lies normal to the sample plane, along the easy axis of anisotropy. Next, an external magnetic field  $\mathbf{H}_{\text{ext}}$  is applied at an angle  $\theta_{\text{ext}} = 60^\circ$  from the easy axis of anisotropy. This results in the canting of the magnetization at an angle  $\theta$  from the easy axis, the size of which depends on the strength of the applied field. Thus, the magnetization is now aligned along the effective field:

$$\mathbf{H}_{\text{eff}}(T) = \mathbf{H}_{\text{ext}} + \mathbf{H}_{\text{a}}(T) + \mathbf{H}_{\text{s}}(T). \quad (4.10)$$

This is the initial condition used in our experiments [Fig. 4.4 a)]. Here  $\mathbf{H}_{\text{ext}}$  is the Zeeman contribution due to the *external magnetic field*.  $\mathbf{H}_{\text{a}}$  is the *anisotropy field* and has its origin in the magneto-crystalline anisotropy energy of the sample  $K_{\text{u}}(T)\sin^2\theta$ , where  $K_{\text{u}}(T)$  is the temperature dependent anisotropy constant. Here, the effective

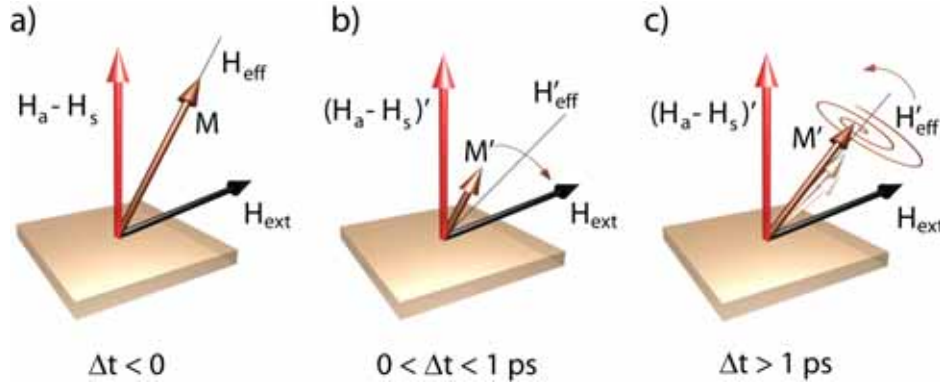


**Figure 4.4:** Schematic illustration of the excitation process. (a) Initially magnetization lies along the effective field  $\mathbf{H}_{\text{eff}}$ . (b) Following laser excitation, magnetization  $\mathbf{M}$  and magneto-crystalline anisotropy are changed. (c) This process triggers the precessional motion of  $\mathbf{M}$  around the new effective field  $\mathbf{H}'_{\text{eff}}(T)$  with an orientation that changes in time due to the thermal diffusion.

anisotropy field is [24]

$$H_a(T) \propto 2K_u(T)/M(T). \quad (4.11)$$

In solids, the magneto-crystalline anisotropy is determined by the asymmetrical overlap of electron distribution of neighboring ions. This asymmetry is translated to the spin via the spin-orbit coupling. In other words, the magneto-crystalline anisotropy is a measure of how strong the spin is locked to a special lattice direction (easy axis) by the spin-orbit coupling. The magneto-crystalline anisotropy energy is therefore minimal when the magnetization lies along the easy axis. In ferromagnetic materials, the spin-orbit interaction energy is relatively small compared to that of the exchange interaction. While its energy is of the order of 10-100 meV, the exchange energy can be as high as 1 eV. However, since the exchange interaction only aligns the magnetic moments (one with respect to the other), regardless of their direction relative to the lattice, the *exchange field* is not taken into account in Eq. 4.10.  $\mathbf{H}_s$  is the *shape anisotropy field*. The origin of this field is in the shape anisotropy energy that is also known as stray field energy, magnetostatic energy or demagnetization field energy. This energy is due to the interaction between the magnetic dipoles. More clearly, it originates from a long range interaction of the magnetic field of the ferromagnetic sample with its own magnetization. In this case, it should indeed depend on the shape of the sample and should be proportional to the magnitude of the sample magnetization. For the thin film case,  $\mathbf{H}_s$  tends to pull the magnetization towards the plane of the sample.

As we have seen in the Chapter 1, a sudden heating of a metallic magnet by a 100 fs laser pulse leads to an ultrafast demagnetization on a time scale shorter than 300 fs. Once the hot electrons and spins thermalize, their subsequent relaxation is mediated by the electron-phonon relaxation that results in an increase of the lattice temperature. After  $\sim 1$  ps electron, spin and lattice temperature are in equilibrium. At this time the magnitude of both the magnetization and the magneto-crystalline anisotropy are changed, leading to a change of both  $\mathbf{H}_a$  and  $\mathbf{H}_s$  and thus of  $\mathbf{H}_{\text{eff}}$  into  $\mathbf{H}'_{\text{eff}}$  [Fig. 4.4 b)]. Following this change, the magnetization  $\mathbf{M}$  will move out of the initial equilibrium towards the new effective field  $\mathbf{H}'_{\text{eff}}$ , via a precessional motion. This precessional motion takes place until the magnetization finds its new equilibrium with  $\mathbf{H}'_{\text{eff}}$  [Fig. 4.4 c)]. Note that  $\mathbf{H}'_{\text{eff}}$  varies in time due to the temperature decrease via heat diffusion. When the heat is completely diffused out of the sample (via lateral diffusion in the metal and a perpendicular heat transfer to the substrate), the magnitude of both  $\mathbf{M}$  and magneto-crystalline anisotropy is restored, thus restoring the initial equilibrium of  $\mathbf{M}$  [Fig. 4.4 a)]. The time required for the thermal diffusion in GdFeCo is a few nanoseconds.

#### 4.1.5 Coherent Magnetization Precession as a Function of the Magnetic Field Amplitude: Ferromagnetic Resonance

Figure 4.5 shows the observed precession excited at a pump fluence of about  $2.2 \text{ mJ/cm}^2$  as a function of the amplitude of the external field in  $\text{Gd}_{22}\text{Fe}_{74.6}\text{Co}_{3.4}$  (20nm). The thermal energy which is transferred from the laser to the material induces a significant increase in the local temperature of the sample at this pump fluence. The temperature indicated in the figure takes into account this heating. Therefore  $T = 350 \text{ K}$  does not represent the static temperature of the sample but instead represents the real temperature at which the spin precession is taking place. Details about how the local increase in temperature due to the laser beam can be experimentally extracted will be presented in the following discussion of this section. Besides the oscillatory character of the  $M_z$  component of the magnetization associated with magnetization precession, Figure 4.5 shows also an instantaneous step-like change of  $M_z$  following laser excitation. The observed step-like process is a result of the ultrafast demagnetization ( $\sim 200 \text{ fs}$ ) [31, 32]. Following this step-like process the magnetization starts a precession motion damped on a time-scale of a few hundred picoseconds. It is interesting to observe that the precession is damped long before the magnetization recovers its magnitude and thus also long before the pump energy is diffused out of the lattice. Therefore, this observation indicates the damping mechanism to be faster than the thermal diffusion time. While for zero applied magnetic field no oscillation of the  $M_z$  component can be observed (not shown here), increasing the amplitude of the magnetic field the amplitude and the frequency of the magnetization precession increase. The strong dependence of the frequency of the oscillatory magneto-optical

response on the magnitude of the magnetic field indicates that this oscillatory signal is related to the temporal variation of the magnetization due to its precessional motion. The increase of the frequency is expected due to the higher Zeeman term in equation 4.10. Thus, as expected, an increase of  $|\mathbf{H}_{\text{eff}}|$  leads to an increase of  $\omega_{\text{FMR}}$  (see Eq. 4.8).

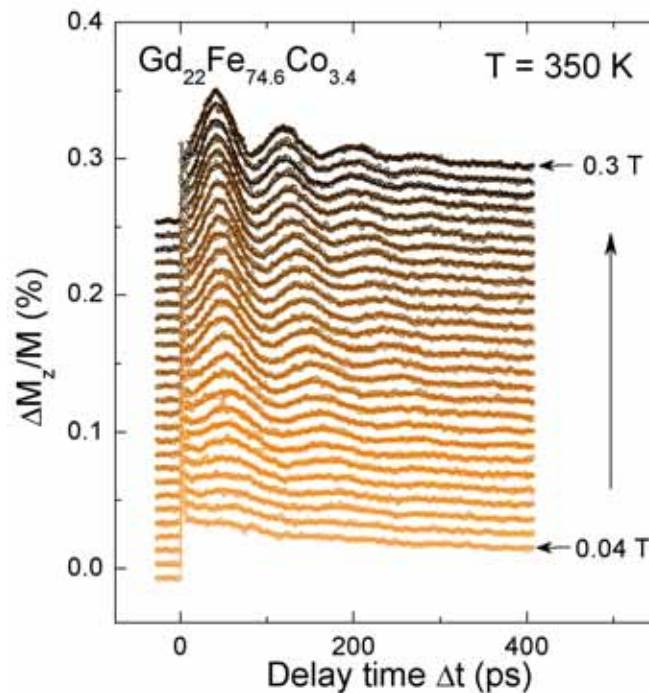


**Figure 4.5:** Magnetization precession in GdFeCo as a function of the applied magnetic field after exciting the sample at a pump fluence of about  $2.2 \text{ mJ/cm}^2$ . The temperature presented in the figure (350 K) includes the temperature increase induced locally by the pump pulses, thus representing the real temperature at which the precession takes place. The data are offset for clarity.

The time resolved magnetic signal can be modelled with an exponentially damped sine wave function added to a linear background. The damped sine function has the form

$$\Delta\theta_F = \Delta\theta_0 \sin(\omega t + \varphi_0) \exp(-t/\tau), \quad (4.12)$$

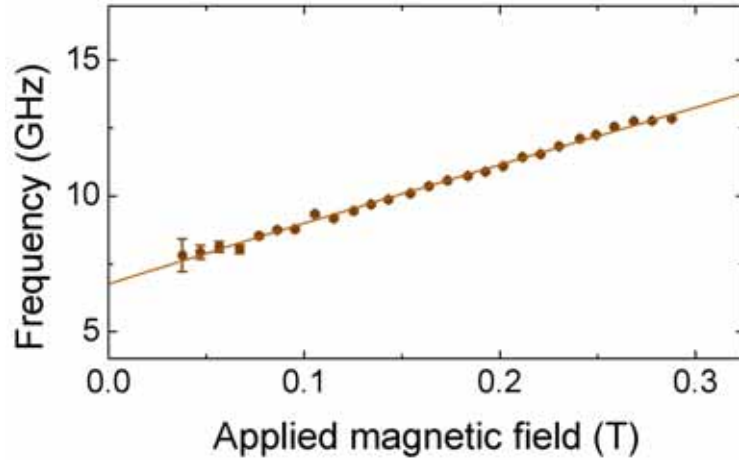


**Figure 4.6:** Frequency spectrum of the  $\omega_{\text{FMR}}$  mode determined from the fitting of the time resolved measurements in Fig. 4.5 with  $\alpha_{\text{eff}} = 0.135$ . The solid line represents the best fit using Eq. 4.13.

representing a precession at a frequency  $\omega$  with an amplitude  $\Delta\theta_0$  and a starting phase  $\varphi_0$  which decays exponentially with the characteristic time  $\tau$ . Thus, such fitting allows a determination of the precessional frequency  $\nu = \omega/2\pi$  and the Gilbert damping parameter  $\alpha_{\text{eff}} = 1/\tau\omega$ . Thus, fitting the experimental data yields precession frequencies of several GHz and a common Gilbert damping  $\alpha_{\text{eff}} = 0.135$ , in good agreement with FMR results [33]. The precession frequencies are well fitted by the Kittel equation which, for the geometry of interest here, is:

$$\omega = \frac{\gamma_{\text{eff}}}{(1 + \alpha_{\text{eff}}^2)} \times \sqrt{(H_{\text{ext}} \cos \theta_{\text{ext}} + |H_{\text{a}} + H_{\text{s}}|)^2 - (H_{\text{ext}} \sin \theta_{\text{ext}})^2}. \quad (4.13)$$

The measurements representing  $T = 350$  K are well described by an internal anisotropy field  $|H_{\text{a}} + H_{\text{s}}| = 0.26$  T and an effective  $g$ -factor  $g_{\text{eff}} = 1.85$ , which is in very good agreement with previous measurement [34] on GdFeCo. This observation indicates on the one hand that the effective gyromagnetic ratio  $\gamma_{\text{eff}}$  is dominated by the spin angular momentum in the GdFeCo case and on the other, that at 350 K only the FMR branch is observed.

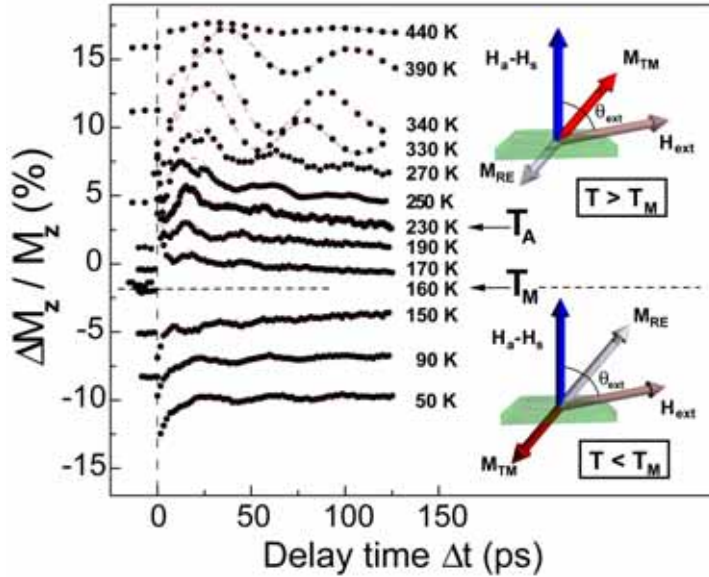
Based on the results presented above we can conclude that:

- a pump fluence of about 2.2 mJ/cm<sup>2</sup> in our experiments triggers a coherent precession with precessional parameters in agreement with the theoretical expectations;
- the precession vanishes long before the electron, spin and lattice temperatures are recovered. As a result, for relatively low laser fluence the magnetization precession frequency is not significantly affected by the heat diffusion;
- the precession observed at 350 K corresponds to the FMR branch described by Eq. 4.8;
- in GdFeCo the effective gyromagnetic ratio  $\gamma_{\text{eff}}$  is dominated by the spin angular momentum.

#### 4.1.6 Magnetization Precession as a Function of Temperature: Ferrimagnetic Resonance

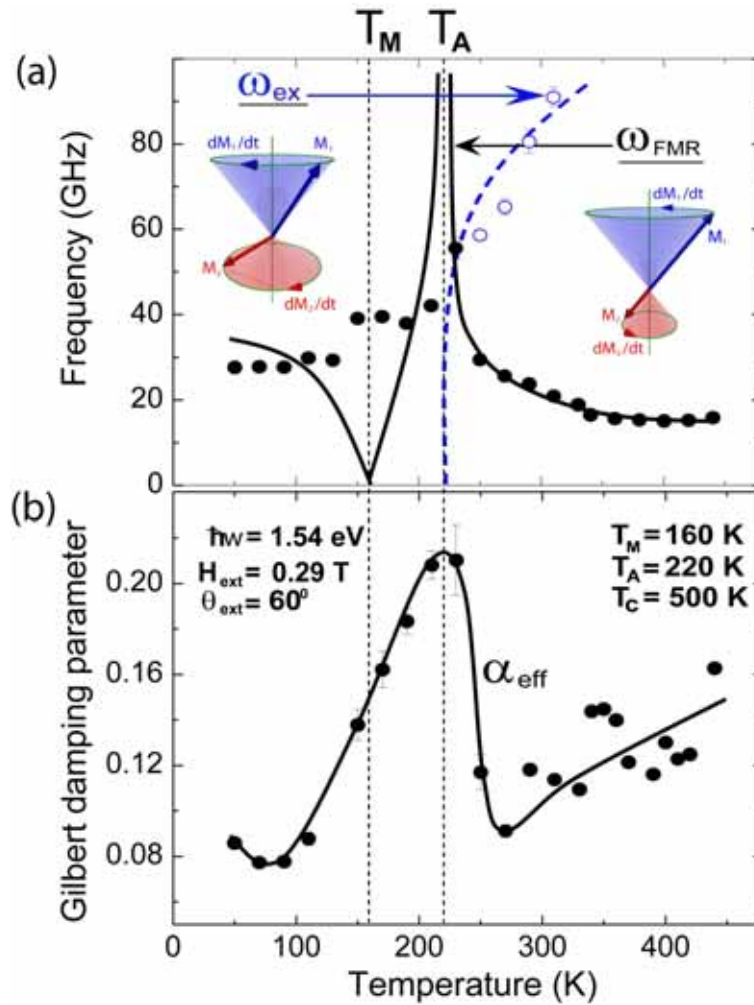
The experiments presented above were done at a temperature where the observed precession represents the ferromagnetic mode. In this case the two coupled Gd and FeCo sublattices precess antiparallel with respect to each other. In order to observe the effect of the ferrimagnetic structure on the resonance of the system we have performed pump-probe experiments as a function of temperature. The temperature dependence of the magnetization dynamics in Gd<sub>22</sub>Fe<sub>74.6</sub>Co<sub>3.4</sub> (20nm), at an external field  $\mathbf{H}_{\text{ext}} = 0.29$  T ( $\theta_{\text{ext}} = 60^\circ$ ), is shown in Figure 4.7. In these experiments, the magnetization precession was excited at a pump fluence of about 2 mJ/cm<sup>2</sup>. Apart from a clear temperature dependence of the frequency and damping, Figure 4.7 shows that the step-like process, representing the ultrafast demagnetization, changes its sign between 150 K and 170 K. This happens because of the presence of the compensation point  $T_M$ . For  $T < T_M$  ( $\sim 160$  K) the TM magnetic moment is smaller than that of Gd. Thus the  $\mathbf{M}_{\text{RE}}$  is aligned along the applied field direction. At  $T > T_M$ ,  $\mathbf{M}_{\text{TM}}$  becomes larger than  $\mathbf{M}_{\text{RE}}$  and the ferrimagnetic system flips, allowing the TM component to be aligned along the direction of the applied field  $\mathbf{H}_{\text{ext}}$ . It is clear that this will lead to a sign change of the observed component of the magnetization,  $\mathbf{M}_{\text{TM}}$ , consistent with the fact that a photon energy of 1.54 eV probes mainly the TM sublattice of the ferrimagnetic system.

Note that the temperature measured on the sample at  $T_M$ , during the magnetization dynamics measurements, was 120 K. However, static measurements performed on the same sample indicate  $T_M$  at 160 K (see Fig. 4.1). The origin of this disagreement is the increase of the temperature induced locally by the pump pulses. From here one can deduce that the 2 mJ/cm<sup>2</sup> laser fluence leads to a local increase of the sample temperature of about 40 K. Therefore, the temperature shown in the figures representing magnetization dynamics has been modified accordingly.



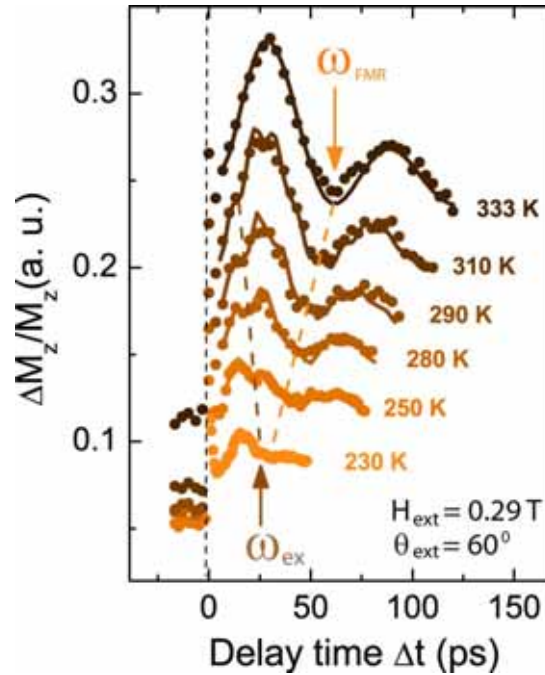
**Figure 4.7:** Temperature dependence of coherent precession of the magnetization in GdFeCo, measured at an external field  $\mathbf{H}_{\text{ext}} = 0.29$  T. Around 160 K magnetic compensation  $T_M$  of the ferrimagnetic system occurs. The inset shows the alignment of the RE-TM system under an external applied field, below and above  $T_M$ .

Figure 4.8 shows the temperature dependence of the magnetization precession frequency (a) and the Gilbert damping parameter (b). At the temperature  $T = 220$  K a significant increase is observed in both the precession frequency and the damping parameter. As expected from Eqs. 4.6 and 4.7, the fact that both  $\alpha_{\text{eff}}$  and  $\omega_{\text{FMR}}$  peak at the same temperature, clearly indicates the existence of angular momentum compensation near this temperature of 220 K. The strong temperature dependence of  $\gamma_{\text{eff}}$  demonstrates the nonequivalent character of the gyromagnetic ratios of the two magnetic sublattices in GdFeCo. In addition to the peak near  $T_A$ , we have also observed an enhancement of  $\alpha_{\text{eff}}$  as the temperature is increased towards the Curie temperature. Again Eq. 4.7 predicts this enhancement under the assumption of temperature independent Landau-Lifshitz damping parameters  $\lambda_{\text{RE}}$  and  $\lambda_{\text{TM}}$ . This enhancement is consistent with earlier data [35, 36]. Our measurements thus demonstrate the consistency of the theoretical prediction of Eq. 4.7 with the temperature dependence of  $\alpha_{\text{eff}}$  in RE-TM alloys like GdFeCo.



**Figure 4.8:** Temperature dependence of: (a) the magnetization precession frequencies  $\omega_{FMR}$  and  $\omega_{ex}$ . As temperature decreases from 310 K towards  $T_A$ , the exchange resonance mode  $\omega_{ex}$  (open circles) softens and mixes with the ordinary FMR resonance  $\omega_{FMR}$  (closed circles). Since around 230 K both FMR and exchange modes have essentially the same frequency, the frequency indicated at 230 K may represent both the FMR and the exchange resonance mode. The insets show schematically the two modes. The solid lines are a qualitative representation of the expected trend of the two resonance branches as indicated by Eq. 4.6 and Eq. 4.9. (b) the Gilbert damping parameter  $\alpha_{eff}$ . Lines are guide to the eye.





**Figure 4.9:** Time traces of the precession excited at temperatures near the angular momentum compensation  $T_A$ . As the temperature of the ferrimagnetic system approaches  $T_A$ , the ferromagnetic mode  $\omega_{\text{FMR}}$  becomes distorted by a high-frequency mode that is identified with the exchange resonance mode  $\omega_{\text{ex}}$ . The time resolved spectra is fitted with a function composed of two damped sine functions such as that defined by Eq. 4.12. The resulted precession frequencies are shown in Fig. 4.8. Due to the actual signal-to-noise ratio, the damping of the mode  $\omega_{\text{ex}}$  could not be determined.

In the temperature region just above  $T_A$  the measured time dependencies reveal two frequencies, one decreasing and another increasing with temperature (see Fig. 4.9). While the former one can be attributed to the FMR mode (see Fig. 4.6), such temperature behavior allows to assign the latter one to the exchange mode (see Eq. 4.9), the frequency of which can be low around  $T_A$  but is usually very high everywhere else.

Although around  $T_A$ , the temperature dependence of the precession frequency appears to be in very good agreement with theory, this is not the case for the region near  $T_M$ . From Eq. 4.6 one would expect a strong decrease of the precession frequency at  $T_M$ . Instead, at this temperature Fig. 4.8 (a) still indicates values of tens of GHz for

the precession frequency and, if anything, an increase rather than a decrease near  $T_M$ . Initially, it was concluded that the high precession frequency observed on the low-temperature side of  $T_M$  could be attributed to an inhomogeneity of the instantaneous temperature distribution in the laser excitation spot [14]. Indeed it can be argued that when excited with a laser pulse in such strong temperature dependence region as near  $T_M$ , a whole spectrum of frequencies can be excited, with the signals from various modes adding up. In this case, it is easy to show that such averaging favors observation of the highest frequency, i.e.

$$\int_0^{\omega_0} \cos \omega t d\omega = \frac{1}{t} \sin \omega_0 t \quad (4.14)$$

However, as it will be further demonstrated, the reason for the apparent disagreement between the experimental observation and the expected trend of the FMR mode is the temperature dependence of the anisotropy field, characteristic for a ferrimagnet that possesses a magnetization compensation point. Near the compensation points the magneto-crystalline anisotropy should be taken into account, no matter how small it is [33]. Since it is inversely proportional to the net magnetic moment (see Eq. 4.11), the anisotropy field should strongly increase towards  $T_M$ , which will have a strong effect on the FMR mode. Thus, from Eq. 4.6, Eq. 4.8, Eq. 4.10 and Eq. 4.11, the temperature dependence of the ferromagnetic mode near  $T_M$  is described essentially by

$$\omega_{\text{FMR}}(T) = \gamma_{\text{eff}}(T) \mathbf{H}_{\text{eff}}(T) \propto \gamma_{\text{eff}}(T) \mathbf{H}_{\text{a}}(T) \propto \frac{M(T)}{A(T)} \cdot \frac{K_{\text{u}}(T)}{M(T)} \propto \frac{K_{\text{u}}(T)}{A(T)} \quad (4.15)$$

The term  $(M(T)/A(T))(\mathbf{H}_{\text{ext}} + \mathbf{H}_{\text{s}})$  was neglected in the above equation as it becomes unimportant near  $T_M$ , while for the rest of the temperature range it behaves in the manner as  $K_{\text{u}}(T)/A(T)$ . Thus, Eq. 4.15 indicates that with the exception of the specific case  $T_M$ , where  $\mathbf{M}$  must also be considered, the temperature dependence of  $\omega_{\text{FMR}}$  in the vicinity of  $T_M$  is mainly defined by the ratio of the magneto-crystalline anisotropy to the angular momentum of the ferrimagnetic system. Consequently, the presence of magneto-crystalline anisotropy should indeed lead to an effective increase of the observed FMR frequency while increasing the sample temperature from both the low- and the high-temperature site, towards  $T_A$ .

In order to illustrate the temperature dependence of the anisotropy field (which according to Eq. 4.11 is expected to increase from both the low- and the high-temperature site, towards  $T_M$ ), we have performed pump-probe experiments on  $\text{Gd}_{22}\text{Fe}_{74.6}\text{Co}_{3.4}$ (20nm) for various fields at different temperatures. The resulting precession frequencies are shown in Figure 4.10. Fitting the precession frequency at 290 K, 310 K and 350 K by the Kittel equation we have obtained the temperature dependence of the internal anisotropy field  $|\mathbf{H}_{\text{a}} + \mathbf{H}_{\text{s}}|$ , presented as the inset in Figure 4.10. A clear

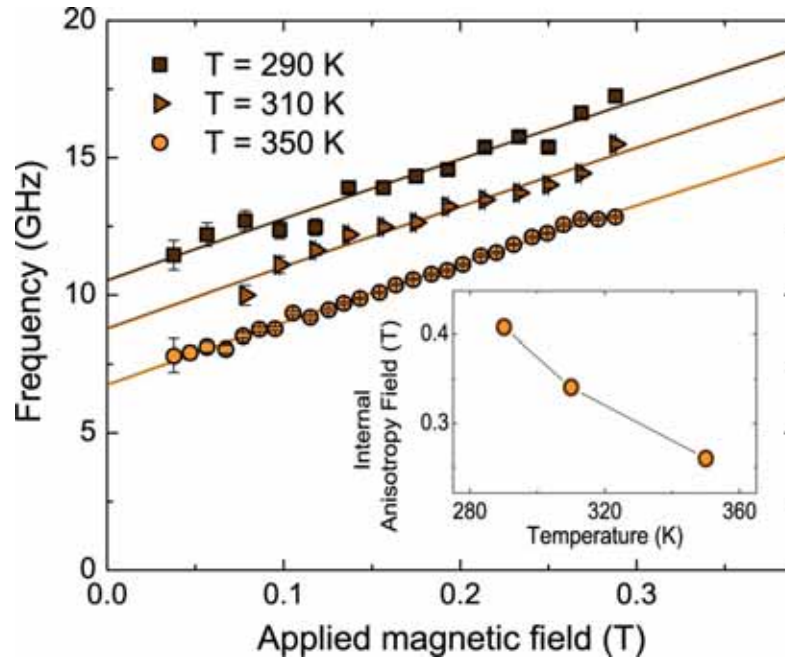


**Figure 4.10:** Magnetization precession frequency for different magnetic field amplitude, at various temperatures in  $\text{Gd}_{22}\text{Fe}_{74.6}\text{Co}_{3.4}$ (20nm). The fitting of the data using Eq. 4.13 reveals an increase of the internal anisotropy field  $|\mathbf{H}_a + \mathbf{H}_s|$  towards  $T_M$ , as expected from Eq. 4.11.

increase of the anisotropy field is observed as the sample temperature approaches  $T_M$ . This enhancement of  $\mathbf{H}_a$  is in agreement with previous observations [37], with Eq. 4.11, and with the temperature dependence of  $\omega_{\text{FMR}}$ . Yet, these experiments show the temperature dependence of  $\mathbf{H}_a$  only on the high-temperature side of  $T_M$ . Nevertheless, the increase of  $\mathbf{H}_a$  towards  $T_M$  on the low-temperature side is fully revealed by the next experiment.

To investigate in more details the magnetization dynamics below  $T_A$  (and  $T_M$ ), we have chosen a GdFeCo sample with the following composition:  $\text{Gd}_{23}\text{Fe}_{73.64}\text{Co}_{3.36}$  (30nm). As can be seen in Fig. 4.1, the magnetization compensation of this sample occurs at about 390 K. Consequently, this high temperature magnetization compensation point allows for the study of the magnetization dynamics in the ferrimagnetic system over a wide range of temperatures below both  $T_A$  and  $T_M$ . The transient Faraday effect traces as a function of temperature in  $\text{Gd}_{23}\text{Fe}_{73.64}\text{Co}_{3.36}$ (30nm) are shown in Figure 4.11. In these experiments the temperature has been varied between

50 K and 370 K. The corresponding precession frequencies are presented in the inset of Figure 4.11. As can be seen, in this case, a clear signature of the (quasi) divergence of the FMR mode towards  $T_A$  can be observed. Since the signature of this divergent trend is already present for temperatures far from  $T_A$ , it can not be attributed to an inhomogeneity of the instantaneous temperature distribution in the laser excitation spot. Therefore, it is clear that below  $T_A$  the trend of the FMR mode is in agreement with Eq. 4.15, thus explaining the high precession frequency observed near  $T_M$  as shown in Figure 4.8.

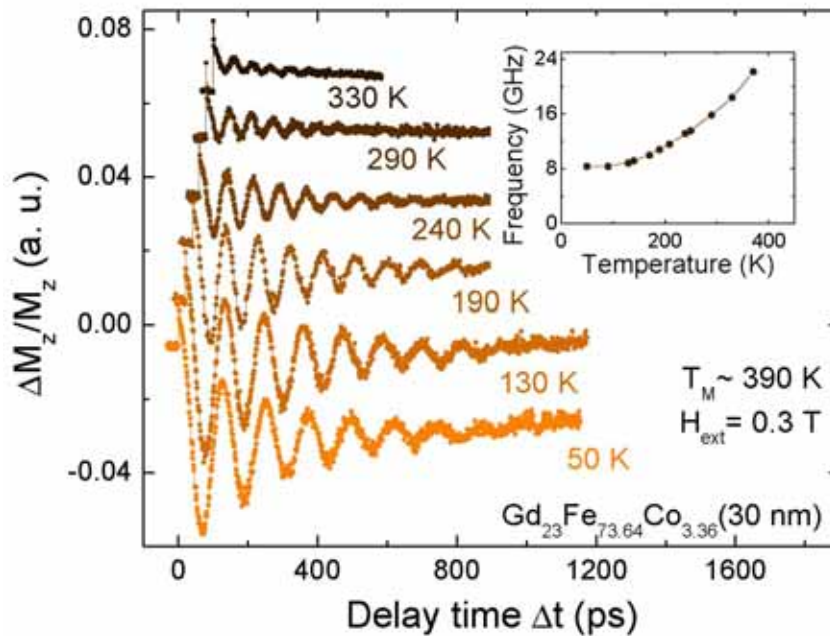


**Figure 4.11:** The transient Faraday effect traces as a function of temperature in  $Gd_{23}Fe_{73.64}Co_{3.36}$  (30 nm), below  $T_M$ . The precession frequencies shown in the inset were determined by nonlinear fitting of the measurements with a damped sine wave function such as Eq. 4.12.

Another feature that can be observed in Figure 4.11 is the initial phase of the magnetization precession, that is opposite from the phase of the precession shown in Figure 4.5. In particular, at temperatures below the magnetization compensation point the magnetization dynamics start from the maximum of the observed precession. This is in contrast to the dynamics taking place at temperatures above  $T_M$

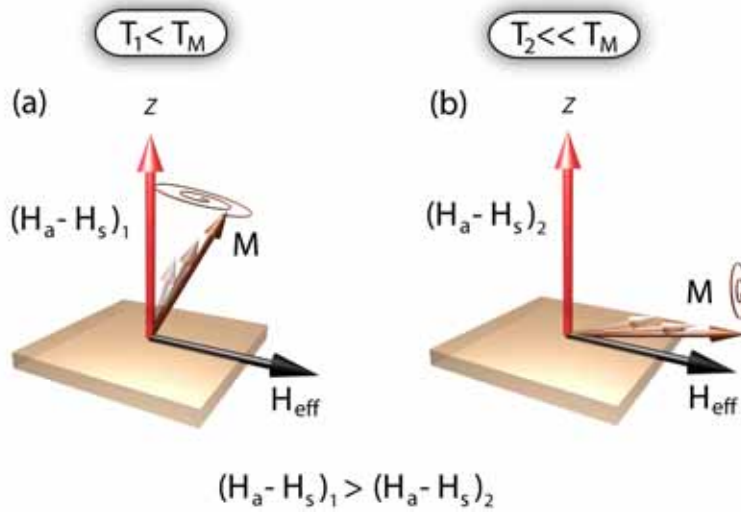


**Figure 4.12:** Schematic illustration of the magnetization dynamics below the magnetization compensation temperature  $T_M$ . (a) At temperatures close to  $T_M$ , because  $\mathbf{H}_a$  is larger, the magnetization vector precesses near the easy axis. (b) At lower temperatures  $\mathbf{H}_a$  decreases and the magnetization vector precesses closer to the plane of the sample. As a result, the z-component of the magnetization vector representing the precessional motion increases while that representing the demagnetization process is reduced (see Fig. 4.11).

where the magnetization starts its precessional motion from a minimum (see Fig. 4.5). This striking difference originates from the different temperature dependence of the anisotropy field below and above  $T_M$ . More specifically, the anisotropy field increases from low temperatures towards  $T_M$  and once  $T_M$  is crossed, the anisotropy field starts decreasing towards  $T_c$ . Therefore, when the temperature of the sample is above  $T_M$ , the pump pulse that triggers the magnetization dynamics leads to a further decrease of the anisotropy field. In this case, the magnetization vector rotates first towards the applied external field of the sample (towards the sample plane). Such precessional dynamics will be observed as an oscillation starting from its minimum (see Fig. 4.5). On the other hand, if the sample temperature is at a temperature below  $T_M$ , the heating induced by the pump pulse will lead to an increase of the anisotropy field. In this case, the step-like process due to the ultrafast demagnetization will be followed by a dynamics where the magnetization vector rotates towards  $\mathbf{H}_a$  (towards the normal to the sample) observed as an oscillation starting from its maximum (see Fig. 4.11).

Besides the change in the phase of the precession in Figure 4.11, we can also note

that upon reducing the temperature of the sample from 330 K down to 50 K, a gradual change in the offset of the equilibrium direction, around which the magnetization precesses, occurs. Note, that the origin of this change is not another magnetization compensation point but instead is again a result of the temperature dependence of the anisotropy field. To explain this behavior it must be noted that the observed step-like process representing the ultrafast demagnetization is reduced with decreasing temperature. This happens because, as the temperature is reduced,  $\mathbf{H}_a$  is also reduced, resulting in a more effective action of  $\mathbf{H}_{\text{ext}}$  that pulls the magnetization towards in-plane (see Fig. 4.12). Since in our geometry we observe the out-of-plane component of the magnetization, the reduction of  $\mathbf{H}_a$  leads to the observation of smaller step-like processes in the magneto-optical signal at lower temperatures, as shown in Fig. 4.11. However, a stronger tilted magnetization vector towards the plane of the sample at low temperatures also implies a precession towards the normal of the sample with a larger projection on the  $\mathbf{k}$ -vector of the probe beam. In other words, decreasing the temperature of the sample (below  $T_M$ ) under a constant applied magnetic field, the demagnetization process becomes less observable in our experiments while the amplitude of the magneto-optical signal representing the precessional motion increases (see Fig. 4.12). This indeed explains the change with temperature in the sign of the equilibrium direction around which magnetization precesses, and the increase in the precessional amplitude, as observed in the experiments shown in Figure 4.11.

Summarizing, the magnetization dynamics of the RE-TM amorphous alloy GdFeCo is drastically affected by the temperature, as expected from the theory of ferrimagnetic resonance [2, 3, 29]. Following the above experimental observations we can draw the following conclusions:

- the all-optical pump-probe technique is a powerful tool, able to reveal the angular momentum compensation temperature  $T_A$  and the magnetization compensation temperature  $T_M$  of a ferrimagnetic RE-TM amorphous alloy;
- due to a difference between the gyromagnetic ratio of the RE and TM sublattices, for GdFeCo we observe a splitting in temperature between  $T_M$  and  $T_A$  of about 60 K;
- both Gilbert damping and precession frequency strongly increase towards  $T_A$  indicating the possibility for high-speed magnetization reversal at  $T_A$ . The increase of the precession frequency (also indicated by Eq. 4.15) is the combined result of both the divergence of the gyromagnetic ratio near  $T_A$  (see Eq. 4.6) and the increase of the anisotropy field towards  $T_M$  (see Eq. 4.11). The elevation of the Gilbert damping is also expected from Eq. 4.7;
- at  $T_A$  the exchange mode softens and becomes observable in our experiments;
- while the strong Gilbert damping is predominant near and above  $T_A$ , it significantly decreases below  $T_A$  to values such as  $\alpha_{\text{eff}} = 0.05$  at  $T = 210$  K (Fig. 4.11).

This is an important temperature range for the MRAM applications where low damping in RE-TM alloys is strongly required, as discussed above.

Other groups have also observed high-speed magnetization dynamics near the ferrimagnetic compensation points of RE-TM alloys [38]. Subsequently, researchers at IBM (USA) have also observed a difference in temperature of about 50 K between  $T_M$  and  $T_A$  in a GdCo amorphous alloy, allowing to study the origin of current-induced magnetization switching and magnetoresistance in spin valves [39].

#### 4.1.7 Conclusions

In conclusion, using magneto-optical techniques we have investigated the spin dynamics in ferrimagnetic GdFeCo films with subpicosecond temporal resolution and in a broad temperature range. Our data unambiguously reveal the angular momentum compensation around  $T_A = 220$  K and the magnetization compensation around  $T_M = 160$  K in  $\text{Gd}_{22}\text{Fe}_{74.6}\text{Co}_{3.4}$  (20nm). The observed difference between the points of magnetization and angular momentum compensation indicate the fact that the two magnetic sublattices in the studied GdFeCo alloy have different g-factors. We have experimentally observed both ferromagnetic and exchange modes of spin precession in the ferrimagnetic material. While the precession frequency and the Gilbert damping strongly increase when the temperature approaches  $T_A$ , the high-frequency exchange mode softens near the angular momentum compensation point  $T_A$ , so that ferromagnetic and exchange modes have similar frequencies. The observed high-speed and strongly damped spin dynamics in the vicinity of the compensation of the angular momentum, might be ideal for ultrafast ringing-free precessional switching in magnetic and magneto-optical recording.

## 4.2 Sub-picosecond Magnetization Reversal across Ferrimagnetic Compensation Points

### 4.2.1 Introduction

The fundamental limit of the magnetization reversal time is presently one of the most intriguing subjects in the physics of magnetism, with crucial consequences for magnetic recording and information processing [5, 14, 40–53]. Traditionally, to reverse the magnetization, a magnetic field is applied in the opposite direction of the magnetization. In that case, the magnetization reversal is achieved by domain-wall motion. Alternatively, by applying a magnetic field perpendicular to the magnetization a coherent precessional switching occurs, known as the fastest way to reverse magnetization [5, 45–47]. A fascinating and even faster way of switching has recently been demonstrated in micromagnetic simulations via ultrafast switching of vortex cores [48]. However, it was also predicted that there is a natural limit of magnetization switching on the picosecond time scale, beyond which magnetization reversal becomes non-deterministic [49]. Thus, finding new approaches to reverse magnetization in a reproducible way on a time scale shorter than picoseconds is a fundamental challenge with important consequences for technology.

Ferrimagnetism represents one of the keys to access the field of sub-picosecond magnetization reversal. This is because a ferrimagnet may possess both a magnetization compensation temperature  $T_M$  and an angular momentum compensation temperature  $T_A$ . A small difference between the gyromagnetic ratio of the two sublattices leads to an angular momentum compensation point  $T_A$  slightly above  $T_M$  [14, 39]. At  $T_A$ , application of a magnetic field should instantaneously flip the magnetization. As we have seen in this chapter, the reason for this is that at  $T_A$  both the frequency of the magnetization precession [14] and the domain-wall velocity [6, 54] increase strongly due to the divergence of the gyromagnetic ratio [2]. In other words, at  $T_A$ , magnetization can be regarded as a mechanical system with no inertia which can be moved by the slightest torque. However, to verify this ultrafast switching, instantaneous application of a magnetic field is required which in real experiments is not feasible. Instead, a DC magnetic field can be applied to the ferrimagnet parallel to the original magnetization direction, at a temperature  $T < T_M$ . When the temperature of the ferrimagnet increases above both  $T_M$  and  $T_A$ , the net magnetization will reverse [55, 56]. Thus a femtosecond (fs) laser pulse heating the sample very rapidly might act as an instantaneously applied magnetic field, allowing the investigation of the magnetization reversal speed at  $T_A$ . An interesting ferrimagnetic system for this study is the family of amorphous rare-earth (RE)-transition-metal (TM) alloys, such as GdFeCo, for which the compensation points can be tuned in a wide temperature range by simply varying its composition [9]. However, due to the localized character of the spins responsible for magnetism in the RE ferrimagnetic sublattice, it is not



clear whether its magnetization can be changed by laser pulses on a fs time scale [68].

In this section, it is experimentally demonstrated that an ultrafast laser induced heating of the GdFeCo ferrimagnetic system over its compensation points under an applied magnetic field results in a sub-picosecond magnetization reversal. Additionally, the observed ultrafast switching implies that the magnetization compensation point is reached on the sub-picosecond time-scale, thus proving that both itinerant TM and localized RE spins are heated on the fs time scale.

### 4.2.2 Experimental Details

In the amorphous ferrimagnetic alloy GdFeCo the FeCo-sublattice is antiferromagnetically coupled to the Gd-sublattice in a collinear alignment [58]. The samples used in this study were grown by magnetron sputtering in the following multilayer structure: glass/AlTi(10nm)/SiN(5nm)/ Gd<sub>23</sub>Fe<sub>73.64</sub>Co<sub>3.36</sub>(20nm)/ SiN(60nm). The ferrimagnetic GdFeCo layer is characterized by a strong perpendicular magnetic anisotropy and a Curie temperature of about 525 K. Given the sample composition, the temperature dependence of the hysteresis loop shows a divergence of the coercive field  $H_c$  at about 370 K (see Fig. 4.1), which indicates the magnetization compensation temperature  $T_M$ .  $T_A$  occurs at a temperature of about 50 K above  $T_M$  [14, 39] (see Fig. 4.1).

To initiate and investigate the magnetization reversal in GdFeCo, we have used an all-optical pump-probe technique employing an amplified Ti:Sapphire laser system with 40 fs laser pulses at a central wavelength of 800 nm and a repetition rate of 1 kHz. The magnetization response resulting from the heating by the pump pulse was investigated by a less intense probe beam, which monitored in time the changes in the Faraday rotation. At nearly normal incidence, the linearly polarized beams were focused on the sample to a spot of 200  $\mu\text{m}$  diameter for the pump and 40  $\mu\text{m}$  for the probe beam. Again, in the present geometry the probe beam is sensitive to the variation in the out-of-plane component of the magnetization,  $\mathbf{M}_z$  while at the 800 nm wavelength, the Faraday signal is mainly given by the FeCo sublattice [14] (Fig. 4.2). The measurements were carried out at room temperature, thus just below  $T_M$ , in air. During this stroboscopic experiment, to ensure the same initial magnetic state for every pump-pulse, a magnetic field  $\mathbf{H}_{\text{ext}}$  larger than the coercive field at room temperature  $H_c^{\text{room}}$  ( $\mathbf{H}_{\text{ext}} = 0.3T > H_c^{\text{room}}$ ) was applied at an angle  $\theta_{\text{ext}} = 60^\circ$  with respect to the easy axis of anisotropy.

### 4.2.3 Results and Discussion: Pump Fluence Dependence

Figure 4.13 shows that the variation of the time-resolved Faraday signal of GdFeCo has a strong laser fluence dependence. In particular, following laser excitation with a low pump fluence (2.5 mJ/cm<sup>2</sup>), a step-like change in the Faraday signal is observed. The step-like process is due to the laser induced change in the magnitude of the

## 4.2 Sub-picosecond Magnetization Reversal across Ferrimagnetic Compensation Points 79

magnetization, representing the ultrafast demagnetization process [32]. Subsequently, the magnetization relaxes back towards the *initial state*. Note that this pump fluence induces an average increase of the local temperature in the sample with  $\approx 50$  K [14] (see Fig. 4.1). As the laser fluence increases one can observe a gradual increase in the transient Faraday signal. Interestingly, after high pump fluence excitation ( $6.29 \text{ mJ/cm}^2$ ), as the heat is diffused out of the sample, the magnetic system relaxes towards the *opposite direction* first, before cooling down and reversing back to the initial state.

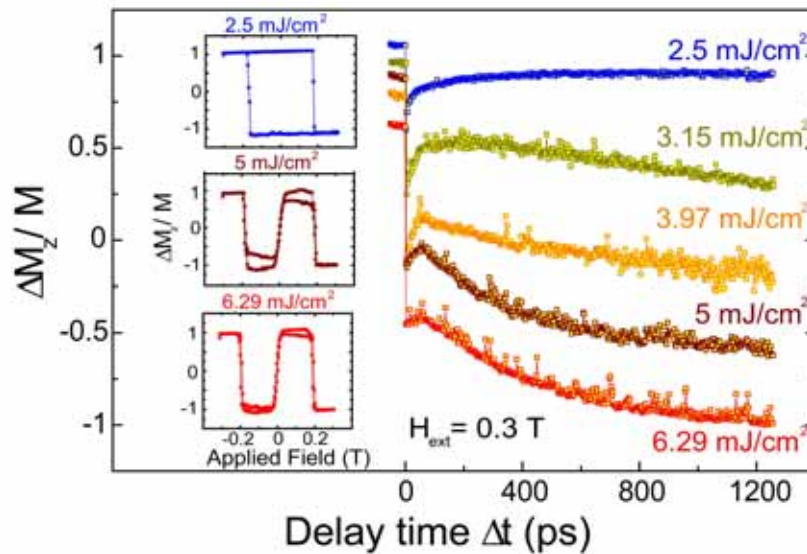


**Figure 4.13:** Transient Faraday effect traces at different pump fluences. The variation of the magneto-optical signal was plotted relative to the total Faraday rotation at room temperature. The data are offset for clarity. Insets: hysteresis loops measured at negative delay for distinct pump fluences.

To investigate the atypical magnetization dynamics observed at pump fluences higher than  $2.5 \text{ mJ/cm}^2$ , we have measured hysteresis loops at negative delay for different pump fluences, shown as insets in Fig. 4.13. Here, a negative delay time implies that the probe pulses were probing the magnetic state long after the pump excitation (1 ms). While at a  $2.5 \text{ mJ/cm}^2$  laser fluence, the measured hysteresis shows no changes due to the laser pumping, the situation changes drastically for the higher pump fluences where anomalous hysteresis loops are observed. To explain these hysteresis loops we must note that at high laser fluences, the sample is heated above  $T_M$ .

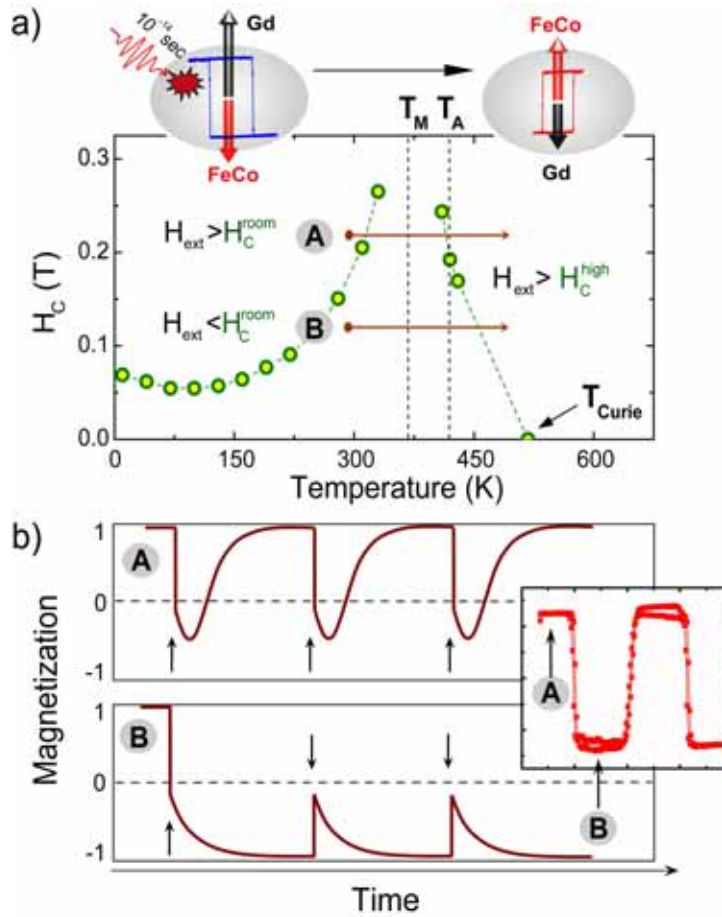


**Figure 4.14:** a) Temperature dependence of the coercive field  $H_c$  in the GdFeCo sample. The divergence of  $H_c$  indicates the presence of  $T_M$ . The inset of the figure shows schematically the ferrimagnetic system in an applied magnetic field below and above  $T_M$ . Depending on the strengths of the applied magnetic field, two different dynamic regimes can be distinguished: (A) for  $H_{ext} > H_c^{room}$  and (B) for  $H_{ext} < H_c^{room}$ . (b) Qualitative description of the magnetization dynamics induced by the first pump pulses, at a  $6.29 \text{ mJ/cm}^2$  fluence, for the two different conditions [(A) and (B)]. The arrows indicate the time when the pump pulses hit the sample (1 ms between two pulses). The inset shows the hysteresis loop measured at negative delay for the  $6.29 \text{ mJ/cm}^2$  pump fluence.

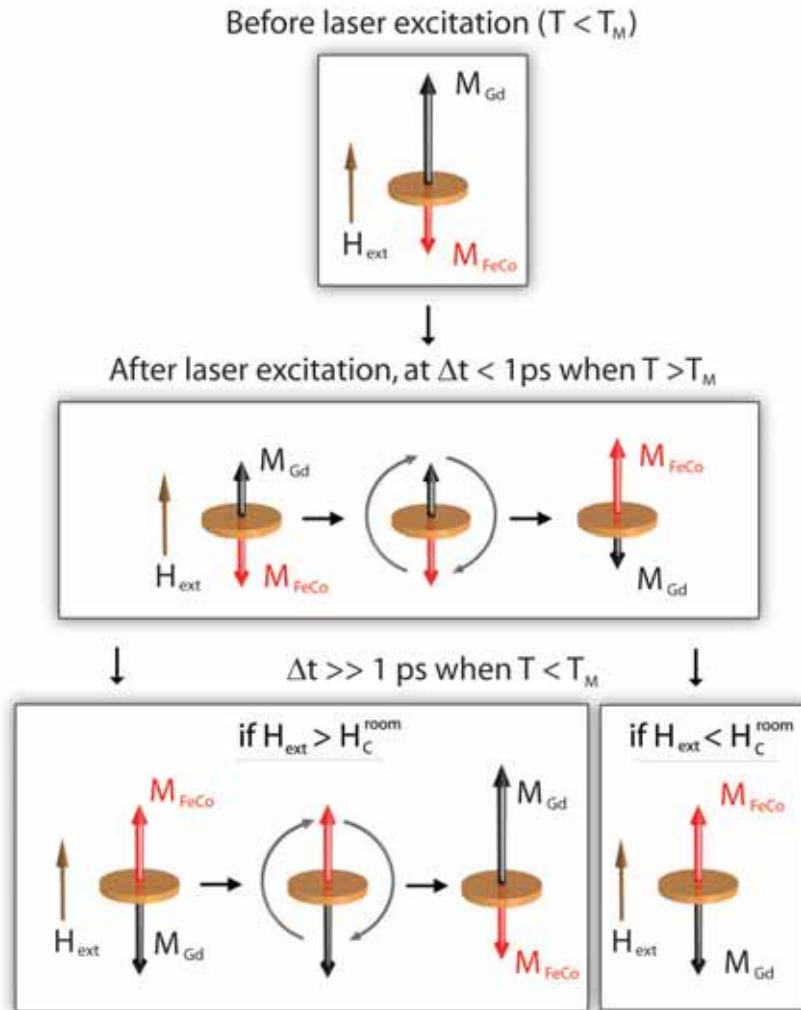


**Figure 4.15:** The behavior of a ferrimagnetic system in an external magnetic field, when heated over the magnetization compensation point  $T_M$ . Note that for  $H_{ext} > H_c^{room}$  the net magnetization reverses back to the initial direction (the same as  $H_{ext}$ ) after the heat is diffused out from the system. In contrast to this, for  $H_{ext} < H_c^{room}$ , the magnetization ends up into a direction opposite to that of the applied field (stable switching).

As shown in Fig. 4.14 (a), depending on the strength of  $\mathbf{H}_{\text{ext}}$  one can distinguish two different scenarios: **(A)** the applied magnetic field is stronger than the coercive field at the initial temperature ( $\mathbf{H}_{\text{ext}} > H_c^{\text{room}}$ ); **(B)** the applied magnetic field is weaker than the coercive field ( $\mathbf{H}_{\text{ext}} < H_c^{\text{room}}$ ).

**(A)** When  $\mathbf{H}_{\text{ext}} > H_c^{\text{room}}$ , below  $T_M$  the Gd magnetic moment, being larger than that of FeCo, aligns parallel to the external field  $\mathbf{H}_{\text{ext}}$ . A sudden laser induced increase of the sample temperature above  $T_M$ , where the FeCo moment becomes dominant, induces switching of the ferrimagnetic system, as long as the coercive field at high temperature  $H_c^{\text{high}} < \mathbf{H}_{\text{ext}}$ . In our experiments this occurs at the 6.29 mJ/cm<sup>2</sup> laser fluence that corresponds to an increase of the local temperature of about 190 K. After the pump pulse, and as long as the spin temperature is still above  $T_M$ , the FeCo sublattice relaxes towards a metastable opposite state. When the sample cools down below  $T_M$ , because  $\mathbf{H}_{\text{ext}} > H_c^{\text{room}}$ , the recovered magnetization will eventually switch back, restoring the initial condition. The same type of dynamics will occur for every pump pulse [see Fig. 4.14 (b)-upper panel]. This clarifies the magnetization dynamics shown in Fig. 4.13 for a laser fluence of 6.29 mJ/cm<sup>2</sup>, where the magnetization is observed to relax towards the opposite magnetic state.

**(B)** A different scenario is taking place when  $H_c^{\text{high}} < \mathbf{H}_{\text{ext}} < H_c^{\text{room}}$ . In this case the first pulse induces the reversal of the magnetization which after the heat is diffused away can not reverse back to the initial state as in the previous case, because  $\mathbf{H}_{\text{ext}} < H_c^{\text{room}}$ . Thus, the magnetization dynamics initiated by the next pulses occur in this opposite magnetic state as shown in the lower panel of Fig. 4.14 (b). In a static view, when the applied magnetic field is weaker than the coercive field at room temperature, the magnetization of the ferrimagnetic system GdFeCo is reversed *oppositely* to the applied magnetic field (see Fig. 4.15). This explains the anomalous hysteresis loops observed at negative delay for laser fluences such as 6.29 mJ/cm<sup>2</sup> and demonstrates the magnetization reversal across  $T_M$  by laser-induced heating.

In order to further compare the magnetization dynamics under applied magnetic field  $\mathbf{H}_{\text{ext}} > H_c^{\text{room}}$  and  $\mathbf{H}_{\text{ext}} < H_c^{\text{room}}$ , we performed pump-probe experiments at a pump fluence of 6.29 mJ/cm<sup>2</sup> for  $\mathbf{H}_{\text{ext}} = 0.13$  T and  $\mathbf{H}_{\text{ext}} = 0.26$  T. The results are shown in Figure 4.16. Note that the orientation of the magnetic field remained the same for both experiments while only its amplitude has been changed. Indeed, it can be clearly observed that the step-like process representing the ultrafast reduction of the magnetization shows opposite sign for the two different amplitudes of the applied magnetic field, as expected from the description in Fig. 4.14.

The hysteresis loop measured at a pump fluence of 5 mJ/cm<sup>2</sup> shows a residual hysteresis in the **(B)** field range. This happens because at lower pump fluence part of the probed area does not fulfill the condition  $\mathbf{H}_{\text{ext}} > H_c^{\text{high}}$ , resulting in an inhomogeneous switching. This also explains the observed gradual increase of the transient Faraday effect with increasing pump fluence shown in Fig. 4.13.

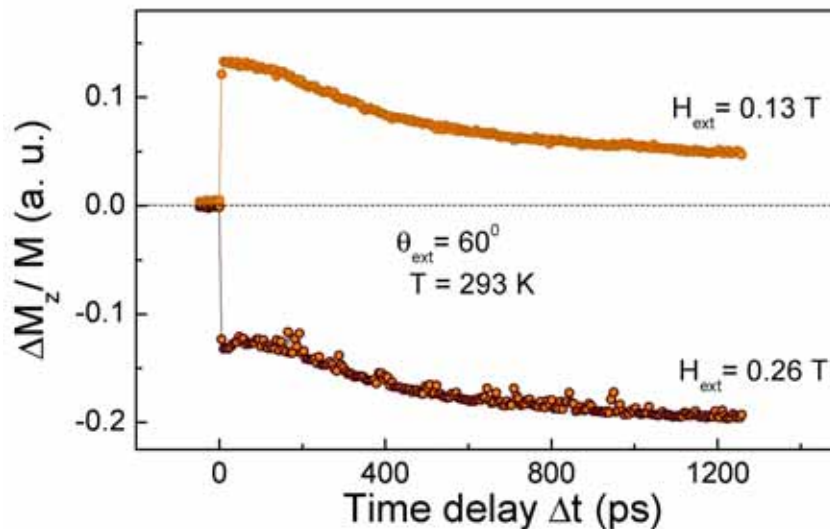


**Figure 4.16:** Transient magnetization dynamics measured for a pump fluence of  $6.29 \text{ mJ/cm}^2$  under  $\mathbf{H}_{\text{ext}} > H_c^{\text{room}}$  and  $\mathbf{H}_{\text{ext}} < H_c^{\text{room}}$ .

#### 4.2.4 Intrinsic Switching Speed

A fundamental question arising from the above demonstrated magnetization switching is: How fast is the intrinsic switching process? To answer this question we have measured hysteresis loops at different time delays after the pump pulses heat the sample with a fluence of  $6.29 \text{ mJ/cm}^2$ . The results are shown in Fig. 4.17. Since only for the condition  $\mathbf{H}_{\text{ext}} > H_c^{\text{room}}$  the system switches and returns to the initial state for each pump pulse, one should focus the attention on the (A) field range of the measured hysteresis. One can clearly observe that in this field range, the measured Faraday signal changes its sign after about 700 fs. The sign change reflects the change of the FeCo sublattice direction towards the applied magnetic field, as the spin temperature of the ferrimagnetic system increases over  $T_M$  in the probed area. This observation unambiguously demonstrates that the magnetization reversal takes place on a sub-picosecond time scale. Note that this reversal time is considerably faster than that found in GdFeCo at temperatures above the compensation points [59]. On the other hand, the growth of the reversed domain to its full 100 % is determined by the cooling rate and takes place at a much longer time scale.

This ultrafast reversal time can be related to the angular momentum compensation

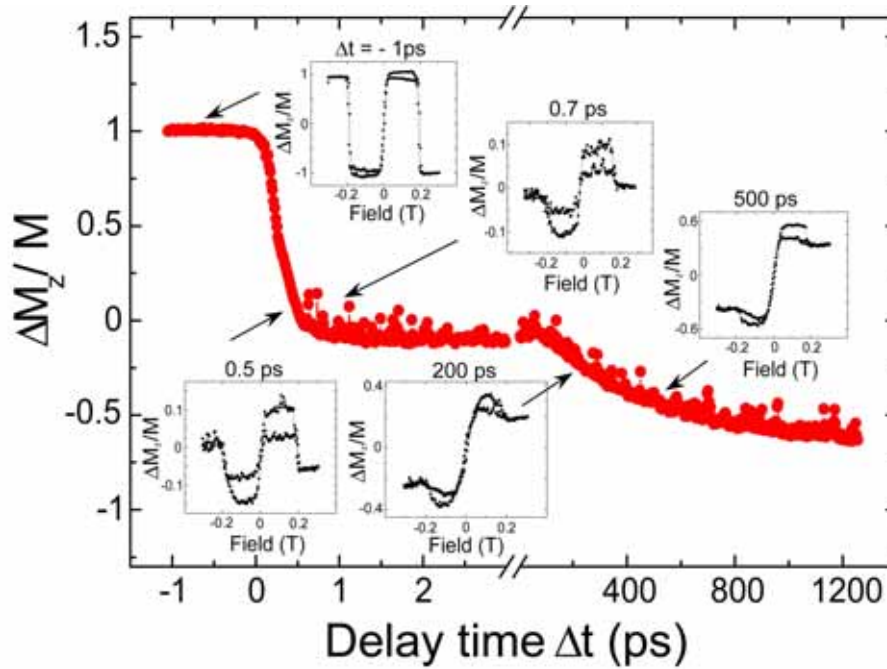


**Figure 4.17:** Transient magnetization reversal dynamics measured for a pump fluence of 6.29 mJ/cm<sup>2</sup>. Insets show hysteresis loops measured at distinct pump-probe delays. The loops demonstrate the magnetization reversal after about 700 fs.

[55, 56]. In GdFeCo, the difference between the gyromagnetic ratios of the Gd and FeCo sublattices induces a separation in temperature between the magnetization and the angular momentum compensation points of about 50 K, where  $T_A > T_M$  [14, 39] [see Fig. 4.14 (a)]. The positive shift of  $T_A$  with respect to  $T_M$  represents an advantage for the present experiment, insuring a  $H_c < H_{ext}$  at  $T_A$  [see Fig. 4.14 (a)]. A laser fluence of 6.29 mJ/cm<sup>2</sup> induces a heating of about 190 K, which implies that the laser pulses locally elevate the sample temperature to above both  $T_M$  and  $T_A$ . Because the effective gyromagnetic ratio of the ferrimagnetic system  $\gamma_{eff}$  is inversely proportional to the total angular momentum of the system ( $\gamma_{eff} = \mathbf{M}/\mathbf{A}$ ), theoretically  $\gamma_{eff}$  diverges when  $T_A$  ( $\mathbf{A} = 0$ ) is reached [2]. In addition, as we have seen in Section 4.1, the anisotropy field also increases due to occurrence of  $T_M$  near  $T_A$ . Thus, in the vicinity of  $T_A$  a many fold increase of the frequency of the spin precession is expected. Consequently, the magnetization reversal will indeed be highly accelerated at  $T_A$ , leading to an ultrafast magnetization reversal. On the other hand,

at  $T_A$ , also the effective Gilbert damping of the ferrimagnetic system shows a peak [14] that could lead to a slower switching. This might be the reason why the switching time at  $T_A$  is not faster than 700 fs as observed in our experiments.

#### 4.2.5 Femtosecond Optical Excitation of Localized Magnetic Moment in Gd

What are the implications of the observed sub-picosecond magnetization reversal? Although it is well known that ultrafast laser excitation of itinerant ferromagnets as Co, Ni or Fe leads to a demagnetization on the femtosecond time scale [40, 60], little is known about how fast the magnetic moments in metals as Gd can be excited, with photon energies in the visible range. This is because in Gd, the optically excited electrons of the  $5d6s$  band carry only  $\approx 9\%$  of the total moment while the localized  $4f$  electrons dominate the magnetic spin moment. However, the  $4f$  levels have a binding energy of about 9 eV and are not accessible with the 1.5 eV photon energy used in our experiments. Thus, the localization of the magnetic moment together with the weak spin-orbit coupling characteristic for Gd, would imply that the transfer of the photon energy to the localized states should be a slow process [61].

Recently, it has been experimentally demonstrated that ultrashort laser pulses can modulate the magnetization at a Gd surface on the femtosecond time scale [66]. Yet, it is still not clear whether this fast demagnetization will also occur in the bulk and whether the  $4f$  moments are involved in this fast magnetization modulation encountered on the Gd surface [65]. In this context it was recently claimed that laser excitation of a CoGd sample resulted in an independent ultrafast excitation of the Co sublattice only [38]. Furthermore, it has been argued that the experiments performed on Gd-TM-alloys until now, were mostly sensitive to the transition metal magnetization while the response time of the Gd component was not determined [68]. Using time-resolved x-ray magnetic circular dichroism with 2 ps time resolution, Bartelt et al. observed a demagnetization time in Gd (Fe/Gd multilayers) of  $2.2 \pm 0.6$  ps.

In contrast to this, we have demonstrated here a sub-picosecond magnetization reversal over the compensation points, which implies that both Gd and FeCo sublattice magnetizations are considerably reduced on the sub-picosecond time scale. In particular, an increase of the spin temperature above  $T_M$  in our experiments produces a partial demagnetization of the FeCo sublattice of  $\sim 25\%$  (see Fig. 4.18). Consequently, the magnetization of the Gd sublattice, which above  $T_M$  is smaller than that of FeCo, must be reduced by more than 25 %. For Gd this represents a reduction of the magnetic moment far larger than that supplied by the itinerant  $5d6s$  electrons. A sub-picosecond change of the localized  $4f$  spin moments is therefore required, thus revealing the important role played by the Gd  $4f$  electrons in this fast reversal process. But how is this possible? What is the mechanism that leads to such ultrafast magnetization reduction of the localized  $4f$  electrons in Gd by 1.5 eV photon energy?

One of the mechanisms that can mediate the laser-induced demagnetization is



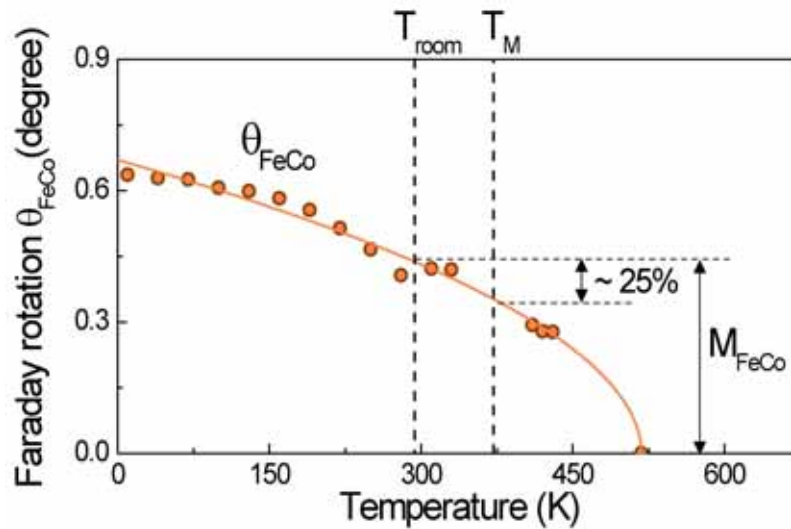


**Figure 4.18:** Faraday rotation  $\theta_{\text{FeCo}}$  at  $\lambda = 805$  nm as a function of temperature representing the temperature dependence of the FeCo-sublattice magnetization. Here  $M_{\text{FeCo}}$  represents the FeCo-sublattice magnetization at the room temperature.

based on the spin-orbit coupling. In this case, following laser irradiation the electronic system is excited. In general, it is assumed that the light can only access the orbital part of the electronic wave function. If the excited system is characterized by a strong spin-orbit coupling, there will be a net momentum transfer from the orbit to the spins. This process will deviate the spins from equilibrium, leading to a spin fluctuation that is equivalent to an increase of the spin temperature and therefore a reduction of the magnetization. Since this process is mediated by the spin-orbit coupling, the time scale on which this demagnetization is taking place is given by the strength of the spin-orbit interaction.

For Gd, the  $4f$  orbital moment vanishes due to the half-filled  $4f$  shell. However, the spin-orbit interaction is not totally vanishing due to the valence band contribution to the magnetic moment. This is the origin of the spin-orbit coupling in Gd that determines its magneto-crystalline anisotropy. Nevertheless, this interaction is weak, of the order of  $16 \mu\text{eV}$  [62]. This translates into a characteristic time in the range of  $10^{-10}$  s that is far too long to lead to a sub-picosecond magnetization reduction as observed in our experiments. Consequently, in normal circumstances, the spin-orbit coupling cannot be responsible for an ultrafast laser-induced demagnetization

mechanism in Gd [64]. Nevertheless, as mentioned in Chapter 1, during optical excitation these circumstances can be modified and an enhanced spin-orbit coupling can be optically induced, which may allow an ultrafast demagnetization [63].

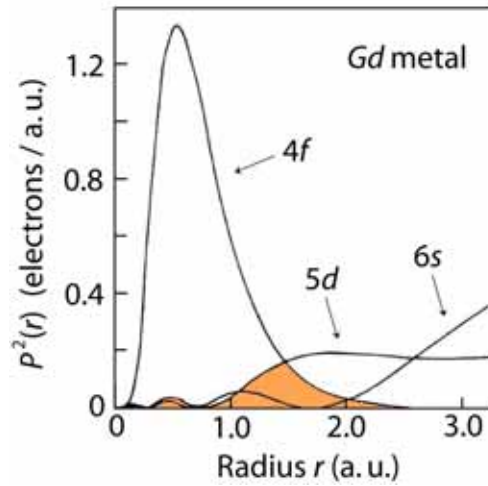


**Figure 4.19:** Typical radial densities of  $s$ -like,  $d$ -like and  $f$ -like wave functions for Gd calculated by Harmon and Freeman [69].  $5d$  has an appreciable overlap with the  $4f$  states (the shaded area) that leads to a strong direct exchange.

Recently a model has been proposed that may also allow the magnetization reduction on a femtosecond timescale without violation of angular momentum conservation but by coupling the  $5d$  spin system to the  $4f$  states [64, 65]. In this case, the ultra-short time scale is indeed allowed in Gd by the strong exchange coupling between  $5d$ - $4f$ , responsible for its ferromagnetic order (see Fig. 4.19). The strength of this intra-atomic exchange is  $\approx 100$  meV [70, 71], corresponding to  $\approx 50$  fs. From these above arguments and in agreement with that observed in our experiments, it follows that indeed the localized  $4f$  spin magnetic moment in Gd can be optically excited on a femtosecond time scale, a time scale comparable with that observed for the itinerant ferromagnets.

Finally, it must be noted that a possible optical excitation of the  $4f$  states in Gd could take place via the optically excited  $3d$  states in Fe. However, such mechanism would have to involve both the intra-atomic (RE)  $4f$ - $5d$  and the inter-atomic (RE-TM)  $5d$ - $3d$  exchange interaction. The Gd-Fe negative (antiferromagnetic) exchange coupling is  $\sim 2.5 \cdot 10^{-22}$  J [72–74] that is 1.56 meV, corresponding to  $\approx 3$  ps. Therefore, this mechanism is too slow to be accounted for a femtosecond excitation of the Gd  $4f$  spins.

### 4.2.6 Conclusions

In conclusion, using a time resolved magneto-optical technique we have unambiguously demonstrated the feasibility of sub-picosecond magnetization reversal in the ferrimagnetic alloy GdFeCo. This ultrafast reversal time is a result of the divergence of the effective gyromagnetic ratio of the ferrimagnetic system at the angular momentum compensation temperature  $T_A$ . These results also imply that the localized moment in Gd can be optically excited on a sub-picosecond time scale. Besides its fundamental importance, the observation reported here might be of real interest for magnetic and magneto-optical recording employing rare-earth-transition-metal alloys [39].

## 4.3 Summary

RE-TM amorphous alloys are magnetic materials widely used in magnetic data storage devices. As previously discussed, these materials are used in both the writing and reading process of the information, processes that are strongly dependent on the magnetization dynamics. However, in spite of this fact and also in spite of the fact that in a ferrimagnet the magnetization dynamics may strongly depend on the temperature, the temperature dependence of the magnetization dynamics in the amorphous RE-TM was not well known.

Therefore, one of the first questions that we addressed in this chapter was how the magnetization dynamics is affected by temperature in ferrimagnetic amorphous systems such as GdFeCo. This investigation has been performed by means of an all-optical pump-probe technique such as presented in Chapter 3, in a wide range of temperature (from 50 K up to 450 K - near Curie temperature). The experiments presented here show a strong increase in both ferromagnetic resonance frequency and damping of the precession near the temperature of 180 K. This observation reveals the angular momentum compensation temperature. The enhancement of both precession frequency and damping parameter near the angular momentum compensation are in agreement with the standard mean-field treatment of the dynamics of total magnetization in a ferrimagnet. At this temperature, the total magnetization can be seen as a mechanical system that is losing its inertia due to the disappearance of its angular momentum. On the other hand, the increase of damping implies that near  $T_A$  the ferrimagnetic system dissipates energy quickly. Thus, *the experiments presented here demonstrate that the angular momentum compensation point is accompanied by a high-speed and strongly damped spin dynamics and thus is ideal for ultrafast ringing-free precessional switching in magnetic and magneto-optical recording.*

As the net angular momentum of the ferrimagnetic system increases at temperatures below  $T_A$ , the two sublattice system dissipates the energy at a much slower rate. As a result, below  $T_A$ , damping parameter values as low as 0.05 are observed.

Thus, the temperature/composition range below  $T_A$  is found to be the most interesting range for MRAM applications, where low damping is desired in order to switch the magnetization of the RE-TM free-layer using the lowest possible currents.

The other investigated subject was the ultrafast magnetization reversal near  $T_A$ . Here, the challenge was to obtain the equivalent of an instantaneously applied magnetic field that would allow to investigate the magnetization reversal speed at  $T_A$ . This problem was solved by ultrafast heating the GdFeCo ferrimagnetic system across its compensation points, under a DC magnetic field applied parallel to the initial magnetization direction. When the spin temperature crosses  $T_M$  the magnetization tends to switch to the opposite direction. In this way a sub-picosecond magnetization reversal is experimentally demonstrated that is related to  $T_A$  on the basis of the above study. *Consequently, the results presented in Section 4.2 demonstrate for the first time the feasibility of sub-picosecond magnetization reversal, breaking the picosecond speed limit of magnetization reversal.* Besides the fast reversal time characteristic for this heat-assisted magnetization reversal, another advantage is that in order to control the magnetization direction, only the amplitude of the magnetic field must be controlled and not its direction.

## References

- [1] J. Z. Sun, IBM J. Res. and Dev. **50**, 81 (2006).
- [2] R. K. Wangsness, Phys. Rev. **91**, 1085 (1953).
- [3] R. K. Wangsness, Phys. Rev. **93**, 68 (1954).
- [21] T. Kobayashi, H. Hayashi, Y. Fujiwara, and S. Shiomi, proceedings INTERMAG 2005.
- [5] H.W.Schumacher, C. Chappert, P. Crozat, R. C. Sousa, P. P. Freitas, J. Militat, J. Fassbender, and B. Hillebrands, Phys. Rev. Lett. **90**, 017201 (2003).
- [6] Robert S. Weng and Mark H. Kryder, IEEE Trans. Magn. **29**, 2177 (1993).
- [7] H. Awano, S. Ohnuki, H. Shirai, N. Ohta, A. Yamaguchi, S. Sumi, and K. Torazawa, Appl. Phys. Lett., **69** (27), 4257 (1996).
- [8] P. Hansen, C. Clausen, G. Much, M. Rosenkranz, and K. Witter, J. Appl. Phys. **66**, 756 (1989).
- [9] P. Chaudhari, J. J. Cuomo, and R. J. Gambino, Appl. Phys. Lett. **22**, 337 (1973).
- [10] R. Malmhäll and T. Chen, J. Appl. Phys. **53**, 7843 (1982).

- 
- [11] Y. Mizusawa and K. Ichihara, Jpn. J. Appl. Phys. Part 1 **30**, 484 (1991).
- [12] S. Tsunashima, S. Masui, T. Kobayashi, and S. Uchiyama, J. Appl. Phys. **53**, 8175 (1982).
- [13] T. Katayama, M. Miyazaki, H. Arimune, and T. Shibata, J. Magn. Soc. Jpn. **8**, 121 (1984).
- [14] C. D. Stanciu, A. V. Kimel, F. Hansteen, A. Tsukamoto, A. Itoh, A. Kirilyuk, and Th. Rasing, Phys. Rev. B **73**, 220402(R) (2006).
- [15] L. Landau and E. Lifshitz, Phys. Z. Sowjetunion. **8**, 153 (1935).
- [16] T. L. Gilbert, Phys. Rev. **100**, 1243, (1955).
- [17] Thomas L. Gilbert, IEEE Trans. Magn. **40**, 3443 (2004).
- [18] C. Kittel, Phys. Rev. **76**, 743 (1949).
- [33] A. G. Gurevich and G. A. Melkov, *Magnetization Oscillations and Waves* (CRC Press, Boca Raton, 1996).
- [20] M. Mansuripur, *The Physical Principles of Magneto-Optical Recording* (Cambridge University Press, Cambridge, 1995).
- [21] T. Kobayashi, H. Hayashi, Y. Fujiwara, and S. Shiomi, IEEE Trans. Magn. **41**, 2848 (2005).
- [22] S.M. Bhagat and P. Lubitz, Phys. Rev. B, **10**, 179 (1974).
- [23] P. Lubitz, J. Schelleng, and C. Vittoria, Solid State Commun. **18**, 965 (1976).
- [24] K. H. J. Buschow and F. R. de Boer, *Physics of Magnetism and Magnetic Materials* (Kluwer Academic Publishers, New York, 2004).
- [25] C. D. Stanciu, A. Tsukamoto, A. V. Kimel, F. Hansteen, A. Kirilyuk, A. Itoh, and Th. Rasing, Phys. Rev. Lett. (*to be published*).
- [26] J. Kaplan and C. Kittel, J. Chem. Phys. **21**, 760 (1953).
- [27] S. Geschwind and L. R. Walker, J. Appl. Phys. **30**, 163S (1959).
- [28] A. J. Sievers, and M. Tinkham, Phys. Rev. **129**, 1995 (1963).
- [29] R. K. Wangsness, Phys. Rev. **97**, 831 (1955).
- [30] Thomas R. McGuire, Phys. Rev. **97**, 831 (1955).

- 
- [31] M. van Kampen, C. Jozsa, J. T. Kohlhepp, P. LeClair, L. Lagae, W. J. M. de Jonge, and B. Koopmans, *Phys. Rev. Lett.* **88**, 227201 (2002).
- [32] M. Vomir, L. H. F. Andrade, L. Guidoni, E. Beaurepaire, and J.-Y. Bigot, *Phys. Rev. Lett.* **94**, 237601 (2005).
- [33] A. G. Gurevich and G. A. Melkov, *Magnetization Oscillations and Waves* (CRC Press, Boca Raton, 1996).
- [34] A. Tsukamoto, K. Nakagawa, A. Itoh, A. Kimel, A. Tsvetkov, H. Awano, N. Ohta, A. Kirilyuk, and Th. Rasing, *J. Magn. Soc. Jpn.* **28**, 318 (2004).
- [35] T. Silva, J. Nibarger, B. Rippard, and B. Stamps, APS Meeting **MAR**, B23011, (2004).
- [36] Yi Li and K. Baberschke, *Phys. Rev. Lett.* **68**, 1208 (1992).
- [37] R. C. Taylor and A. Gangulee, *J. Appl. Phys.* **47**, 4666 (1976); **48**, 358 (1977).
- [38] M. Binder, A. Weber, O. Mosendz, G. Woltersdorf, M. Izquierdo, I. Neudecker, J. R. Dahn, T. D. Hatchard, J.-U. Thiele, C. H. Back, and M. R. Scheinfein, *Phys. Rev. B* **74**, 134404 (2006).
- [39] Xin Jiang, Li Gao, Jonathan Z. Sun, and Stuart S. P. Parkin, *Phys. Rev. Lett.* **97**, 217202 (2006).
- [40] E. Beaurepaire, J.-C. Merle, A. Daunois, and J.-Y. Bigot, *Phys. Rev. Lett.* **76**, 4250 (1996).
- [41] A. Scholl, L. Baumgarten, R. Jacquemin, and W. Eberhardt, *Phys. Rev. Lett.* **79**, 5146 (1997).
- [42] J. Hohlfeld, E. Matthias, R. Knorren, and K. H. Bennemann, *Phys. Rev. Lett.* **78**, 4861 (1997).
- [43] G. Ju, A. V. Nurmikko, R. F. C. Farrow, R. F. Marks, M. J. Carey, and B. A. Gurney, *Phys. Rev. Lett.* **82**, 3705 (1999).
- [44] A. V. Kimel, A. Kirilyuk, A. Tsvetkov, R. V. Pisarev, and Th. Rasing, *Nature* **429**, 850 (2004).
- [45] B. C. Choi, M. Belov, W. K. Hiebert, G. E. Ballentine, and M. R. Freeman, *Phys. Rev. Lett.* **86**, 728 (2001).
- [46] C. H. Back, D. Weller, J. Heidmann, D. Mauri, D. Guarisco, E. L. Garwin, and H. C. Siegmann, *Phys. Rev. Lett.* **81**, 3251 (1998).

- 
- [47] Th. Gerrits, H. A. M. van den Berg, J. Hohlfeld, L. Br. Th. Rasing, *Nature* **418**, 509 (2002).
- [48] R. Hertel, S. Gliga, M. Fähnle, and C. M. Schneider, *Phys. Rev. Lett.* **98**, 117201 (2007).
- [49] C.H. Back and D. Pescia *et al.*, *Nature* **428**, 808 (2004).
- [50] K. Yu. Guslienko, O. Chubykalo-Fesenko, O. Mryasov, R. Chantrell, and D. Weller, *Phys. Rev. B* **70**, 104405 (2004).
- [51] G. Ju, J. Hohlfeld, B. Bergman, R. J. M. van de Veerdonk, O. N. Mryasov, J.-Y. Kim, X. Wu, D. Weller, and B. Koopmans, *Phys. Rev. Lett.* **93**, 197403 (2004).
- [52] C. D. Stanciu, F. Hansteen, A. V. Kimel, A. Tsukamoto, A. Itoh, A. Kirilyuk, and Th. Rasing, *Phys. Rev. Lett.* **98**, 207401 (2007).
- [53] D. Cimpoesu, A. Stancu and L. Spinu, *J. Appl. Phys.* **102**, 013915 (2007).
- [54] V. V. Randoshkin, V. A. Polezhaev, N. N. Sysoev and Yu. N. Sazhin, *Physics of the Solid State* **45**, 513 (2003).
- [55] M. Aeschlimann, A. Vaterlaus, M. Lutz, M. Stampanoni, F. Meier, and H. C. Siegmann, *Appl. Phys. Lett.*, **59** (17), 2189 (1991).
- [56] M. Aeschlimann, A. Vaterlaus, M. Lutz, M. Stampanoni, and F. Meier, *J. Appl. Phys.* **67**, 4438 (1990).
- [68] A. F. Bartelt, A. Comin, J. Feng, J. R. Nasiatka, T. Eimüller, B. Ludescher, G. Schütz, H. A. Padmore, A. T. Young, and A. Scholl, *Appl. Phys. Lett.* **90**, 162503 (2007).
- [58] O. S. Anilturk and A. R. Koymen, *Phys. Rev. B* **68**, 024430 (2003).
- [59] J. Hohlfeld, Th. Gerrits, M. Bilderbeek, Th. Rasing, H. Awano, and N. Ohta, *Phys. Rev. B* **65**, 012413 (2002).
- [60] H.-S. Rhie, H. A. Dürr, and W. Eberhardt, *Phys. Rev. Lett.* **90**, 247201 (2003).
- [61] A. Vaterlaus, T. Beutler, and F. Meier, *Phys. Rev. Lett.* **67**, 3314 (1991).
- [62] M. Colarieti-Tosti, S. I. Simak, R. Ahuja, L. Nordström, O. Eriksson, D. Åberg, S. Edvardsson, and M. S. S. Brooks, *Phys. Rev. Lett.* **91**, 157201 (2003).
- [63] C. Stamm, T. Kachel, N. Pontius, R. Mitzner, T. Quast, K. Holldack, S. Khan, C. Lupulescu, E. F. Aziz, M. Wietstruk, H. A. Dürr and W. Eberhardt, *Nature Materials* **6**, 740 (2007).

- 
- [64] U. Bovensiepen, Appl. Phys. A **82**, 395 (2006).
- [65] I. Radu, Ph.D. thesis, Berlin, Germany, 2006.
- [66] A. Melnikov, I. Radu, U. Bovensiepen, O. Krupin, K. Starke, E. Matthias, and M. Wolf, Phys. Rev. Lett. **91**, 227403 (2003).
- [74] J. P. Liu, F. R. de Boer, P. F. de Chatel, R. Coehoorn, K. H. J. Buschow, J. Magn. Magnet. Mat. **132**, 159 (1994).
- [68] A. F. Bartelt, A. Comin, J. Feng, J. R. Nasiatka, T. Eimüller, B. Ludescher, G. Schütz, H. A. Padmore, A. T. Young, and A. Scholl, Appl. Phys. Lett. **90**, 162503 (2007).
- [69] B. N. Harmon and A. J. Freeman, Phys. Rev. B **10**, 1979 (1974).
- [70] M. S. S. Brooks, L. Nordström, B. Johansson, J. Appl. Phys. **69**, 5683 (1991).
- [71] R. Ahuja, S. Auluck, B. Johansson, M.S.S. Brooks, Phys. Rev. B **50**, 5147 (1994).
- [72] P. Hansen. *Crytalline and amorphous films with rare earth and 3d transition elements.*, Landolt-Bornstein, Group III, Vol. **19g**, 204 (Springer, Berlin, 1988).
- [73] Rainer Lübbers, Ph.D. thesis, Paderborn, Germany, 2000.
- [74] J. P. Liu, F. R. de Boer, P. F. de Chatel, R. Coehoorn, K. H. J. Buschow, J. Magn. Magnet. Mat. **132**, 159 (1994).





## CHAPTER 5

---

## The Role of Photon Angular Momentum <sup>1</sup>

---

**C**an light alone switch a magnet? A positive answer to this question would indicate a bright future where the manipulation of the data would take place at unimaginable speeds. Indeed, due to the tremendous development of ultrafast laser sources over the past years, the laser pulse has become one of the shortest man-made events. As a result, commercial laser sources can now generate light pulses with duration shorter than 50 fs, while lasers in laboratory experiments today already operate on a time scale as short as 130 attoseconds (1 as =  $10^{-18}$  s) [1]. In fact, an all-optical manipulation of magnetization would not only strongly enhance the speed of manipulating information but also simplify it. In this way the data would not only be transmitted but also stored purely by light.

When a light pulse is circularly polarized, it contains photons (light quanta of energy  $h\nu$ ) that carry angular momentum<sup>2</sup>, *i.e.* exhibit a rotation in space. The angular momentum of a photon is fixed and intrinsic, with eigenvalues  $+\hbar$  and  $-\hbar$  independent on the photon energy. On the other hand, the essence of magnetization is angular momentum. This similarity suggests that a circularly polarized wave may

---

<sup>1</sup>Adapted from: C. D. Stanciu, F. Hansteen, A. V. Kimel, A. Tsukamoto, A. Itoh, A. Kirilyuk, and Th. Rasing, *Phys. Rev. Lett.* **98**, 207401 (2007), and C. D. Stanciu, F. Hansteen, A. V. Kimel, A. Kirilyuk, A. Tsukamoto, A. Itoh, and Th. Rasing, *Phys. Rev. Lett.* **99**, 047601 (2007).

<sup>2</sup>Note that with the demonstration of photon states such as an *optical vortex*, in the recent literature there is a distinction between the photon (orbital) angular momentum and the spin characteristic of circularly polarized photons [2]. However, in the literature and throughout this thesis, in conjunction with magnetism the photon spin is referred to as *photon angular momentum*.

directly couple with the spins of the electrons, via its angular momentum. And since a  $180^\circ$  rotation in space changes the sign of the angular momentum of the circularly polarized photons ( $+\hbar \leftrightarrow -\hbar$ ), one might envisage the possibility of controlling the electron spins in magnets by simply changing the handed temporal motion of the interacting photons.

Earlier studies in plasmas [3] and paramagnetic solids [4] demonstrated that excitation of a medium with a circularly polarized laser pulse corresponds to the action of an effective magnetic field. Because phenomenologically this phenomena seems to be the opposite of the magneto-optical Faraday Effect and because both effects are mediated by the same magneto-optical susceptibility tensor, it has been called the Inverse Faraday Effect (IFE)<sup>3</sup>. Later, the nonthermal control of the magnetization by light was also reported in ferromagnetic III-V semiconducting compounds [6]. Recently, this opto-magnetic effect has been observed even in dielectric materials such as orthoferrites [7, 8] and garnets [9, 10], induced by 100 fs laser pulses. In particular, it has been demonstrated that left- and right-handed circularly polarized light can excite spin oscillations (in antiferromagnets) and spin precession (in ferrimagnets) with an opposite phase. Although the effective optically-induced magnetic field was high (in the order of Tesla's), *the maximum achieved reorientation of the magnetization was only a few degrees*. In addition, all these experiments were performed for rather model materials irrelevant for magnetic recording. As will be further discussed, in metallic magnets (materials that are relevant for data storage) the effect of the angular momentum of the photons has never been observed and considered to be too small to be taken into account. Consequently, *all-optical switching, particularly in materials of actual interest for applications, remained both a fundamental and technological challenge (see also Section 1.5)*.

As will be further shown, with this thesis, the all-optical switching of magnetization by circularly polarized light in metallic magnets such as RE-TM alloys will no longer represent a challenge. In the first section of this chapter, it is shown how, by turning a GdFeCo sample into a multi-domain state and thereby suppressing the observation of the heating effect of light, it is possible to demonstrate an ultrafast nonthermal excitation of spin waves by circularly polarized laser pulses, with a phase that depends on the angular momentum of the photons.

In the second section of the chapter it is demonstrated that under the proper conditions, the effect of the angular momentum shown in Section 5.1 can be fully exploited. More specifically, *it is experimentally demonstrated that the magnetization can be reversed in a reproducible manner by a single 40 femtosecond circularly polarized laser pulse, without any applied magnetic field*. The direction of this opto-magnetic switching is determined only by the helicity of light. This finding reveals an ultrafast and efficient pathway for writing magnetic bits at record-breaking speeds.

<sup>3</sup>This axial magnetic field with the origins in the angular momentum of the photons has been sometimes referred in the literature as the field  $\mathbf{B}^{(3)}$  [5].

## 5.1 Ultrafast Interaction of the Angular Momentum of Photons with Spins in GdFeCo

### 5.1.1 Introduction

The strongly nonequilibrium conditions developed in magnetic materials following excitation by intense femtosecond laser pulses represent a subject that has attracted a continuously growing interest over the last two decades [7–16, 18–23, 25–27, 48]. However, due to this strong non-equilibrium, the conventional description of magnetic phenomena in terms of thermodynamics is no longer valid. As a result, the ultrafast channels for transfer the energy and the angular momentum between photons, electrons, spins and phonons remain elusive and a subject of debate [11].

As detailed in Chapter 1, in metallic magnets, the absorbed ultrashort laser pulses excite collective modes (plasmons) and electron-hole pairs (quasiparticles) within tens of femtoseconds, which acquire a large kinetic energy far above the Fermi level [12, 13]. The electron-hole pairs then thermalize to a hot Fermi-Dirac distribution due to electron-electron, hole-hole and electron-hole scattering processes, on a time scale of a few hundred fs [12]. During this thermalization time an ultrafast demagnetization may occur [14]. This process is followed by a quasistatic equilibrium at which the spins follow the electronic temperature [15]. Subsequently, the electron-phonon interaction leads to an increase of the lattice temperature while the electrons cool down ( $t < 2$  ps) [16]. Throughout this section, the above described processes will be referred to as *heat-driven* effects. Surprisingly, it has been reported that laser excitation of a magnetic metallic film may lead to a demagnetization of the material within 50 fs, thus much faster than the typical spin-lattice characteristic time [48]. Furthermore, it has recently been demonstrated that light can excite a metallic spin system also before electron thermalization, via excitation of coherent optical phonons [18]. Such intriguing observations raise fundamental questions about the mechanisms responsible for the ultrafast optical excitation of spins in metals.

In this context it has been suggested that in a metallic magnet, photons may also excite spins nonthermally via an ultrafast interaction between the angular momentum of the photons and the spin system [19]. However, it has been argued that the number of photons involved in real experiments is too low to support such an action on the spin system in metals, based on the transfer of photon angular momentum via absorption (see Subsection 1.5.3) [20]. Indeed, several attempts to detect an ultrafast effect of the light helicity in ferromagnetic metals such as Ni and other transition metals have remained unsuccessful [21–24] and heat-driven effects of light were found to dominate in all these experiments.

Here it is demonstrated that via careful tuning of the conditions in all-optical pump-probe experiments, in particular turning the sample into a multi-domain state, it is possible to minimize the observation of the usually dominating heat-driven effects

of light on the magnetization in the metallic ferrimagnet GdFeCo. Consequently, an ultrafast nonthermal interaction mechanism between photons and spins is revealed where the phase of the excited spin wave is given by the photon angular momentum. The ultrashort laser pulse acts on the ensemble of strongly correlated spins as a magnetic field pulse [7, 9]. It is suggested that this *opto-magnetic* mechanism takes place not by absorption of the angular momentum of the photons but via a different type of mechanism such as a Raman-like coherent optical scattering process. Therefore it does not require annihilation of photons, indicating that one single photon might effectively interact with more than one spin, in this way yielding an efficient interaction between photons and spins.

### 5.1.2 Experimental Details

The material chosen for this study was the ferrimagnetic alloy GdFeCo, grown by magnetron sputtering in the following multilayer structure: glass/AlTi(10 nm)/SiN(5 nm)/Gd<sub>22</sub>Fe<sub>74.6</sub>Co<sub>3.4</sub>(20 nm)/SiN(60 nm). The AlTi layer serves as a heat sink. The GdFeCo layer is an amorphous alloy characterized by a Curie temperature of about 500 K.

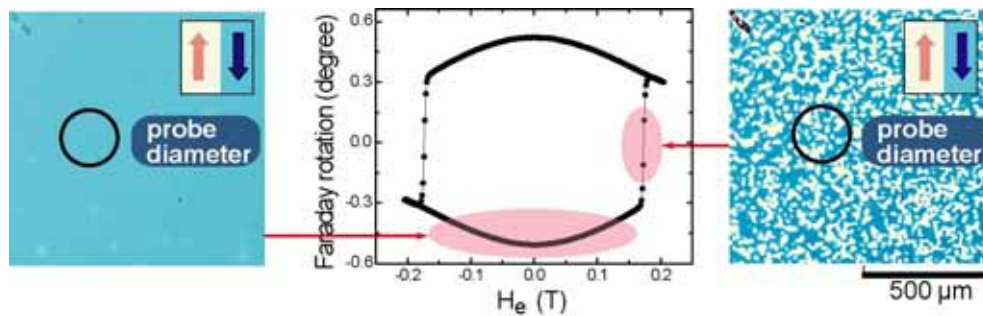


**Figure 5.1:** The initial magnetic state of the GdFeCo sample is a single domain state (left image). Certain values of an external field applied at an angle from the normal to the sample, turn the sample into a multi-domain state (right image) with magnetic domains much smaller than the probe spot diameter. The images were captured by means of a polarization microscope.

Laser induced spin dynamics was investigated using a pump-probe technique. We have applied an external and nearly in-plane magnetic field  $\mathbf{H}_e$  and excited the ferrimagnetic film by circularly polarized 100 fs laser pulses of 0.87 eV photon energy from an amplified Ti:Sapphire laser with a repetition rate of 1 kHz. A less intense linearly polarized probe beam of the same energy was used to detect the changes in

the magnetic system induced by the pump via measurements of the magneto-optical Faraday effect. The pump and probe beams had an intensity ratio of about 100. At nearly normal incidence, the beams were focused on the sample to a spot of  $200 \mu\text{m}$  diameter for the pump and somewhat smaller for the probe beam. The present geometry is sensitive to the out-of-plane component of the magnetization,  $M_z$ . The measurements were performed at room temperature.

### 5.1.3 Averaging Out the Laser Induced Heating Effects

The laser fluence used in our experiments to excite coherent precession of the magnetization in GdFeCo [25] was relatively high (about  $2 \text{ mJ/cm}^2$ ). Hence, heat-driven effects of light on the magnetic order in the metallic ferrimagnet GdFeCo could be very strong. In order to suppress the observation of such heating effects and thus to allow observation of nonthermal effects, we used the concept of turning the sample into a multi-domain state. In addition we used fairly low energy photons of  $0.87 \text{ eV}$  ( $\lambda = 1.42 \mu\text{m}$ ).

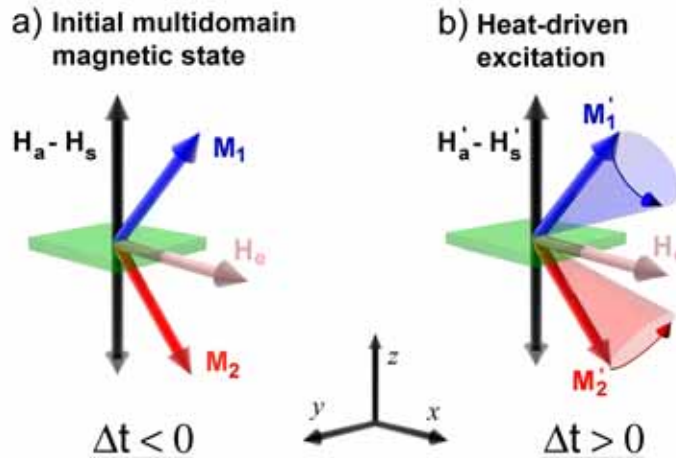


**Figure 5.2:** (a) At  $\Delta t < 0$ , the magnetizations  $M_1$  and  $M_2$  of oppositely magnetized domains are tilted due to the balance between magnetocrystalline anisotropy field  $H_a$ , shape anisotropy field  $H_s$  and external field  $H_e$ . (b) After photoexcitation,  $\Delta t > 0$ , heating induces out of phase oscillations of the z-components of  $M_1$  and  $M_2$ .

As shown in Fig. 5.1, the initial magnetic state of our sample is a single domain

state. The application of an out of plane field of opposite orientation with respect to the magnetization would reverse the magnetization via a few large ( $>100 \mu m$ ) domains, while the simultaneous presence of an in-plane external magnetic field results in the nucleation of a large numbers of small domains [30], with sizes much smaller than the probe area (see Fig. 5.1). Due to the coercivity, these magnetic domains are sufficiently stable in time and thus suitable for the stroboscopic pump-probe experiments. The balance between magnetocrystalline anisotropy field  $\mathbf{H}_a$ , shape anisotropy field  $\mathbf{H}_s$  and external field  $\mathbf{H}_e$ , creates an initial state for these experiments such that the magnetization in each of the domains will be tilted [see Fig. 5.2 (a)]. Laser-heating excitation of such a sample induces locally a change of the magneto-crystalline and shape anisotropy due to heating. This leads to a change of the equilibrium orientation for the magnetization and triggers a precession of the magnetic moments of the domains. These precessions proceed in such a way that the  $z$ -components of the magnetization in oppositely oriented domains (like  $\mathbf{M}_1$  and  $\mathbf{M}_2$  in [Fig. 5.2 (b)]) always oscillate out of phase. Since the probe beam is averaging over a large number of such oppositely oriented domains, the heat-driven effect of light on the magnetization is effectively averaged out in the Faraday signal by achieving  $\sum \delta\mathbf{M}_1^i + \sum \delta\mathbf{M}_2^i \approx 0$ , where the sums are taken over all the domains within the probe area. Experimentally, the optimum cancellation is achieved by adjusting the external magnetic field  $\mathbf{H}_e$ . On the other hand, the effect of a possible optically induced magnetic field, using circularly polarized light is the same for  $\mathbf{M}_1$  and  $\mathbf{M}_2$  as the optically induced field is given by the  $k$ -vector and helicity of the incident laser pulse, *i.e.* the opto-magnetic effect will not be averaged out in a multi-domain sample.

#### 5.1.4 Observation of an Opto-Magnetic Effect in GdFeCo

The results of these time-resolved measurements of the magneto-optical Faraday effect for right-  $\sigma^+$  and left-handed  $\sigma^-$  circularly polarized pump pulses at different  $\mathbf{H}_e$  are shown in Fig. 5.3. The variation of the magneto-optical signal  $\Delta\theta_F$  representing the oscillatory behavior of  $\mathbf{M}_z$  was plotted relative to the total Faraday rotation of the sample  $\theta_F$ . On the scale of 500 ps one can clearly distinguish two different processes. At zero time delay, instantaneous changes of the Faraday rotation are observed that result partly from ultrafast demagnetization and partly from changes of the magneto-crystalline anisotropy [16]. These instantaneous changes of the Faraday rotation are followed by oscillations with a frequency of about 7 GHz, which can clearly be ascribed to precession of the magnetization [25]. The strong damping observed can be understood as a result of the averaging over the many domains. Fig. 5.3 shows that the difference between the magneto-optical Faraday signal for right- and left-handed excitation strongly depends on the external applied field  $\mathbf{H}_e$ . At  $\mathbf{H}_e = 0.172$  T the  $\sigma^+$  and  $\sigma^-$  pump pulses excite precession of opposite phase. Because the phase of the spin precession is given by the angular momentum of the exciting photons, this observation

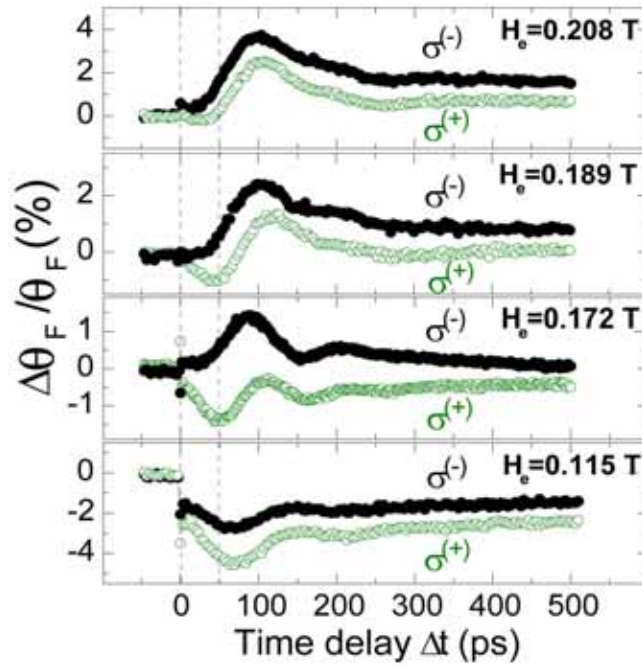


**Figure 5.3:** Precession of the magnetization excited by circularly polarized pump pulses in GdFeCo, probed via the magneto-optical Faraday effect. For certain values of the external field  $\mathbf{H}_e$ , the two helicities  $\sigma^+$  and  $\sigma^-$  give rise to precession with different phase. The lines are guides to the eye.

provides a first indication of an opto-magnetic effect in a metallic ferrimagnet.

In order to better separate this opto-magnetic effect from the heat-driven ones, we have calculated the sum and the difference of the magneto-optical signals resulting from excitation with  $\sigma^+$  and  $\sigma^-$  pump pulses. While the sum of the magneto-optical signals shows the helicity independent heat-driven effect of light on the magnetization  $\Delta M_{\text{heat}} \sim \Delta\theta_F(\sigma^-) + \Delta\theta_F(\sigma^+)$ , the difference corresponds to the opto-magnetic effect  $\Delta M_{\text{opto}} \sim \Delta\theta_F(\sigma^-) - \Delta\theta_F(\sigma^+)$  [21]. The results of the thus analyzed experimental data are plotted in Fig. 5.4. In the opto-magnetic signal [Fig. 5.4 (a)] one can identify an instantaneous change in  $\Delta\theta_F$  after excitation. Although the origin of this instantaneous change is the demagnetization, which is a heat-driven effect, its observation here is a result of the opto-magnetic effect. More specifically, the  $\sigma^+$  and  $\sigma^-$  pump pulses act on the magnetization in opposite directions resulting



in different projections of the demagnetization process on the  $\mathbf{k}$ -vector of the probe beam. This will indeed lead to the observation of a step in  $\Delta M_{\text{opto}}$  as observed in Fig. 5.4 (a). As the strength of  $\mathbf{H}_e$  increases, the magnetization is pulled towards

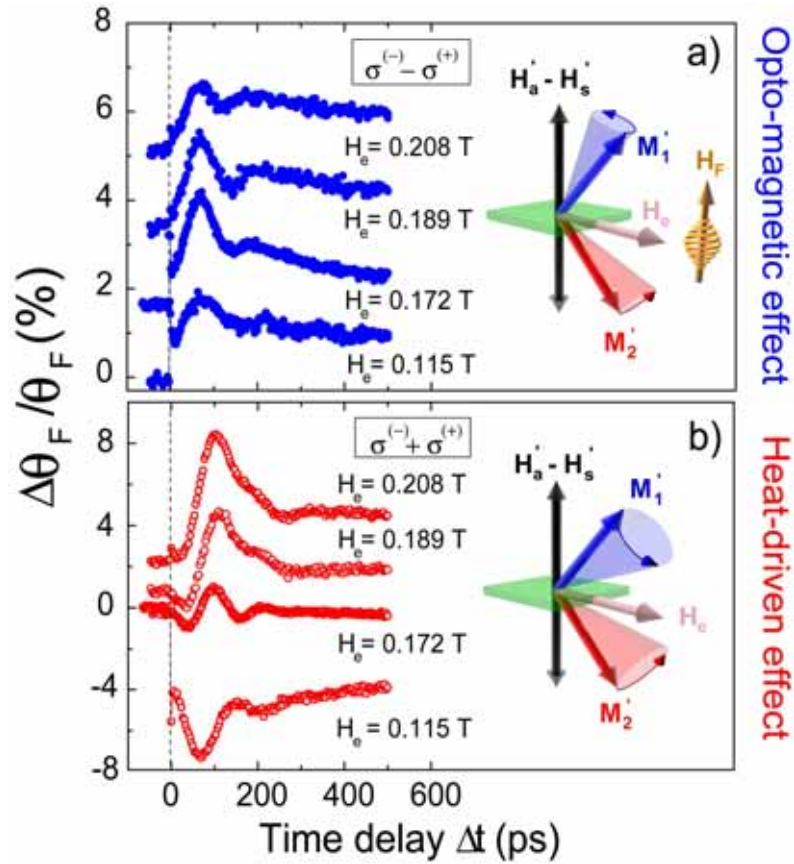


**Figure 5.4:** The difference (a) and the sum (b) of the experimental data resulting from excitations by  $\sigma^+$  and  $\sigma^-$  pump pulses, representing the opto-magnetic and the heat-driven excitation, respectively. The curves are vertically displaced for clarity. The insets of the figure are schematic representations of the opto-magnetic and the heat-driven excitation mechanisms.

the plane of the sample and this difference is gradually reduced. It can also be seen that the sign of the opto-magnetic effect does not depend on the value of  $\mathbf{H}_e$  while the heat-driven one [Fig. 5.4 (b)] is characterized by a strong field dependence and

changes sign at  $\mathbf{H}_e \approx 0.172$  T. Since the amplitude of the heat-driven effect is strongly reduced at  $\mathbf{H}_e = 0.172$  T, it is clear that around this point the averaging out of the heating effect in the Faraday signal is most efficient, allowing the observation of the opto-magnetic effect as was shown in Fig. 5.3. By fine tuning of the external field one may balance the magnetic domains even more precisely and thus suppress the observation of the heat-driven effect completely. At a laser fluence of  $2 \text{ mJ/cm}^2$ , the ratio  $\Delta M_{\text{opto}}/\Delta M_{\text{heat}}$  was estimated to be about 0.21 [31].

### 5.1.5 A Possible Mechanism: The Inverse Faraday Effect

The observed opto-magnetic effect can be described under the assumption that the effect of the laser pulse on the magnetic system is equivalent to the action of a magnetic field pulse  $\mathbf{H}_F$  directed along the wave vector of light [7, 9, 10]. This effective field pulse along the  $z$ -axis triggers a precession of the magnetization, but now the  $z$ -components of  $\mathbf{M}_1$  and  $\mathbf{M}_2$  oscillate in-phase, in contrast to the heat-driven effect where the  $z$ -components of the magnetization in the two opposite domains oscillate out of phase (see inset Fig. 5.4). As a result, the opto-magnetic effect can be detected.

This opto-magnetic effect was suggested to be due to the inverse Faraday effect [4, 32], which can phenomenologically be described as an axial magnetic field

$$\mathbf{H}(0) = (\chi/16\pi)[\mathbf{E}(\omega) \times \mathbf{E}^*(\omega)], \quad (5.1)$$

were  $\mathbf{E}(\omega)$  and  $\mathbf{E}^*(\omega)$  are the electric field of the light wave and its complex conjugate, respectively;  $\chi$  is the magneto-optical susceptibility. Equation 5.1 indicates that the axial magnetic field is induced by circularly polarized light along its  $\mathbf{k}$ -vector. In addition, the sign of this induced field depends on the helicity of light [7–9].

How is it possible that photons affect spins? The optical electric dipole transition cannot change the spin magnetic quantum number. Another mechanism present during the interaction of light with a ferromagnetic solid is the magnetic dipole transition. This mechanism can indeed be responsible for some spin-flip processes. Nevertheless, such mechanism requires annihilation of the photon. It therefore leads to a low efficiency that can not explain the strong opto-magnetic effects such as observed in the experiments presented in this chapter. In addition, in solids, because the orbital angular momentum is in general largely suppressed by the crystal field [33–36] (some exceptions are for example the non-S state RE ions where the unfilled  $4f$  are well screened from the crystal field by the filled outer shells), the spin-orbit interaction is also suppressed. It follows from here that a more effective spin-flip must occur during an optical transition, when the wavefunction of the electron is a superposition of several eigenstates, while it is far less effective for an electron in one of these stationary states. Indeed, it has been recently demonstrated that even if the spin-orbit interaction in the stationary states might be small, the intense laser radiation can cause a laser-enhanced spin-orbit coupling and lead to ultrafast nonthermal demagnetization of materials [37].

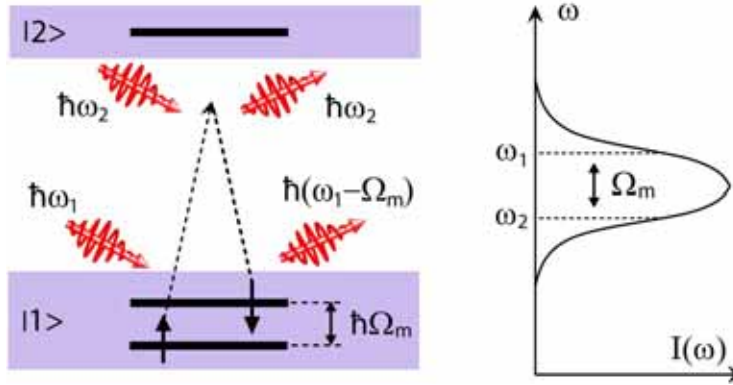


**Figure 5.5:** Schematic illustration of ultrafast spin-flip via the stimulated Raman-like coherent scattering mechanism, believed to be responsible for the ultrafast optically generated magnetic field, as shown in Ref. [10]. Two frequency components of electromagnetic radiation ( $\omega_1$  and  $\omega_2$ ) from the spectrally broad laser pulse ( $\Delta\omega \sim 5$  THz for a laser pulse with duration  $\Delta t=100$  fs) take part in the process.

To account for the speed and efficiency of the opto-magnetic effect, a stimulated Raman-like coherent scattering process has been suggested [7, 9, 29] (see Fig. 5.5). The following picture is in this case considered: Initially, the electron is in the ground state  $|1\rangle$  with its spin up. If it is an orbital singlet (a non-degenerate state), the spin-orbit interaction for this electron can be neglected. When a photon of energy  $\hbar\omega_1$  is acting on this electron, the wave function of the electron becomes a superposition of different eigenstates. This excitation unquenches the orbital angular momentum of the electron. Since the electrons carries also a spin, this process will lead to a strong spin-orbit interaction, unavailable without the presence of the photon, that will lead to an intensification of the spin-flip processes. If the energy of the photon is smaller than the energy required to bring the electron into the nearest excited state  $|2\rangle$ , the electron will be excited into a virtual state. A photon of energy  $\hbar\omega_2$  also present in the optical pulse can now stimulate the de-excitation process from the virtual state back into the ground state with a spin-flip. This spin-flip is due to the fact that circularly polarized light mixes a part of the excited state wave function with the ground state [29]. The relaxation is accompanied by the coherent emission of a photon of energy  $\hbar(\omega_1 - \Omega_m) = \hbar\omega_2$  and the creation of a magnon of energy  $\hbar\Omega_m$ . Because this spin-flip process involves a transition through a virtual state with a strong spin-orbit interaction, it is expected to be very fast, of the order of  $\tau \sim \hbar/E_{s-o} \sim 20$  fs (considering a spin-orbit coupling  $E_{s-o} = 50$  meV).

## 5.1 Ultrafast Interaction of the Angular Momentum of Photons with Spins in GdFeCo 105

---

Therefore,  $\Delta M_{\text{heat}}$  and  $\Delta M_{\text{opto}}$  separate two completely different effects which are coexisting in this metallic system, following laser excitation. While the heat-driven excitation is based on the absorption of light, the opto-magnetic effect is due to the ultrafast interaction of the photon angular momentum with the magnetic system, and is expected to take place via a stimulated Raman-like coherent optical scattering process [7, 10, 29]. Thus, this opto-magnetic mechanism does not require annihilation of a photon. Instead, the photons stimulate the transfer of the required angular momentum from the lattice to the spins. As the energy loss per scattering event is very small ( $\hbar\Omega_m \ll$  photon energy), one single photon can effectively interact with more than one spin, explaining the efficiency of this effect for metallic materials. It is observed from Eq. 5.1, that the strength of the effective magnetic field  $\mathbf{H}_F$  depends on the laser fluence. Although in our experiments we used a relatively high laser fluence for a metallic magnetic material (2 mJ/cm<sup>2</sup>), this is still low compared with the experiments on nonabsorbing dielectrics (e.g. 60 mJ/cm<sup>2</sup> [10]) where a strong opto-magnetic effect was observed. Therefore the usual experimental conditions on metallic magnets, of low laser fluence in addition to a strong heat-driven effect, require a special technique for the detection of ultrafast opto-magnetic effects, as was shown here. On the other hand, under the proper conditions, the effect of the angular momentum can be fully exploited (see Section 5.2).

### 5.1.6 Conclusion

The observation of the opto-magnetic effect in a metallic magnet reported here, together with the previously reported observation of this effect in orthoferrites [7, 8] and garnets [9], indicate that this mechanism does not rely on specific material properties but is a general phenomenon (see also [27]). Thus, it must also occur in ferromagnetic materials such as Ni, and it is a question of the observation technique to detect it.

In conclusion, by using an all optical pump-probe set-up and turning the GdFeCo alloy into a state with small magnetic domains, we have been able to average out the laser induced heating effects in the Faraday signal. Consequently, we have observed that photoexcitation with right and left handed circularly polarized laser pulses results in spin precessions of different phase. This observation clearly demonstrates that in the metallic ferrimagnetic alloy GdFeCo an ultrafast nonthermal coupling between spins and the angular momentum of photons exists.

## 5.2 All-Optical Magnetic Recording with Circularly Polarized Light

### 5.2.1 Introduction

The ever increasing operation speed of modern electronics as well as the push to increase the capacity of storing information motivates the search for faster approaches to process and magnetically record information [7, 9, 25, 38–45]. In magnetic memory devices, logical bits ("ones" and "zeros") are stored by setting the magnetization vector of individual magnetic domains either 'up' or 'down'. The conventional way to record a bit is to reverse the magnetization  $\mathbf{M}$  by applying an external magnetic field  $\mathbf{H}$  [38–42, 46] (see also subsection 1.5.1). However, optical pulses could serve as an alternative stimulus to trigger magnetization reversal. In principle, circularly polarized light should have the ability to act upon a magnetic system in a way similar to a magnetic field directed parallel to the wave-vector of the light via the inverse Faraday effect [4, 32]. Moreover, right- and left-handed circularly polarized waves should act as magnetic fields of opposite sign. This effect was only recently confirmed experimentally [7, 45], and has also been demonstrated to be an efficient tool for coherently controlling the small angle precessional magnetization dynamics in magnetic dielectrics [9, 47] and metals (see Section 5.1).

However, magnetization reversal induced by a sub-picosecond stimulus, i.e. a true  $180^\circ$  switching of the magnetization into a stable and oppositely magnetized state, has remained an important fundamental and technological challenge. Further adding to this challenge is the fact that for direct transfer of angular momentum from the light to the magnetic system, the number of photons available in optical experiments is far from enough [20]. Despite the predicted speed limit and shortage of photons, we here demonstrate that a single 40 femtosecond circularly polarized laser pulse can cause well controlled permanent magnetization reversal in materials typically used for data storage. The optical excitation causes an ultrafast heating of the magnetic system which makes it highly susceptible to the magnetic field simultaneously generated by the circularly polarized light pulse. The combination of these two effects leads to magnetization reversal in a reproducible way. No external magnetic field is required for this opto-magnetic switching, and the stable final state of the magnetization is unambiguously determined by the helicity of the laser pulse.

### 5.2.2 Experimental Details

For our experiments we have chosen a GdFeCo sample, with a composition of  $\text{Gd}_{22}\text{Fe}_{74.6}\text{Co}_{3.4}$  grown in a multilayer structure: glass/AlTi(10 nm)/SiN(5 nm)/GdFeCo(20 nm)/SiN(60 nm), characterized by strong perpendicular magnetic anisotropy, a saturation magnetization of about  $4\pi M = 1000$  G at room temperature, and a Curie point  $T_C = 500$  K.

The experiments were performed by placing the sample under a polarizing microscope, where domains with magnetization "up" and "down" could be observed as white and black regions, respectively. To excite the material we used regeneratively amplified pulses from a Ti:sapphire laser at a wavelength of  $\lambda = 800$  nm and a repetition rate of 1 kHz. Each pulse had a Gaussian intensity profile, with a width at half-maximum of 40 fs. The laser pulses were incident normal to the sample surface, so that an effective optically generated magnetic field would be directed along the magnetization. The beam was focused down to a  $100 \mu\text{m}$  spot and the laser-induced magnetic changes were studied by recording magneto-optical images of the domain patterns before, during and after the laser excitation. This is a well known technique for studying the magnetic material response to ultrashort field pulses [38, 39, 43]. The experiments were performed at room temperature in air.

### 5.2.3 Demonstration of All-Optical Magnetization Reversal

The effect of polarized laser pulses on the magnetization is most readily demonstrated by slowly sweeping a laser beam across the surface of the sample. Figure 5.6 shows how three different sweeps, with the laser beam right-handed circularly polarized ( $\sigma^+$ ), linearly polarized (L), and left-handed ( $\sigma^-$ ) circularly polarized, affect the initial domain pattern in dramatically different ways. The region exposed to linearly polarized light is turned into small domains randomly oriented up or down. In striking contrast, the magnetization of the regions exposed to circularly polarized light is completely switched into an "up"- or "down"-state (white or black) determined only by the helicity of the optical excitation.

Despite the very clean switching behavior observed when scanning the laser beam across the sample, a scramble of the magnetization remains near the right end of each scan line, at the point where the laser beam was shut off. To further investigate its origin we focused the laser beam onto a domain wall, as shown in Figure 5.7, and acquired magneto-optical images *during* the pulsed laser excitation for the three different polarizations of the beam  $\sigma^+$ , L and  $\sigma^-$ . The gray area observed in the center of the laser spot has a contrast in-between that of the white and black magnetic regions. This represents a demagnetized state consisting of small domains which are randomly oriented by each excitation event, and not sensitive to the light polarization. The demagnetized region is formed due to the strong heating in the central part of the Gaussian laser beam. An increase of the spin temperature to above the Curie point corresponds to a total demagnetization, and subsequent cooling in zero magnetic field favors the formation of a random multi-domain state, as observed in this experiment. Note that the concept of spin temperature used above indicates the amount of energy deposited into the magnetic system by the laser excitation.

At the outer perimeter of the gray demagnetized area a white (black) ring with perfect contrast can be seen in the case of  $\sigma^+$  ( $\sigma^-$ ) circularly polarized excitation.

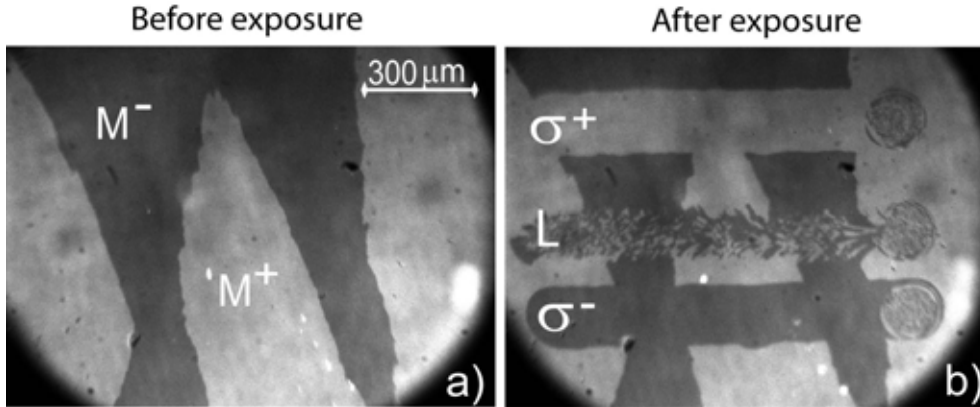


**Figure 5.6:** The effect of ultrashort polarized laser pulses on magnetic domains in  $\text{Gd}_{22}\text{Fe}_{74.6}\text{Co}_{3.4}$ . (a) Magneto-optical image of the initial magnetic state of the sample before laser exposure. White and black areas correspond to "up" ( $M^+$ ) and "down" ( $M^-$ ) magnetic domains, respectively. (b) Domain pattern obtained by sweeping at low speed ( $\sim 30 \mu\text{m/s}$ ) linear (L), right-handed ( $\sigma^+$ ) and left-handed ( $\sigma^-$ ) circularly polarized beams across the surface of the sample, with a laser fluence of about  $11.4 \text{ mJ/cm}^2$ . The central area of the remaining spots at the end of each scan line consists of small magnetic domains, where the ratio of "up" to "down" magnetic domains is close to 1.

When the laser polarization is linear this ring-like switching does not occur, and the demagnetized gray area simply defines the region where the laser fluence is sufficiently high to cause heating above  $T_C$ . This area has the exact same size for all three polarizations, implying that at the outer perimeter of the laser spot, where the opto-magnetic switching occurs, the temperature always remains below the Curie point. Hence, the laser-induced magnetization reversal can be explained as the result of two cooperating effects: First, part of the pulse energy is absorbed in the metal bringing it into a strongly non-equilibrium state with the spin temperature increasing to a level slightly below  $T_C$ . Second, the circularly polarized laser pulse acts on this excited magnetic system as an effective magnetic field directed antiparallel to the small remaining magnetization [4, 7, 9, 32]. According to the theory of second-order magnetic phase transitions, the magnetic susceptibility diverges when the spin temperatures approaches the Curie point [49]. The observed all-optical magnetization reversal can therefore be seen as the combined result of a diverging magnetic susceptibility and a laser-induced effective magnetic field. This switching process is in some respects similar to the recently developed Heat Assisted Magnetic Recording (HAMR) scheme [50], but with the major difference that the laser pulse in our case not only

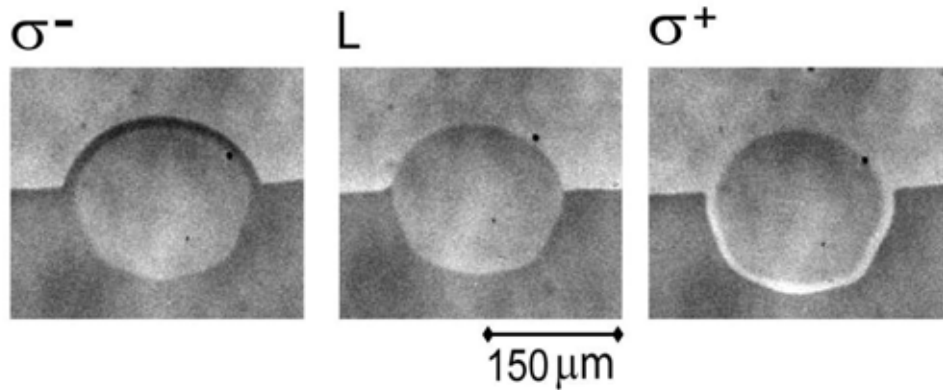


**Figure 5.7:** Images of the laser spot focused onto a domain wall *during* the 1 kHz pulsed laser-excitation with linear (L), right- ( $\sigma^+$ ) and left-handed ( $\sigma^-$ ) circular polarization. The images were obtained for a pulse fluence of about 11.4 mJ/cm<sup>2</sup>. In all three cases the central region of the optically excited area is demagnetized (grey color) due to heating. For circularly polarized excitation ( $\sigma^+$  and  $\sigma^-$ ) opto-magnetic switching takes place on the perimeter of the excited area, where the temperature is just below  $T_C$ .

heats the medium, but does this ultrafast and simultaneously acts as a magnetic field.

The above described picture suggests that by simply reducing the laser power one should be able to cleanly reverse the magnetization in the center of the excited area, without causing overheating and demagnetization of the environment. Figure 5.8 shows how the switching depends on the excitation fluence. The sample was initially magnetized in the "up" direction, and then exposed to laser pulses for about 20 ms. High laser fluences produce similar random multi-domain magnetic states for both  $\sigma^+$  and  $\sigma^-$  excitation, while the lower fluence excitations lead to drastically different results for the two helicities. In particular at 2.9 mJ/cm<sup>2</sup>, the  $\sigma^+$  pulses leave the initial magnetic state unchanged, while the  $\sigma^-$  excitation cleanly reverses the magnetization only in the central part of the irradiated area.



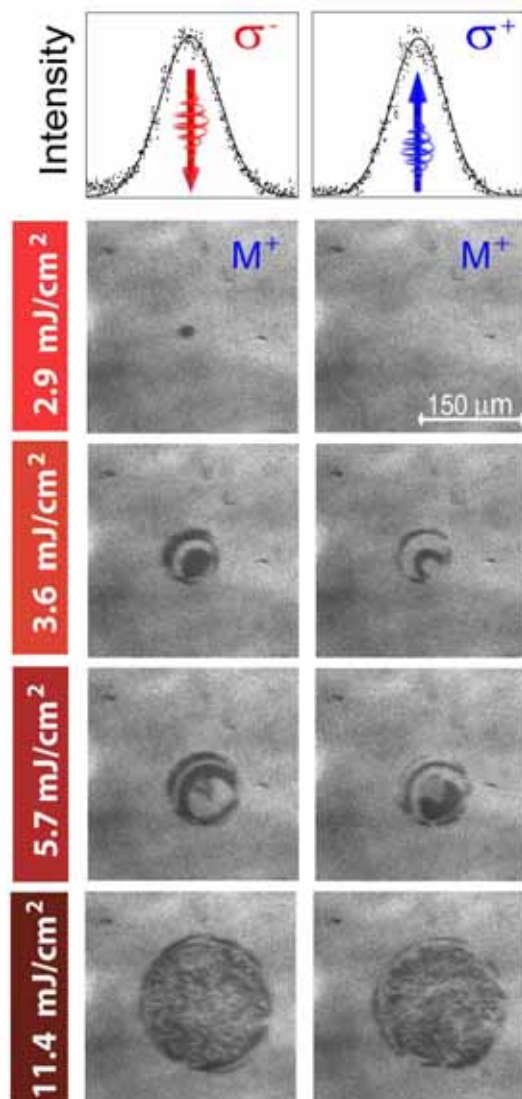


**Figure 5.8:** Images of the magnetic film after exposure to  $\sim 20$  ultrashort left-handed  $\sigma^-$  (left column) and right-handed  $\sigma^+$  (right column) circularly polarized laser pulses at different pulse energies. Before each exposure, the sample was saturated in the "up" ( $M^+$ ) state. The graphs at the top show the intensity profile of the laser beams used for excitation.

### 5.2.4 Magnetization Reversal with Single 40-fs Circular Polarized Laser Pulses

In order to unambiguously determine whether excitation by a single 40 fs laser pulse is sufficient to reverse the magnetization, the laser beam was swept at high speed across the sample, so that each pulse landed at a different spot. The results of this experiment are shown in Figure 5.9 for the two helicities of the laser excitation. One can see that each of the  $\sigma^+$  pulses reverses the magnetization in the black domain, but does not affect the magnetization of the white domain. The opposite situation is observed when the sample is exposed to  $\sigma^-$  pulses. Thus, during the presence of a single 40 fs laser pulse, information about the photons' angular momentum is transferred to the magnetic medium, and subsequently recording occurs. These experiments unambiguously demonstrate that all-optical magnetization reversal can be achieved by single 40 femtosecond circularly polarized laser pulses without the aid of an external magnetic field.

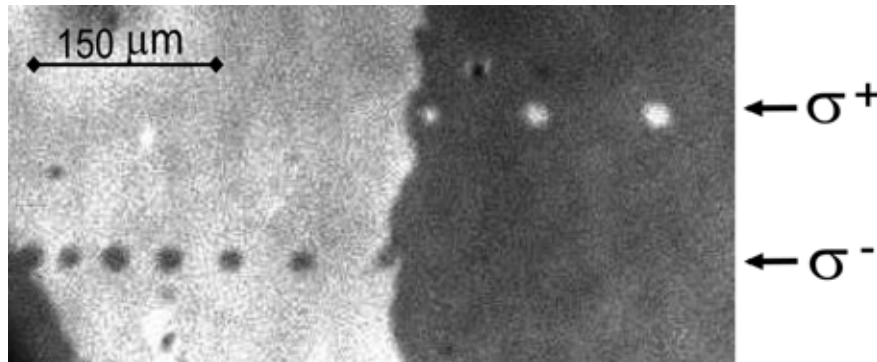


**Figure 5.9:** The effect of single 40-fs circular polarized laser pulses on the magnetic domains in  $\text{Gd}_{22}\text{Fe}_{74.6}\text{Co}_{3.4}$ . The domain pattern was obtained by sweeping at high-speed ( $\sim 50$  mm/s) circularly polarized beams across the surface so that every single laser pulse landed at a different spot. The laser fluence was about  $2.9$  mJ/cm<sup>2</sup>. The small size variation of the written domains is caused by the pulse-to-pulse fluctuation of the laser intensity.

The actual speed of the magnetization reversal is still an intriguing question. It can be answered quite accurately by considering the coherence time of optical excitations in metals. During the 40 fs interaction of the optical pulse with the sample, information about the angular momentum of the photons is transferred to the electrons via electric-dipole transitions. However, the electrons lose this information very rapidly, typically within 200 fs, due to decoherence processes such as electron-electron and electron-phonon collisions [22, 51]. Moreover, the optical spectrum of

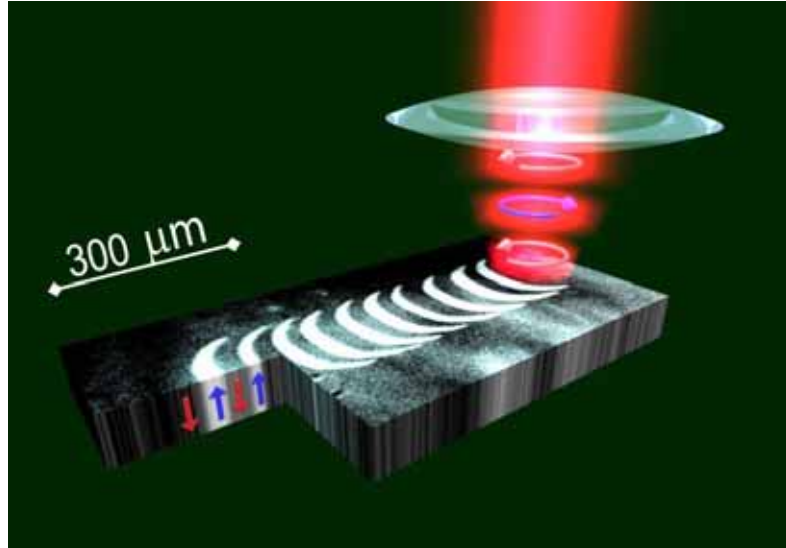


**Figure 5.10:** Demonstration of compact all-optical recording of magnetic bits. This was achieved by scanning a circularly polarized laser beam across the sample and simultaneously modulating the polarization of the beam between left- and right circular.

$\text{Gd}_{22}\text{Fe}_{74.6}\text{Co}_{3.4}$  does not show any narrow lines, thus excluding the possibility of any long-lived electronic states acting as a reservoir of angular momentum. It follows that the actual magnetization reversal must take place on a sub-picosecond time scale, as this is the only way for the helicity information to survive on longer time scales. Consequently, the magnetization is changed on the time scale of the laser pulse, which implies an ultrafast channel of angular momentum transfer between spins and the lattice. This is an important implication of the present results, since currently, the microscopic spin-flip mechanisms leading to the observed ultrafast reduction of macroscopic magnetization are still a matter of debate [15, 52, 53]. Because the spin temperature of the area where all-optical magnetization reversal occurs remains below the Curie point, some domains of the magnetically ordered phase are still present [54]. The fact that a circularly polarized laser pulse reverses the magnetization means that the magnetic field generated by the laser is able to reverse the magnetization in these domains. The complete recovery of the magnetization in the new state is a much slower process determined mainly by the speed of heat diffusion in the sample. During this recovery process no magnetic field is present to set the magnetization, but the magnetization direction is well determined.

As a simple illustration of opto-magnetic recording, it is shown in Figure 5.10 how optically written bits can be overlapped and made much smaller than the beam waist by modulating the polarization between  $\sigma^+$  and  $\sigma^-$  as the laser beam is swept across the sample. High density recording may also be achieved by employing especially designed near-field antenna structures [50] such as those currently being developed for HAMR. With the recent development of compact ultrafast laser systems [55] and the successful incorporation of lasers in magnetic storage devices [50], the present demonstration of ultrafast and all-optical magnetization reversal might spur the realization of a new generation of magnetic recording devices.

### 5.2.5 Conclusion

In conclusion, we have demonstrated that the magnetization of a 20 nm metallic GdFeCo film can be reversed in a controllable way with a single 40 fs circularly polarized laser pulse without the aid of any applied magnetic field. The direction of this switching is determined only by the helicity of the light pulse. Besides its clear technological importance, we believe that the observations reported here will lead to a better understanding of the interaction of light with magnetic systems on ultrashort time scales.

## 5.3 Summary

In this chapter the role of the angular momentum of the photons on spins in the metallic amorphous alloy GdFeCo has been investigated by means of both magneto-optical imaging and all-optical time-resolved pump-probe techniques. In the first section of this chapter, it is experimentally demonstrated that via careful tuning of the conditions in all-optical pump-probe experiments, one can suppress the observation of the usual thermal induced effects on the spin system. In this way a nonthermal action of the angular momentum of the photons on the spin system was revealed, where the phase of the excited spin precession depends on the light helicity. Consequently, the relevance of the photon angular momentum in the interaction process of ultrafast light pulses with metallic magnets was demonstrated for the first time experimentally.

Besides the control of the magnetization precession phase, it is demonstrated in the second section of the present chapter that circularly polarized light can induce all-optical magnetization reversal in GdFeCo. It was demonstrated that the magnetization can be reversed in a reproducible manner by a single femtosecond circularly polarized laser pulse, without any applied magnetic field. The direction of this opto-magnetic switching is determined only by the direction of the angular momentum of the photons. It follows that this magnetization reversal must take place on a subpicosecond time scale, as this is the only way for the helicity information to survive on longer time scales.

## References

- [1] G. Sansone, E. Benedetti, F. Calegari, C. Vozzi, L. Avaldi, R. Flammini, L. Poletto, P. Villoresi, C. Altucci, R. Velotta, S. Stagira, S. De Silvestri, M. Nisoli, *Science* **314**, 443 (2006).
- [2] Gabriel Molina-Terriza, Juan P. Torres, and Lluís Torner, *Nature Physics* **3**, 305 (2007).
- [3] J. Deschamps, M. Fitaire, and M. Lagoutte, *Phys. Rev. Lett.* **25**, 1330 (1970).
- [4] J. P. van der Ziel, P. S. Pershan, and L. D. Malmstrom, *Phys. Rev. Lett.* **15**, 190 (1965).
- [5] M. W. Evans and J. P. Vigièr, *The Enigmatic Photon* (Kluwer Academic Publishers, 1994).
- [6] A. Oiwa, Y. Mitsumori, R. Moriya, T. Slupinski, and H. Munekata, *Phys. Rev. Lett.* **88**, 137202 (2002).
- [7] A. V. Kimel, A. Kirilyuk, P. A. Usachev, R. V. Pisarev, A. M. Balbashov and Th. Rasing, *Nature* **435**, 655 (2005).
- [8] A. V. Kimel, C. D. Stanciu, P. A. Usachev, R. V. Pisarev, V. N. Gridnev, A. Kirilyuk, and Th. Rasing, *Phys. Rev. B* **74**, 060403 (2006).
- [9] F. Hansteen, A. Kimel, A. Kirilyuk, and Th. Rasing, *Phys. Rev. Lett.* **95**, 047402 (2005).
- [10] F. Hansteen, A. Kimel, A. Kirilyuk, and Th. Rasing, *Phys. Rev. B* **73**, 014421 (2006).
- [11] J. Stöhr and H. C. Siegmann, *Magnetism: From Fundamentals to Nanoscale Dynamics* (Springer Verlag, New York, 2006).
- [12] J.-Y. Bigot, *C. R. Acad. Sci. Ser. IV (Paris)* **2**, 1483 (2001).
- [13] N. Del Fatti, C. Voisin, M. Achermann, S. Tzortzakis, D. Christofilos, and F. Valleé, *Phys. Rev. B* **61**, 16956 (2000).
- [14] A. Scholl, L. Baumgarten, R. Jacquemin, and W. Eberhardt, *Phys. Rev. Lett.* **79**, 5146 (1997).
- [15] E. Beaupaire, J.-C. Merle, A. Daunois, and J.-Y. Bigot, *Phys. Rev. Lett.* **76**, 4250 (1996).

- 
- [16] M. Vomir, L. H. F. Andrade, L. Guidoni, E. Beaurepaire, and J.-Y. Bigot, Phys. Rev. Lett. **94**, 237601 (2005).
- [48] L. Guidoni, Eric Beaurepaire, and Jean-Yves Bigot, Phys. Rev. Lett. **89**, 017401 (2002).
- [18] A. Melnikov, I. Radu, U. Bovensiepen, O. Krupin, K. Starke, E. Matthias, and M. Wolf, Phys. Rev. Lett. **91**, 227403 (2003).
- [19] G. P. Zhang and W. Hübner, Phys. Rev. Lett. **85**, 3025 (2000).
- [20] B. Koopmans, M. van Kampen, J. T. Kohlhepp, and W. J. M. de Jonge, Phys. Rev. Lett. **85**, 844 (2000).
- [21] G. Ju, A. Vertikov, A. V. Nurmikko, C. Canady, Gang Xiao, R. F. C. Farrow and A. Cebollada, Phys. Rev. B **57**, R700 (1998).
- [22] V. V. Kruglyak, R. J. Hicken, M. Ali, B. J. Hickey, A. T. G. Pym, and B. K. Tanner, Phys. Rev. B **71**, 233104 (2005).
- [23] R. Wilks, R. J. Hicken, M. Ali, B. J. Hickey, J. D. R. Buchanan, A. T. G. Pym, and B. K. Tanner, J. Appl. Phys. **95**, 7441 (2004).
- [24] F. Dalla Longa, J. T. Kohlhepp, W. J. M. de Jonge, and B. Koopmans, Phys. Rev. B **75**, 224431 (2007).
- [25] C. D. Stanciu, A. V. Kimel, F. Hansteen, A. Tsukamoto, A. Itoh, A. Kirilyuk, and Th. Rasing, Phys. Rev. B **73**, 220402(R) (2006).
- [26] J. Hohlfeld, Th. Gerrits, M. Bilderbeek, Th. Rasing, H. Awano, and N. Ohta, Phys. Rev. B **65**, 012413 (2001).
- [27] R. Hertel, J. Magn. Magn. Mater. **303**, L1 (2005).
- [28] A. K. Zvezdin and V. A. Kotov, *Modern Magneto-Optics and Magneto-Optical Materials* (IoP Publishing, Bristol, 1997).
- [29] P. S. Pershan, J. P. van der Ziel, and L. D. Malmstrom, Phys. Rev. **143**, 574 (1966).
- [30] Te-ho Wu, J. Appl. Phys. **81**, 5321 (1997); M. Kisielewski, A. Maziewski, V. Zablotskii, T. Polyakova, J. M. Garcia, A. Wawro, and L. T. Baczewski, J. Appl. Phys. **93**, 6966 (2003).
- [31] The magnitude of the heat-driven effect was obtained from the single domain experiment.

- [32] L. P. Pitaevskii, Sov. Phys. JETP **12**, 1008 (1961).
- [33] Harvey Brooks, Phys. Rev. **58**, 909 (1940).
- [34] J. H. Van Vleck, Rev. Mod. Phys. **17**, 27 (1945).
- [35] Charles Kittel, Rev. Mod. Phys. **21**, 541 (1949).
- [36] Peter Mohn, *Magnetism in the Solid State: An Introduction*, p-206 (Springer-Verlag Berlin Heidelberg, 2006).
- [37] C. Stamm, T. Kachel, N. Pontius, R. Mitzner, T. Quast, K. Holldack, S. Khan, C. Lupulescu, E. F. Aziz, M. Wietstruk, H. A. Dürr and W. Eberhardt, Nature Materials **6**, 740 (2007).
- [38] C. H. Back, R. Allenspach, W. Weber, S. S. P. Parkin, D. Weller, E. L. Garwin, H. C. Siegmann, Science **285**, 864 (1999).
- [39] C. H. Back, D. Weller, J. Heidmann, D. Mauri, D. Guarisco, E. L. Garwin, and H. C. Siegmann, Phys. Rev. Lett. **81**, 3251 (1998).
- [40] S. Kaka, S. E. Russek, Appl. Phys. Lett. **86**, 2958 (2002).
- [41] H. W. Schumacher, C. Chappert, P. Crozat, R. C. Sousa, P. P. Freitas, J. Miltat, J. Fassbender, and B. Hillebrands, Phys. Rev. Lett. **90**, 017201 (2003).
- [42] Th. Gerrits, H. A. M. van den Berg, J. Hohlfeld, L. Bär, Th. Rasing, Nature **418**, 509 (2002).
- [43] I. Tudosa, C. Stamm, A. B. Kashuba, F. King, H. C. Siegmann, J. Stöhr, G. Ju, B. Lu, D. Weller, Nature **428**, 831 (2004).
- [44] Ganping Ju, Julius Hohlfeld, Bastiaan Bergman, René J. M. van de Veerdonk, Oleg N. Mryasov, Jai-Young Kim, Xiaowei Wu, Dieter Weller, and Bert Koopmans, Phys. Rev. Lett. **93**, 197403 (2004).
- [45] C. D. Stanciu, F. Hansteen, A. V. Kimel, A. Tsukamoto, A. Itoh, A. Kirilyuk, and Th. Rasing, Phys. Rev. Lett. **98**, 207401 (2007).
- [46] M. Mansuripur, *Physical Principles of Magneto-Optical Recording* (Cambridge University Press, Cambridge, 1998).
- [47] A.V. Kimel, A. Kirilyuk, F. Hansteen, and Th. Rasing, J. Phys.: Condens. Matter **19**, 043201 (2007).
- [48] L. Guidoni, E. Beaurepaire, J.-Y. Bigot, Phys. Rev. Lett. **89**, 017401 (2002).

- 
- [49] L. D. Landau, E. M. Lifshitz, *Electrodynamics of Continuous Media* (Pergamon, Oxford, 1984).
- [50] W. A. Challener, T. W. McDaniel, C. D. Mihalcea, K. R. Mountfield, K. Pelhos and I. K. Sendur, *Jpn. J. Appl. Phys.* **42**, 981 (2003).
- [51] H. Petek, and S. Ogawa, *Progress in Surface Science* **56**, 239 (1997).
- [52] Uwe Bovensiepen, *J. Phys. Cond. Matter* **19**, 083201 (2007).
- [53] M. Cinchetti, M. Sánchez Albaneda, D. Hoffmann, T. Roth, J.-P. Wüstenberg, M. Krauß, O. Andreyev, H. C. Schneider, M. Bauer, and M. Aeschlimann, *Phys. Rev. Lett.* **97**, 177201 (2006).
- [54] O. Chubykalo-Fesenko, U. Nowak, R. W. Chantrell, and D. Garanin, *Phys. Rev. B* **74**, 094436 (2006).
- [55] U. Keller, *Nature* **424**, 831 (2003).





---

## Summary and Outlook

---

A hard disk drive (HDD) stores information in the form of small magnetic areas magnetized in opposite directions, like tiny bar magnets pointing north or south. Depending on the orientation of these bits the information can be later retrieved as "ones" and "zeros". The higher the information density on a hard disk, the *smaller* the magnetic bits must be. The higher the writing speed of information on a hard disk, the *faster* the manipulation (*i.e.* reversal) of the tiny bar magnets must become. Thus *smaller* and *faster* represents the driving force for the advancement of the hard disk drive technology in particular, and of the magnetic storage technology in general.

*This thesis focuses on the speed of manipulating the magnetization in metallic magnets relevant for data storage.*

The conventional way to reverse the magnetization is by applying a magnetic field pulse either parallel or perpendicular to the magnetization of a bit, as described in Chapter 1 of this thesis. Today, a HDD stores a magnetic bit in  $\sim 1$  nanosecond. The speed of this process is proportional to the magnetic field strength. This would imply that the reorientation time could be as short as desired, provided that sufficiently high fields would be available. However, it was recently predicted that there is a natural limit of magnetization switching on the picosecond time scale, beyond which magnetization reversal becomes chaotic<sup>1</sup>. Thus, finding new approaches to reverse magnetization in a reproducible way on a time scale shorter than picoseconds is a fundamental challenge with important consequences for magnetic data storage technology.

*In this thesis two different ways of reversing the magnetization faster than picosecond were experimentally demonstrated, breaking what was previously called the speed*

---

<sup>1</sup>[http : //physicsworld.com/cws/article/news/19401](http://physicsworld.com/cws/article/news/19401)

*limit of magnetic recording. In addition, this thesis demonstrates the feasibility of an effect that was previously believed fundamentally impossible in metals: controlled magnetization reversal with circularly polarized light.*

The experiments were performed on a rare-earth transition-metal (RE-TM) amorphous alloy, *i.e.* GdFeCo. The magnetic and magneto-optical properties of the RE-TM metallic magnets are detailed in Chapter 2. The main experimental techniques used to investigate and control the magnetization dynamics on the femtosecond time-scales are presented in Chapter 3. The results are presented in Chapter 4 and Chapter 5.

Chapter 4 shows that the angular momentum compensation point, that can be present in some ferrimagnetic materials such as GdFeCo, is accompanied by a high-speed and strongly damped spin dynamics. Next, by ultrafast heating the ferrimagnet across its compensation points, under an applied magnetic field, a subpicosecond magnetization reversal is experimentally demonstrated. This shows for the first time the feasibility of subpicosecond magnetization reversal, in a time-resolved experiment.

In Chapter 5, the effect of the angular momentum of the photons on spins in metallic systems was investigated. Previously, this effect was thought to be of no relevance. A full  $180^\circ$  reorientation of a magnet by femtosecond laser pulses was considered to be even less possible based on the physics as known today (see Subsection 1.5.3). However, it is demonstrated here that the magnetization of the metallic amorphous alloy GdFeCo can be reversed in a reproducible manner by a single 40 femtosecond circularly polarized laser pulse, without any applied magnetic field. Nevertheless, the actual speed of this all-optical induced magnetization reversal remained an open question.

In collaboration with dr. Julius Hohlfeld and dr. Adnan Rebei (Seagate, Pittsburgh, USA) we have recently succeeded to observe a subpicosecond all-optical magnetization reversal induced by 500 fs circularly polarized laser pulses. In addition to the importance of this observation, it is remarkable that near-picosecond long laser pulses are still able to switch the magnetization. This is an important issue from the applications point of view, since currently lasers with near-picosecond long pulses are relatively cheap and of small size, in contrast to the expensive femtosecond lasers.

In addition to the experiments on GdFeCo we have also performed experiments on all-optical switching in ferrimagnetic RE-TM amorphous alloys such as TbFeCo and DyFeCo. The all-optical switching has been also observed in these experiments. In addition, the observation of all-optical switching in materials such as the ferromagnetic crystalline  $\text{SmCo}_5$  has been recently reported by J. Hohlfeld and A. Rebei<sup>2</sup>. From this it follows that the all-optical switching is taking place no matter whether the magnetic material is amorphous or has a crystalline structure or, whether it has a low coercivity such as  $\sim 0.01$  T in GdFeCo or a high coercivity such as more than 1 T in TbFeCo and  $\text{SmCo}_5$ , or whether the magnetic system is ferromagnetic or ferrimagnetic. Yet,

<sup>2</sup>J. Hohlfeld and A. Rebei, talk at THz Dynamics, Grenoble 2007.

as observed in our experiments, the all-optical switching depends on the spot size of the laser beam and on the thickness of the sample. In particular, we observed (in collaboration with J.-Y. Bigot in Strasbourg, France) that a few micrometer spot-size leads to a nondeterministic switching of magnetization. The reason for this is that due to the relatively low anisotropy of the sample, for certain compositions the minimum domain-size in GdFeCo is a few micrometers. Consequently, under these experimental conditions there is a large chance that the created domain collapses. As the optical penetration depth in metals is  $\sim 20$  nm, if the sample is too thick the all-optical switched domain might also collapse. This has been also observed in a 50 nm thick GdFeCo sample. Therefore, in order to better understand the required conditions for the feasibility of the all-optical switching, more quantitative studies must be performed such as the dependence on pulse-duration, spot-size, sample shape and thickness. It must also be noted here that, in the presence of an external magnetic field, the effect of the angular momentum of the photons is suppressed. A quantitative study of the all-optical switching as a function of applied field strength for various sample compositions is therefore also required.

Yet, until now all-optical switching has been only observed in magnetic systems involving rare-earths. Therefore, it would be very interesting to study the effect of the photon angular momentum on metallic magnets such as for example Co (with perpendicular anisotropy). This study would indicate whether the switching mechanism is mainly driven by the localized effects in the RE or whether the itinerant character of the spins of the TM is required as well.

Furthermore, it was very recently demonstrated that the magnetization switching in current-induced magnetic switching experiments, where the injected electrons transfer their angular momentum to the magnetic material, is a process associated not with the magnetization but with the angular momentum of the magnetic material<sup>3</sup>. In this respect it will be very interesting to study and compare the effect of the angular momentum of the photons on magnetic materials characterized by various total angular momenta.

From the present experiments it appears, that the optically induced ultrafast magnetization reversal is the combined result of femtosecond laser heating of the magnetic system to just below the Curie point, and circularly polarized light simultaneously acting as a magnetic field. On the other hand, it has been also shown elsewhere that the opto-magnetic effect in dielectric materials is proportional to the laser fluence<sup>4</sup>. However, the increase of the laser fluence in metallic materials is limited by the strong optical absorption. In order to better understand the importance of laser fluence and whether the sample temperature must indeed be elevated to near the Curie tempera-

---

<sup>3</sup>Xin Jiang, Li Gao, Jonathan Z. Sun, and Stuart S. P. Parkin, *Phys. Rev. Lett.* **97**, 217202 (2006).

<sup>4</sup>A. V. Kimel, A. Kirilyuk, P. A. Usachev, R. V. Pisarev, A. M. Balbashov and Th. Rasing, *Nature* **435**, 655 (2005).

ture to achieve the all-optical switching, a systematic study should be performed on all-optical switching as a function of the laser fluence at lower temperatures. Alternatively, the experiment can also be performed at various laser wavelengths, and specifically in the range where the magnetic sample shows low optical absorption. These experiments would be relevant not only for a better understanding of the switching mechanism but also from a technological point of view, since for storage purpose it is highly desirable to reduce the temperature involved in the magnetization reversal process.

With this thesis a new avenue in the field of ultrafast magnetization reversal has been opened. Since the experiments presented here are the first to demonstrate the feasibility of an effect that was previously believed fundamentally impossible, the microscopic mechanism responsible for this effect is still a matter of debate<sup>5</sup>. As described above, many experiments have to be performed in order to completely understand the opto-magnetic switching mechanism.

Finally, it must be noted that although the all-optical magnetization reversal by circularly polarized light is presented from the point of view of applications in the data storage, it is obvious that this new effect has the potential to strongly affect also other fields of research and technology.

---

<sup>5</sup>A. Rebei and J. Hohlfield, *Physics Letters A* **372**, 1915 (2008).

---

## Samenvatting en Vooruitblik

---

Op een harde schijf wordt informatie opgeslagen in de vorm van kleine magnetische gebieden, welke in tegenovergestelde richting zijn gemagnetiseerd, net als kleine magneetjes die naar het noorden of zuiden wijzen. Afhankelijk van hun orientatie kunnen deze "bits" als digitale "een" of "nul" worden uitgelezen. Hoe hoger de informatie dichtheid, hoe kleiner de magnetische bits moeten zijn. En hoe hoger de schrijfsnelheid, hoe sneller de magneetjes moeten worden omgepoold. *Kleiner* en *sneller* zijn dus de drijvende krachten achter de ontwikkeling van de harde schijf technologie, en van magnetische data opslag in zijn algemeenheid.

*Dit proefschrift richt zich op de snelheid van het ompolen van de magnetisatie in metalische materialen welke relevant zijn voor magnetische data opslag.*

De conventionele manier om de magnetisatie om te keren is gebeurd met behulp van een korte magneetveldpuls parallel of loodrecht op de magnetisatie van een bit, zoals beschreven in hoofdstuk 1. De snelheid van dit proces is evenredig met de veldsterkte. Recentelijk echter werd voorspeld dat er een natuurlijke snelheidslimiet van enkele picoseconden bestaat, waar voorbij het omkeren van de magnetisatie chaotisch dreigt te verlopen<sup>1</sup>. Het vinden van nieuwe manieren om de magnetisatie op een gecontroleerde wijze sneller dan een picoseconde om te polen is daarom een grote fundamentele uitdaging met belangrijke praktische consequenties met name voor magnetische dataopslag.

*In dit proefschrift worden twee manieren om de magnetisatie binnen een picoseconde om te polen experimenteel gedemonstreerd.* De experimenten werden uitgevoerd met GdFeCo, een amorfe legering van zeldzaam aarde overgangsmetalen (ZA-OM). De magnetische en magneto-optische eigenschappen van deze ZA-OM magnetische

<sup>1</sup><http://physicsworld.com/cws/article/news/19401>

legering worden besproken in hoofdstuk 2. De belangrijkste experimentele technieken welke werden gebruikt om de magnetisatie dynamica op een femtoseconde tijdschaal te bestuderen en manipuleren worden beschreven in hoofdstuk 3, terwijl de hoofdstukken 4 en 5 de verkregen resultaten bevatten.

In hoofdstuk 4 wordt eerst aangetoond dat het draaimoment-compensatie punt, wat aanwezig is in sommige ferrimagnetische materialen zoals GdFeCo, aanleiding geeft tot zeer snelle en sterk gedemptespin dynamica. Daarna wordt aangetoond dat in de buurt van zo'n compensatiepunt, subpicoseconde magnetisatie omkeer mogelijk is door de ferrimagneet zeer snel te verhitten in de aanwezigheid van een extern magneetveld. Dit is, zover bekend, de eerste keer dat een magnetisatie omkering binnen een picoseconde is gedemonstreerd.

In hoofdstuk 5 wordt de wisselwerking van het draaimoment van fotonen met de magnetische spins bestudeerd. Oorspronkelijk wordt dit als een verwaarloosbaar effect beschouwd. Een volledige  $180^\circ$  omkering van de magnetisatie door femtoseconden laserpulsen werd zelfs voor volledig onmogelijk gehouden uitgaande van de momenteel bekende natuurkunde (zie 1.5.3). Echter hoofdstuk 5 laat zien dat de magnetisatie in GdFeCo op een reproduceerbare wijze kan worden omgepoold met behulp van een enkele 40 femtoseconde circulair gepolariseerde laserpuls. De snelheid van dit omkering proces zelf blijft hierbij nog een onbeantwoorde vraag.

In samenwerking met dr. Julius Hohfeld en dr. Adnan Rebei (Seagate, Pittsburgh, USA) is recentelijk een subpicoseconde, geheel optisch geïnduceerde magnetisatie ompoling gedemonstreerd met behulp van 500 femtoseconde circulair gepolariseerde laserpulsen. Naast het intrinsiek belang van deze waarneming is het bijzonder dat zelfs laserpulsen van bijna een picoseconde in staat zijn de magnetisatie om te polen. Dit is van belang voor eventuele toepassingen, omdat picoseconde lasers veel kleiner en goedkoper zijn dan de huidige dure femtoseconde lasers.

Behalve in GdFeCo hebben we ook in andere ferrimagnetische ZA-OM amorfe legeringen, zoals TbFeCo en DyFeCo volledig optisch geïnduceerde magnetisatie omkering waargenomen. Daarnaast hebben J. Hohfeld en A. Rebei recentelijk ook volledig optisch geïnduceerde ompoling in de kristallijne ferromagneet  $\text{SmCo}_5$  waargenomen<sup>2</sup>. Uit dit alles blijkt dat het volledig optisch schakelen niet afhankelijk is van de kristalstructuur, noch van de coërciviteit, welke zeer laag is in GdFeCo ( $\sim 0,01$  T) en zeer laag in TbFeCo en  $\text{SmCo}_5$  (meer dan 1T), noch van het ferri- of het ferromagnetische karakter van het betreffende magnetische systeem. Echter, in onze experimenten hebben we gezien dat het optisch ompolen wel afhangt van de grootte van de laser spot en de dichtheid van de magnetische film. In samenwerking met J. -Y. Bigot in Strasbourg hebben we geconstateerd dat een spot grootte van enkele micrometer aanleiding geeft tot een niet-deterministisch schakelgedrag. De reden hiervoor is dat vanwege de lage anisotropie, de domeingrootte voor bepaalde preparaat samenstellingen enkele micrometer is. Als gevolg hiervan is er een grote kans dat een nieuw

<sup>2</sup>J. Hohfeld and A. Rebei, talk at THz Dynamics, Grenoble 2007.

gevormd magnetisch domein verdwijnt. Ditzelfde kan gebeuren bij een te dichte film, aangezien de optische indringdiepte in metalen ongeveer 20 nm is. Dit is inderdaad waargenomen voor een 50 nm dik GdFeCo preparaat. Het is daarom duidelijk dat er meer kwantitatieve metingen moeten worden gedaan om een beter inzicht te krijgen in de vereiste omstandigheden voor de verwezenlijking van volledig optisch schakelen, zoals de afhankelijkheid van pulsduur, spotgrootte, preparaatvorm en dikte. Daarnaast is het goed te realiseren dat het effect van het fotondraaimoment wordt onderdrukt door de aanwezigheid van een uitwendig magneetveld, hetgeen ook verdere kwantitatieve studies van verschillende preparaat composities vereist.

Tot nu toe is het volledig optisch schakelen alleen waargenomen in materialen waarin zeldame aarden voorkomen. Het is daarom interessant om het effect van het draaimoment van fotonen op magnetische metalen zoals Co (met loodrechte anisotropie) te bestuderen. Een dergelijk studie kan misschien verduidelijken of het schakelen voornamelijk afhangt van de sterk gelocaliseerde magnetische momenten in de ZA of dat het gedelocaliseerde karakter van de OM-spins ook een rol speelt.

Recente experimenten met spin-gepolariseerde electronen hebben laten zien dat bij dit stroom geïnduceerde schakelen waarbij het draaimoment van de electronen wordt overgedragen naar het magnetisch materiaal, niet de magnetisatie maar het draaimoment van het materiaal van belang is<sup>3</sup>. In dit verband is het dan ook interessant om het optisch schakelen te bestuderen in materialen met verschillend totaal draaimoment.

De huidige experimenten lijken aan te geven dat het optisch schakelen het resultaat is van het gecombineerde effect van het opwarmen van het magnetisch materiaal tot vlak onder de Curie temperatuur en het optisch geïnduceerde magnetische veld. Anderzijds dielectrisch materialen reeds aangetoond dat de sterkte van dit veld evenredig is met de laserintensiteit. Echter, de sterke optische absorptie beperkt het opvoeren van de laser intensiteit in metalen. Om het belang van het al dan niet verwarmen tot de Curie temperatuur beter te begrijpen zijn meer systematische experimenten noodzakelijk bij lagere temperaturen. Anderzijds kan men ook de gebruikte golflengte variëren met name in een gebied met lage absorptie. Deze experimenten zijn niet alleen van belang voor een beter fundamenteel begrip maar ook voor mogelijke toepassingen, omdat ook dan een lagere temperatuur wenselijk is.

Met dit proefschrift is er een nieuwe weg ingeslagen op het gebied van ultrasnelle magnetisatie ompoling. Aangezien de hier gepresenteerde experimenten de eerste zijn die een effect demonstreren dat tot voor kort onmogelijk werd geacht, is het microscopisch mechanisme wat er voor verantwoordelijk is nog steeds onderwerp van discussie<sup>4</sup>. Zoals hierboven opgemerkt zullen er nog veel experimenten nodig zijn om

<sup>3</sup>Xin Jiang, Li Gao, Jonathan Z. Sun, and Stuart S. P. Parkin, *Phys. Rev. Lett.* **97**, 217202 (2006).

<sup>3</sup>A. V. Kimel, A. Kirilyuk, P. A. Usachev, R. V. Pisarev, A. M. Balbashov and Th. Rasing, *Nature* **435**, 655 (2005).

<sup>4</sup>A. Rebei and J. Hohlfield, *Physics Letters A* **372**, 1915 (2008).



tot een beter inzicht in dit optomagnetisch schakel effect te komen.

Ten slotte dient te worden opgemerkt dat hoewel de hier beschreven resultaten met name in het licht van data-opslag zijn gepresenteerd, het duidelijk moge zijn dat dit nieuwe effect ook grote mogelijkheden biedt in andere gebieden van onderzoek en technologie.

---

## Rezumat

---

**Î**ntr-un hard disk (HDD) informația este stocată sub forma unor regiuni magnetice extrem de mici, magnetizate în direcții opuse, precum mici magneti orientați către nord sau sud. În funcție de orientarea acestor mici regiuni magnetice, denumite biți, informația poate fi accesată mai târziu ca "unu" sau "zero". Pentru a crește capacitatea de stocare a informației a unui HDD, dimensiunea biților magnetici trebuie redusă. Pe de altă parte, pentru a crește viteza de scriere a informației, reorientarea micilor magneti trebuie să devină mai rapidă. De aceea *mai mic* și *mai rapid* sunt cuvintele cheie ce guvernează avansarea tehnologiei în HDD-uri în particular, și al tehnologiei de stocarea a informației în general.

*În această teză atenția este concentrată asupra vitezei de manipulare a magnetizării în materiale magnetice metalice, relevante tehnologiei stocării de date.*

În mod convențional, reorientarea rapidă a magnetizării, în direcția opusă celei inițiale, este produsă cu ajutorul unui câmp magnetic pulsatoriu. Acesta este aplicat fie paralel, fie perpendicular în raport cu magnetizarea unui bit, așa cum a fost descris în Capitolul 1 al acestei teze. În zilele noastre, într-un HDD, un bit magnetic este stocat în  $\sim 1$  nanosecunda. Viteza acestui proces este proporțională cu amplitudinea câmpului magnetic aplicat. Acest lucru ar implica faptul că, viteza de scriere a informației poate fi infinit de mare atât timp cât există disponibil câmp magnetic cu amplitudine suficient de mare. Cu toate acestea, după cum a fost prezis recent de oamenii de știință ai Universității din Stanford, USA, există o limită fundamentală a vitezei de reorientare a magnetizării<sup>1</sup>. Aceștia, au indicat o limită de ordinul a câteva picosecunde ( $ps = 10^{-12}s$ ). La durate de timp mai scurte, cum ar fi fem-

---

<sup>1</sup><http://physicsworld.com/cws/article/news/19401>

tosecunde ( $1 \text{ femtosecundă} = 10^{-15} \text{ s}$ ), s-a sugerat că reorientarea magnetizării devine necontrolabilă/haotică. Evident, acest fenomen nedorit duce la incapacitatea de a controla biții de informație în mediile de stocare a datelor, astfel impunând o limită fundamentală vitezei de stocare a informației a HDD-urilor. De aceea, descoperirea unei noi metode de manipulare/reorientare a magnetizării într-un mod reproductibil, pe o scală de timp mai scurtă de o picosecundă, este o problemă fundamentală cu consecințe importante pentru tehnologia de stocare a datelor.

*În această teză sunt demonstrate experimental două metode diferite de reorientare a magnetizării pe durate de timp mai scurte de o picosecundă, distrugând astfel ceea ce cu doar puțin timp în urmă era numită limita de viteză a stocării de informație pe căi magnetice. În plus, această teză demonstrează un efect fizic fundamental, crezut în literatura de specialitate ca fiind imposibil: controlul magnetizării în metale numai cu ajutorul luminii polarizate.*

Experimentele au fost realizate pe aliaje amorfe de pamanturi-rare și metale-de-tranziție (RE-TM), mai exact GdFeCo. Acest tip de material este extrem de folosit ca mediu de stocare a informației în aparatele de stocare magneto-optice. Proprietățile magnetice și magneto-optice ale acestui material sunt detaliate în Capitolul 2. Tehnicile principale folosite pentru studiul și controlul dinamicii magnetizării în aceste materiale, la nivel de femtosecunde, au fost bazate pe laseri cu pulsuri extrem de scurte, cum ar fi 40 de femtosecunde. Aceste tehnici sunt detaliate în Capitolul 3. Rezultatele experimentale sunt prezentate în Capitolul 4 și Capitolul 5.

Capitolul 4 demonstrează cum punctul de compensare al momentului unghiular (caracteristic anumitor materiale ferrimagnetice cum ar fi GdFeCo) este acompaniat de o viteză foarte mare și o amortizare puternică a dinamicii magnetizării. Mai departe, este demonstrat cum încălzirea ultra-rapidă a ferrimagnetului peste punctele sale de compensare, în timp ce un câmp magnetic este aplicat, duce la reorientarea magnetizării pe o scală de timp de ordinul femtosecundelor. Acest experiment demonstrează pentru prima dată experimental fezabilitatea procesului de reorientare a magnetizării pe durate de timp mai scurte de 1 picosecundă, fenomen considerat imposibil cu doar un an în urmă. Un alt lucru fascinant caracteristic acestui experiment este că reorientarea magnetizării se produce în direcția opusă direcției câmpului magnetic aplicat.

În Capitolul 5, este investigată influența momentului unghiular al fotonilor asupra magnetizării materialelor magnetice metalice. Cu doar cațiva ani în urmă, acest efect era crezut nerelevant în procesul de interacțiune al luminii cu magnetizarea metalelor. O totală reorientare de  $180^\circ$  a magnetizării cu pulsuri laser ultra-scurte era considerat și mai puțin probabil după cum ne indică fizica cunoscută în zilele noastre (vezi Subsecțiunea 1.5.3). În ciuda acestui fapt aceasta teză demonstrează experimental  $180^\circ$  reorientarea magnetizării într-un mod reproductibil, în aliajul metalic amorf GdFeCo. Este demonstrat cum un singur puls laser cu lungime de 40 de femtosecunde conduce la reorientarea magnetizării, fără ajutorul nici unui câmp magnetic aplicat.

Direcția finală a magnetizării depinde de polarizarea luminii laser (circular-stanga sau circular-dreapta). Aceste experimente demonstrează o metodă *pur-optică* de stocare a informației, simplă, rapidă și total nouă, indicând o cale de a scrie informația cu o viteză de  $\sim 50.000$  de ori mai mare decât viteza actuală de scriere a informației într-un HDD.

În colaborare cu dr. Julius Hohlfeld și dr. Adnan Rebei (Seagate, Pittsburgh, USA) am reușit să observăm evoluția în timp a reorientării magnetizării, indusă prin metoda *pur-optică* cu pulsuri relativ lungi, de ordinul a 500 femtosecunde. Reorientarea a fost observată ca având loc la o scală de timp de ordinul femtosecundelor. În plus față de acest important rezultat, este remarcabil faptul că pulsuri laser relativ lungi (de  $\sim 1$  picosecundă) reușesc să reorienteze magnetizarea. Acest lucru este important din punct de vedere al aplicațiilor, deoarece în zilele noastre laserele cu durata pulsurilor de  $\sim 1$  picosecunda sunt relativ mici și ieftine, în contrast cu scumpele laserele cu pulsuri de ordinul femtosecundelor, o condiție necesară integrării lor în instrumentelor de stocare a datelor.

Pe lângă experimentele pe GdFeCo, am studiat efectul momentului unghiular al fotonilor și în alte aliaje feromagnetice de tipul RE -TM, ca de exemplu TbFeCo și DyFeCo. Și în aceste materiale pulsurile laser circular polarizate conduc la reorientarea magnetizării. În plus, acest efect a fost foarte recent observat și în materiale cristaline feromagnetice cum ar fi SmCo<sub>5</sub> de către J. Hohlfeld și A. Rebei<sup>2</sup>. De aici rezultă că metoda de reorientare a magnetizării *pur-optică* are loc indiferent dacă materialul este amorf sau are structură cristalină, dacă are coercivitate redusă (cum ar fi  $\sim 0.01$  T în cazul GdFeCo) sau foarte mare (cum ar fi 1 T în TbFeCo și SmCo<sub>5</sub>), sau dacă sistemul magnetic este feromagnetic sau ferimagnetic. Totuși, după cum am observat în experimentele noastre, reorientarea optică a magnetizării depinde de diametrul spotului laser focalizat pe materialul magnetic și de grosimea probei. Mai precis, în laboratoarele prof. J. -Y. Bigot, Strasbourg, Franța, am observat cum un spot laser cu diametrul de câțiva micrometri conduce la o reorientare haotică a magnetizării în GdFeCo. Acest lucru se datorează probabil faptului că GdFeCo este caracterizat de o anizotropie magnetică relativ redusă ceea ce conduce la o dimensiune minimă a domeniilor magnetice de ordinul micrometrilor. Așadar, în aceste condiții experimentale, există mari șanse ca domeniile magnetice reorientate să colapseze. Deoarece distanța de penetrare optică în metale este de  $\sim 20$  nm, dacă proba este prea groasă, domeniul magnetic reorientat optic poate de asemenea să colapseze. Acest lucru a fost observat într-o probă GdFeCo cu grosimea de 50 nm. De aceea, pentru a înțelege mai bine condițiile necesare pentru o reorientare *pur-optică* fezabilă a magnetizării, mai multe analize trebuie realizate, ca de exemplu analiza dependenței reorientării magnetice în funcție de durata pulsului, diametrul spotului, forma și grosimea probei. Trebuie de asemenea menționat că, în prezența unui câmp magnetic extern efectul momentului unghiular al fotonilor este suprimat. De aceea,

<sup>2</sup>J. Hohlfeld și A. Rebei, prezentare la THz Dynamics, Grenoble 2007.

un studiu cantitativ al comportamentului reorientării magnetizării pe cale optică în funcție de un câmp magnetic extern este de asemenea dorit.

Cu toate acestea, până acum reorientarea magnetizării pe cale *pur-optică* a fost observată numai în sisteme magnetice având în compoziția lor pământuri rare (RE). Din această cauză ar fi foarte interesant a fi studiat efectul momentului unghiular al fotonilor în materiale magnetice metalice cum ar fi de exemplu Co (cu anizotropie magnetică perpendiculară). Acest studiu va indica și totodată clarifica dacă mecanismul de reorientare optică a magnetizării este dominat de efecte cauzate de localizarea spinilor în RE sau dacă este necesar caracterul itinerant al spinilor din metalele de tranziție (TM).

Mai mult, foarte recent a fost demonstrată reorientarea magnetizării prin metoda inducerii de curent (așa numitul *current induced switching*), este un proces datorat interacțiunii momentului unghiular al electronilor nu cu magnetizarea (așa cum era crezut) ci cu momentul unghiular al materialului magnetic<sup>3</sup>. De aceea, ar fi foarte interesant un studiu care să investigheze efectul momentului unghiular al fotonilor pe materiale magnetice caracterizate de moment-unghiular-total diferit.

Din experimentele prezentate aici, se indică faptul că reorientarea magnetizării *pur-optică* este rezultatul combinat al încălzirii ultra-rapide a sistemului magnetic la temperaturi aproape de punctul Curie, și lumina circular polarizată acționând simultan precum un câmp magnetic local de ordinul a câțiva Tesla. Pe de altă parte a fost de asemenea arătat recent că în materialele dielectrice acest efect opto-magnetic este proporțional cu fluența laserului<sup>4</sup>. Totuși, în materialele metalice creșterea fluenței este limitată de absorbția optică puternică. Pentru a clarifica importanța fluenței laser și necesitatea creșterii temperaturii materialului în apropierea punctului Curie, un studiu sistematic va trebui realizat pe reorientarea magnetizării *pur-optică*, în funcție de fluența laserului, la temperaturi reduse. Alternativ, acest experiment poate fi de asemenea realizat la diferite lungimi de undă, mai specific în zona lungimilor de undă pentru care proba magnetică prezintă o absorbție optică redusă. Acest experiment este relevant nu doar pentru o mai bună înțelegere a mecanismului de reorientare *pur-optică* a magnetizării, ci și din punct de vedere tehnologic. Acest lucru se datorează faptului că pentru viitorul stocării informației este foarte important ca temperatura implicată în procesul de reorientare magnetică să fie redusă pe cât de mult posibil.

Cu această teză a fost deschisă o cale cu totul nouă în domeniul reorientării magnetice ultra-rapide. Deoarece experimentele prezentate aici sunt primele experimente care au demonstrat fezabilitatea unui efect crezut imposibil cu doar puțin timp în urmă, mecanismul microscopic responsabil pentru acest efect este încă un subiect neînțeleș

<sup>3</sup>Xin Jiang, Li Gao, Jonathan Z. Sun, and Stuart S. P. Parkin, *Phys. Rev. Lett.* **97**, 217202 (2006).

<sup>4</sup>A. V. Kimel, A. Kirilyuk, P. A. Usachev, R. V. Pisarev, A. M. Balbashov and Th. Rasing, *Nature* **435**, 655 (2005).

complet<sup>5</sup>. După cum a fost detaliat aici, multe experimente trebuie realizate pentru a înțelege complet acest nou mecanism de control al magnetizării, *pur-optic*.

În final, trebuie menționat că, chiar dacă reorientarea magnetică indusă de lumina circular polarizată este prezentată aici din punct de vedere al aplicațiilor în tehnologia de socare a datelor, este evident faptul că datorită caracterului său fundamental, acest nou efect are potențialul de a afecta puternic și alte domenii ale științei și tehnologiei.

---

<sup>5</sup>A. Rebei and J. Hohlfeld, Physics Letters A **372**, 1915 (2008).



---

## List of Publications

---

### Journal Articles

#### **Thermal-induced Magnetization Dynamics in GdFeCo**

C. D. Stanciu, A. V. Kimel, A. Kirilyuk, F. Hansteen, A. Tsukamoto, A. Itoh, and Th. Rasing, *in preparation*.

#### **Subpicosecond Magnetization Reversal across Ferrimagnetic Compensation Points**

C. D. Stanciu, A. Tsukamoto, A. V. Kimel, F. Hansteen, A. Kirilyuk, A. Itoh, and Th. Rasing, *Physical Review Letters*, vol. 99, p. 217204 (2007).

Also published in Virtual Journal of Ultrafast Science, Volume 6, Issue 12 (2007).

#### **All-optical Magnetic Recording with Circularly Polarized Light**

C. D. Stanciu, F. Hansteen, A. V. Kimel, A. Kirilyuk, A. Tsukamoto, A. Itoh, and Th. Rasing, *Physical Review Letters*, vol. 99, p. 047601 (2007).

This article has been selected as "Editors' Suggestions" and presented as the Cover of *Physical Review Letters*.

Also published in Virtual Journal of Ultrafast Science, Volume 6, Issue 8 (2007).

#### **Ultrafast Interaction of the Angular Momentum of Photons with Spins in the Metallic Amorphous Alloy GdFeCo**

C. D. Stanciu, F. Hansteen, A. V. Kimel, A. Tsukamoto, A. Itoh, A. Kirilyuk, and Th. Rasing, *Physical Review Letters*, vol. 98, p. 207401 (2007).

Also published in Virtual Journal of Ultrafast Science, Volume 6, Issue 6 (2007).

#### **Ultrafast spin dynamics across compensation points in ferrimagnetic GdFeCo: The role of angular momentum compensation**

C. D. Stanciu, A. V. Kimel, F. Hansteen, A. Tsukamoto, A. Itoh, A. Kirilyuk, and Th. Rasing, *Physical Review B*, vol. 73, p. 220402 (2006) (Rapid Communications).



**Optical excitation of antiferromagnetic resonance in TmFeO<sub>3</sub>**

A. V. Kimel, C. D. Stanciu, P. A. Usachev, R. V. Pisarev, V. N. Gridnev, A. Kirilyuk, and Th. Rasing, *Physical Review B*, vol. 74, p. 060403 (2006) (Rapid Communications).

**Observation and Control of Ultrafast Dynamics of GdFeCo Thin Films by Femtosecond Laser Pulses**

A. Tsukamoto, N. Jumpei, A. Itoh, D. Stanciu, A. Kimel, F. Hansteen, A. Kirilyuk, T. Rasing, *IEIC Technical Report*, vol. 105, p. 1 (2006).

**Ultrafast dynamics of GdFeCo ferrimagnetic film**

A. Tsukamoto, A. Itoh, D. Stanciu, A. Kimel, F. Hansteen, A. Kirilyuk, T. Rasing, *Bulletin of Topical Symposium of the Magnetism Society of Japan*, vol. 151, p. 19 (2006).

**Patents****Magneto-optical switching device and method for switching a magnetizable medium**

C. D. Stanciu, F. Hansteen, A. V. Kimel, A. Kirilyuk, A. Tsukamoto, A. Itoh, and Th. Rasing, *International Patent* WO2007136243 (2007).



---

## Curriculum Vitae

---

**Claudiu Daniel Stanciu,**  
born on 20th December 1979 in Pitești, Romania

1994–1998	Highschool, Grupul Școlar de Chimie Industrială Nr. 4, Pitești, Romania
1998–2002	Undergraduate studies at the Physics Faculty, West University of Timișoara, Romania
2002–2003	Post-University studies on Magnetic Nano-Microsistems at the Physics Faculty, West University of Timișoara, Romania.
2002–2004	Physicist at the National R&D Institute for Welding and Materials Testing, Timișoara, Romania
2004–2008	Ph.D. studies at Radboud University Nijmegen, The Netherlands, under the supervision of Prof. Th. Rasing.
2006 & 2007	One month, research guest at Institut de Physique et Chimie des Matériaux de Strasbourg, France, in the research group of Prof. J.-Y. Bigot.
2007	One month, Technical Intern at Seagate Research, Pittsburgh, USA.
2008– present	Researcher at Océ Technologies, Venlo, The Netherlands.





